EXPERIMENTAL INVESTIGATION ON FLEXURAL AND SHEAR BEHAVIOUR OF REINFORCED CONCRETE BEAMS USING GFRP REINFORCEMENT

By

Urvesh N. Barot
(07MCL002)

DEPARTMENT OF CIVIL ENGINEERING
Ahmedabad 382481
May-2009

EXPERIMENTAL INVESTIGATION ON FLEXURAL AND SHEAR BEHAVIOUR OF REINFORCED CONCRETE BEAMS USING GFRP REINFORCEMENT

Major Project

Submitted in partial fulfillment of the requirements

For the degree of

Master of Technology in Civil Engineering
(Computer Aided Structural Analysis & Design)

By
Urvesh N. Barot
(07MCL002)

Guide
Prof. U. V. Dave

DEPARTMENT OF CIVIL ENGINEERING
Ahmedabad 382481
May-2009

CERTIFICATE

This is to certify that the Major Project entitled “Experimental Investigation on Flexural and Shear Behaviour of Reinforced Concrete Beams using GFRP Reinforcement” submitted by Mr. Urvesh N. Barot (07MCL002), towards the partial fulfillment of the requirements for the degree of Master of Technology in Civil Engineering (Computer Aided Structural Analysis and Design) of Nirma University of Science and Technology, Ahmedabad is the record of work carried out by him under my supervision and guidance. In my opinion, the submitted work has reached a level required for being accepted for examination. The results embodied in this major project, to the best of my knowledge, haven’t been submitted to any other university or institution for award of any degree or diploma.

Prof. U. V. Dave,
Guide, Associate Professor,
Department of Civil Engineering,
Institute of Technology,
Nirma University,
Ahmedabad

Dr. P. H. Shah
Professor and Head,
Department of Civil Engineering,
Institute of Technology,
Nirma University,
Ahmedabad

Dr. K Kotecha
Director,
Institute of Technology,
Nirma University,
Ahmedabad

Examiner,

Examiner

Date of Examination

ACKNOWLEDGEMENT

With great pleasure I express my sincere gratitude towards my guide **Prof. U. V. Dave**, Associate Professor, Department of Civil Engineering, Institute of Technology, Nirma University, Ahmedabad for his valuable guidance and continual support. He has taken lots of effort to make contact between us and other companies. I would like to give my thanks for his continual help in technical and other problems throughout the Major Project. From the very beginning of the work, his valuable discussions, continuous reviews and suggestions have helped me a lot during this study.

My special thanks are to **Prof. G. N. Patel** and **Dr. P. V. Patel**, Professors, and **Dr. P. H. Shah**, Head, Department of Civil Engineering, Institute of Technology, Nirma University, Ahmedabad who have constantly encouraged me throughout the Major Project. I would like to thank **Prof. C. H. Shah,** structural consultant for his valuable suggestions to improve quality of my work. I am also thankful to **Dr. K Kotecha**, Director, Institute of Technology for his kind support in all respects during my study.

I would further like to thank **Shri Viren Pandya**, Lecturer, Department of Electrical Engineering, Institute of Technology, Nirma University for his valuable guidance and for extending all possible help.

I am really thankful to my classmates especially Mr. Jignesh I. Patel and roommates who have been great supporters in my Major Project work.

Most importantly, I express my special gratitude towards my parents, for their endless love and moral support.

I would also like to convey my sincere thanks to, all others who have helped me directly and indirectly.

Urvesh N. Barot
Roll No.07MCL002

ABSTRACT

New types of materials are always a matter of research interest. Researchers have attempted improvement different properties of structural members by using different types of innovative materials and techniques. Improvement in flexural, shear properties and durability for beams is one of the important aspects related to overall behaviour for structures. FRP is a material which withstands higher tensile strength as well as having other advantages like non-corroded and non-magnetic. FRP reinforcement is one of the most innovative solutions to replace a conventional steel reinforcement partially or fully. Hence, an attempt has been made hereby to check comparative performance of RC beams using various combinations of conventional and FRP rebars. FRP rebars have been used as tensile and shear reinforcement for beams. Replacement of conventional reinforcement of HYSD rebars has been tried with FRP rebars for RC beams in the present investigation.

Total twelve beams having cross sectional dimensions 150mm x 200mm with effective span of 2.1 m are cast in experimental programme. Variations has been employed in study by changing main reinforcement for RC beams. Total six categories of beams have been divided assuming two beams as identical in each category to take an average results. First three category of beams consist main reinforcement as HYSD rebars, combined HYSD and GFRP rebars, and third category has been consists of GFRP rebars only. All beams in first three categories have been used mild steel stirrups respectively. Another three categories of beams have same main reinforcement GFRP stirrups have been used. Different parameters like moment capacity, failure load, crack pattern, strain and deflection have been measured experimentally for all beams.

Design for RC beams has been done and relevant checks have been made. Different codal provisions have been used for design of beams using IS 456:2000 and ACI 440.1R-03 respectively. Moment capacities for different beams have been computed. It has been observed that failure load obtained for RC beams with minimum FRP reinforcement can give comparable results for beams with higher amount of HYSD reinforcement.

Tensile testing of GFRP as well as HYSD bars have been conducted under universal testing machine. Here GFRP bars show good amount of strength compared to HYSD bars.

Testing of beams have been conducted using two point load. Comparable failure loads and moment capacity has been observed for RC beams with FRP rebars and conventional HYSD rebars. RC beam with combined rebars have performed better compared to all other beams in terms of load and moment capacity. GFRP stirrups have exhibited superior performance compared to mild-steel stirrups in failure loads and moment capacities for all RC beams.

As per theoretical as well as experimental evaluation, shear strength of RC beams with conventional reinforcement proves better compared to RC beams with GFRP reinforcement. Experimental shear strength higher of RC beams with combined reinforcement has been observed higher compared to all other beam specimens.

Higher magnitude of deflection and strain has been observed for RC beams with GFRP rebars compared to RC beams with conventional rebars. RC beams with GFRP stirrups have exhibited lower deflections compared to RC beams with mild-steel stirrups. GFRP rebars have ruptured suddenly, compared to conventional HYSD bars. FRP stirrups also have been failed suddenly with loud noise compared to mild steel stirrups.

Thus, it can be concluded that GFRP rebars have proved better material to replace conventional HYSD bars because of comparable strength and other benefits like light in weight, non-corrosive, non-magnetic etc. Partial replacement of conventional HYSD bars with GFRP rebars has exhibited higher strength and capacity for RC beams. However, more experimental and analytical investigations are required in this area for generalizing use of FRP rebars in Structural Engineering applications.

CONTENTS

LIST OF FIGURES

LIST OF TABLES

ABBREVIATION NOTATION AND NOMENCLATURE

RC	Reinforced Concrete
FRP	Fiber Reinforced Polymer composite
HYSD	High Yield Strength Deformed Bar
HYSD-MS	RC beam with HYSD reinforcement and mild-steel stirrups
HYSD-GFS	RC beam with HYSD reinforcement and GFRP stirrups
Mix-MS	RC beam with combined reinforcement and mild-steel stirrups
Mix-GFS	RC beam with combined reinforcement and GFRP stirrups
GFRP-MS	RC beam with GFRP reinforcement and mild-steel stirrups
GFRP-GFS	RC beam with GFRP reinforcement and GFRP stirrups
b	Width of Section (Beam)
D	Depth of Section (Beam)
W	Working Load
W_u	Ultimate Load
M_u	Ultimate Bending Moment
M_{ur}	Ultimate Moment of resistance
P_{tmax}	Maximum percentage of steel
A_{st}	Area of steel reinforcement
f_{ck}	Characteristic compressive strength of concrete
f_y	Characteristic yield strength of steel
D_c	Density of Concrete
g	Acceleration due to gravity
W_{ud}	Ultimate design load
V_{ud}	Ultimate shear force
M_{DL}	Bending moment due to live load
M_{LL}	Bending moment due to dead load
A	Cross sectional area of member
M	Bending Moment
Z	Section Modulus
x_u	Linear co-ordinate or depth of neutral axis
D	Overall depth of section
f_{fu}	Design tensile strength of FRP bar
f_{fu}^*	Guaranteed tensile strength of FRP bar
C_E	Environmental reduction factor

ρ_f	FRP reinforcement ratio
A_f	Area of FRP reinforcement
f_r	Rupture strength of concrete
E_f	Guaranteed modulus of elasticity of FRP
E_s	Modulus of elasticity of steel
M_n	Nominal Moment Capacity
ρ_{fb}	FRP reinforcement ratio producing balanced strain conditions
β1	factor for concrete strength
fc’	specified compressive strength of concrete
εcu	Ultimate strain in concrete
V_{cf}	nominal shear strength
Vu	factored shear force
I_g	Gross moment of inertia
f_c’	specified compressive strength of concrete
Ec	modulus of elasticity of conrete
P_j	jacking load
Δf_{cr}	Change in flexural tensile srength
C_C	Torsional moment of inertia
ε_s	Strain in steel reinforcement
f_{pe}	effective stress in tendon
e	eccentricity
Φ	strength reduction factor
X_u	depth of neutral axis
£	Pounds

1. INTRODUCTION

1.1 General

It is a need of the hour today to find different kind of new types of materials to improve quality and behavior of structures with economical touch. Looking back into history, many new materials have been found to improve properties of structures. In last few decades, FRP (Fiber Reinforced Plastics) has arise as a new construction and repair material. Improvements in FRP in last 10 years have made its use feasible in different civil engineering applications.

1.2 FRP Reinforcement

A structural reinforcing bar made from filaments or fibers held in polymeric resin matrix binder is known as a FRP reinforcing bar.

Different types of FRP reinforcement are presented in Fig. 1.1, 1.2 and 1.3 respectively.

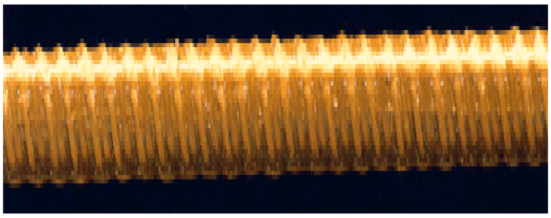

Fig. 1.1 AFRP (Aramid Fiber Reinforced Polymer) rebars

Fig. 1.2 GFRP (Glass Fiber Reinforced Polymer) rebars (Ref. Sunna et al. [15])

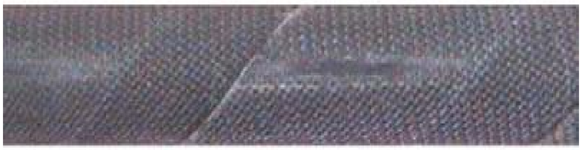

Fig. 1.3 CFRP (Carbon Fiber Reinforced Polymer) rebars (Ref. Sunna et al.[15])

FRP rebars are a new type of structural material for civil engineering community. Basic constituent materials for reinforced concrete design have changed very little in last 100 years. Traditionally, composite materials were being used extensively in aerospace and consumer sporting goods to exploit their high strength to weight characteristics. Now a day's FRP has become very popular. Therefore, FRP has been used more in construction industry. FRP reinforcing bars have become innovative solution to structure repairs.

Basic advantages of FRP reinforcement are as follows

- High longitudinal strength to weight ratio
- Corrosion resistant
- Non-magnetic
- High fatigue endurance (Aramid and Carbon fibres)
- Low thermal and electric conductivity
- Lighter in weight (about 1/4th in comparison of steel)

Popular applications of FRP reinforcement in different conditions have been listed as follows.

1. Corrosive applications
    - Concrete exposed to deicing salts such as bridge decks, approach slabs, parking structures, railroad crossing, salt storage facilities etc.
    - Seawalls**,** buildings and structures near waterfronts**,** Aquaculture operations**,** Floating marine docks, Tunnel work, Brine tanks, Swimming pools
    - RC work in chemical plants and containers
    - Architectural precast and cast stone elements (Where adequate cover not available)
2. Electromagnetic applications
    - MRI rooms in hospitals
    - Airport radio and compass calibration pads
    - Electrical high voltage transformer vaults
3. Masonry and Structural strengthening work.

FRP reinforcements were originated in 60's. But advances in field of polymers, production techniques and implementation of authoritative design guidelines have resulted in a rapid increase in their usage in last 15 years. Use of FRP reinforcement in Europe began in Germany with construction of a prestressed FRP highway bridge in 1986. Since construction of this bridge, intensive efforts have been made to increase research related to applications of FRP reinforcement in Europe.

Canadian civil engineers have been continuing to develop applications related to FRP reinforcement in Canadian Highway Bridge Design Code and have constructed a number of demonstration projects. Headingly Bridge in Manitoba included both CFRP and GFRP reinforcement. Additionally, Kent County Road No. 10 Bridge used CFRP grids to reinforce negative moment regions.

Joffre Bridge, located over St-François River in Sherbrooke, Quebec, included CFRP grids in deck slab and GFRP reinforcing bars in traffic barrier and sidewalk. This bridge was opened for traffic in December 1997, which included fiber-optic sensors that were structurally integrated into FRP reinforcement for remotely monitoring strains. Applications of FRP reinforcement in bridges and building have been given in Fig. 1.4 and 1.5. Typical uses of FRP reinforcement (In United States) have been reported in ACI 440.1[23]. Recent applications of FRP reinforcements in bridge deck construction have been given in Fig. 1.6 and 1.7 respectively.

Fig.1.4 GFRP bars installed during Construction of crowchild bridge in Calgary, Alberta

Fig. 1.5 GFRP bars used in winery in British Columbia

Fig. 1.6 FRP reinforced deck constructed in Lima, Ohio

Fig. 1.7 GFRP bars used in redecking of Ohio’s Salem avenue bridge

FRP reinforcement differs from conventional steel reinforcement from following viewpoints

- No yielding before failure
- Low transverse strength
- Low elastic modulus (especially for glass)
- Susceptible to UV rays
- Sensitive to moisture
- Sensitive to alkaline environment
- High coefficient of thermal expansion perpendicular to fibers.

1.3 Material Characteristics of FRP Reinforcement

Physical and mechanical properties of FRP reinforcing bars have been presented here. It is anticipate that these properties are helpful to develop a fundamental understanding of behavior of bars their use in concrete structures. FRP bars are anisotropic in nature and are manufactured using a variety of techniques like as pultrusion, braiding, and weaving. Factors such as fiber volume, type of fiber, type of resin, fiber orientation, dimensional effects, and quality control during manufacturing all play a significant role in establishing characteristics of an FRP bar.

1.3.1 Physical properties

1. *Density*

   FRP bars have a density ranging from 1.25 to 2.1 g/cm^3, which is estimate to one-sixth to one-fourth that of steel.

2. *Coefficient of thermal expansion*

   Coefficients of thermal expansion of FRP bars vary in longitudinal and transverse directions depending on types of fiber, resin, and volume fraction of fiber. Longitudinal coefficient of thermal expansion dominated by properties of fibers, on the other hand transverse coefficient is dominated by resin. Longitudinal and transverse coefficients of thermal expansion for typical FRP bars and steel bars have been presented in Table 1.1. Negative coefficient of thermal expansion indicates that material contracts with increase in temperature and expands with decrease in temperature. Concrete has a coefficient of thermal expansion that varies from 7.2×10^{-6} to 10.8×10^{-6}/C and is usually assumed to be isotropic.

Table 1.1 Physical properties of FRP reinforcing bar*

Properties	Direction	Steel	GFRP	CFRP	AFRP
Density (gm/cm^3)	-	7.9	1.25 - 2.1	1.5-1.6	1.25-1.4
Coefficient of thermal expansion (x 10^{-6}/C)	Longitudinal, α_L	11.7	6 – 10	-9 to 0	-6 to -2
	Transverse, α_T	11.7	21 – 23	74-104	60-80
Tensile strength (MPa)	-	414	552	2070	1172
Elastic modulus (GPa)	-	200	35 – 51	120 - 580	41-125
Rupture strain (%)	-	6 to 12	1.2 to 3.1	0.5 - 1.7	1.9-4.4
Reinforcement ratio (ρ_{fb})	-	0.0335	0.0078	0.002	0.0035

*****Typical values for fiber volume fraction ranging from 0.5 to 0.7.

1.3.2 Mechanical properties and Behavior

1. *Tensile behavior*

FRP bars do not exhibit any plastic behavior (yielding) before rupture. (When loaded in tension) and Tensile behavior of FRP bars consisting of one type of fiber material is characterized by a linearly elastic stress-strain relationship until failure. Tensile properties of commonly used FRP bars have been summarized in Table 1.1.

Tensile strength and stiffness of an FRP bar have been dependent on specific factors. As fibers in a FRP bar are main load-carrying constituents, ratio of volume of fiber to overall volume of FRP i.e. fiber-volume fraction significantly affects tensile properties of a FRP bar. Strength and stiffness variations have been observed in bars with various fiber-volume fractions respectively, even in bars with same diameter, appearance, and constituents. Rate of curing, manufacturing process and quality control also affect mechanical properties of FRP bar. Unlike steel bars, FRP bars exhibit a substantial effect of cross/sectional area on tensile strength. Typical stress-strain curve for a GFRP bar has been shown in Fig. 1.8.

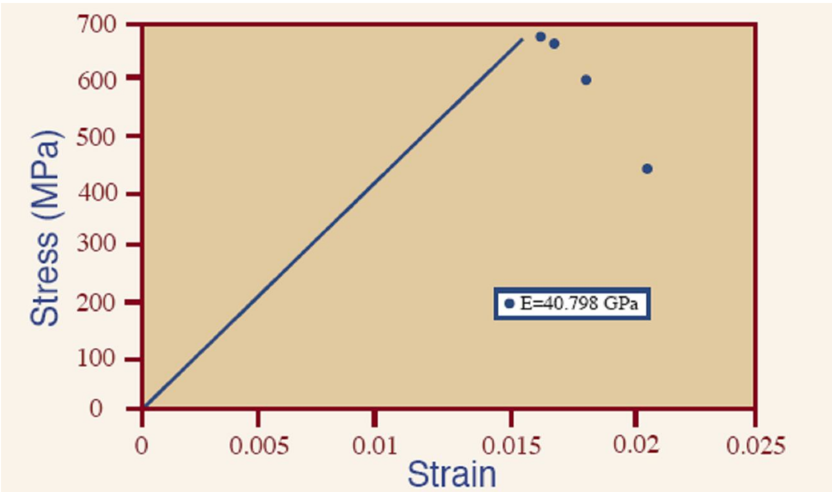

Fig 1.8 Typical stress-strain curve for GFRP bar (Ref. Manufacturer data sheet)

2. *Compressive behaviour—*

FRP bars are not very reliable for resisting compressive stresses. Tests on FRP bars with a length to diameter ratio from 1:1 to 2:1 have shown that compressive strength is refer than tensile strength. Mode of failure for FRP bars subjected to longitudinal compression has exhibited transverse tensile failure, fiber microbuckling, and shear failure. Mode of failure depends on type of fiber, fiber-volume fraction and type of resin. Compressive strength of 55%, 78%, and 20% of tensile strength has been reported for GFRP, CFRP, and AFRP, respectively (ACI 440.1[23]). Compressive strength is higher for bars with higher tensile strengths in general. However, AFRP bars where fibers exhibit nonlinear behavior in compression at a relatively low level of stress opposite behaviour has been observed occasionally (ACI 440.1[23]).

3. *Shear behaviour*

Majority of FRP bars are relatively weak in interlaminar shear where layers of unreinforced resin lie between layers of fibers. Interlaminar shear strength is governed by relatively weak polymer matrix (because there is usually no reinforcement across layers). Orientation of fibers in an off-axis direction across layers of fiber increase shear resistance depending upon the degree of offset. This can be accomplished (For FRP bars) by braiding or winding fibers transverse to main fibers. Off-axis fibers are also placed in pultrusion process by introducing continuous strand mat in roving/mat creel. Standard test methods are not yet established to characterize shear behavior of FRP bars. Shear properties of a particular FRP bar are generally obtained from bar manufacturer. Manufacturer should provide a description of test method used to obtain reported shear values.

4. *Bond behaviour*

Bond performance of a FRP bar is dependent on design, manufacturing process, mechanical properties of bar itself, and environmental conditions. When anchoring a reinforcing bar in concrete, bond force is be transferred in different ways as follows.

a) Adhesion resistance of interface, known as chemical bond.
b) Frictional resistance of interface against slip.
c) Mechanical interlock due to irregularity of interface.

It is postulated that bond force is transferred through resin to the reinforcement fibers, and a bond-shear failure (For FRP bars) in resin is also possible. When a bonded deformed bar is subjected to increasing tension, adhesion between bar and surrounding concrete breaks down.

Deformations on surface of bar causes inclined contact forces between bar and surrounding concrete. Stress at surface of bar resulting from force component in direction of bar can be considered bond stress between bar and concrete. Unlike reinforcing steel, bond of FRP rebars appears not to be influenced significantly by concrete compressive strength provided adequate concrete cover exists to prevent longitudinal splitting.

1.4 Research Significance

From discussion of properties and advantages given above, it has been observed that tensile strength of FRP bars is more than that of steel. RC structures using steel reinforcement have been designed by maximum moment capacity. It has been assumed that steel is a ductile material. Therefore steel is assumed to fails first and there after concrete crushes. It has been reported that FRP bars are heterogeneous (ACI 440[23]). Hence, if beams with FRP reinforcement are designed assuming rupture of FRP reinforcement then design is to be deals with minimum FRP reinforcement. Hence, an attempt has been made here to evaluate viability of using minimum FRP bars as tensile reinforcement. It has been also tried to use FRP rebars as shear reinforcement in place of steel reinforcement. Whether flexural strength, and moment capacity reaches at the level of steel RC beam with conventional reinforcement also has been tried to evaluate. Partial replacement of conventional reinforcement with FRP rebars also has been planned to check through experimental study.

1.5 Scope of Work

Scope of work of major project includes theoretical work and laboratory work related to flexure and shear behaviour of RC beams using GFRP reinforcement.

Theoretical work includes the following.

- Calculation of maximum moment resisting capacity and ultimate load of RC beams using design provisions of IS: 456[23] and ACI 440.1[21].
- Calculation of cross-section dimension, span, diameter of reinforcement, number of bars etc. for RC beams.
- Evaluation of maximum displacement and strain for RC beams.

Laboratory work consists following

- Testing of FRP reinforcement for tensile strength.
- 12 RC Beams of 150mm x 200mm x 2100mm are to be cast in laboratory. The beams are to be tested for flexure and shear behaviour respectively. Details of RC beams have been given in Fig. 1.9.
- For all RC Beams M25 grade concrete is to be used.
- Average results of two beams are required to be considered as final result in terms of load, displacement, strain etc. for beams of all categories.

Following measurements are required to be taken after testing of all beams with two point loading

- Ultimate failure load
- Deflection
- Strain measurement at external surface of concrete using strain gauges
- Crack and failure patterns

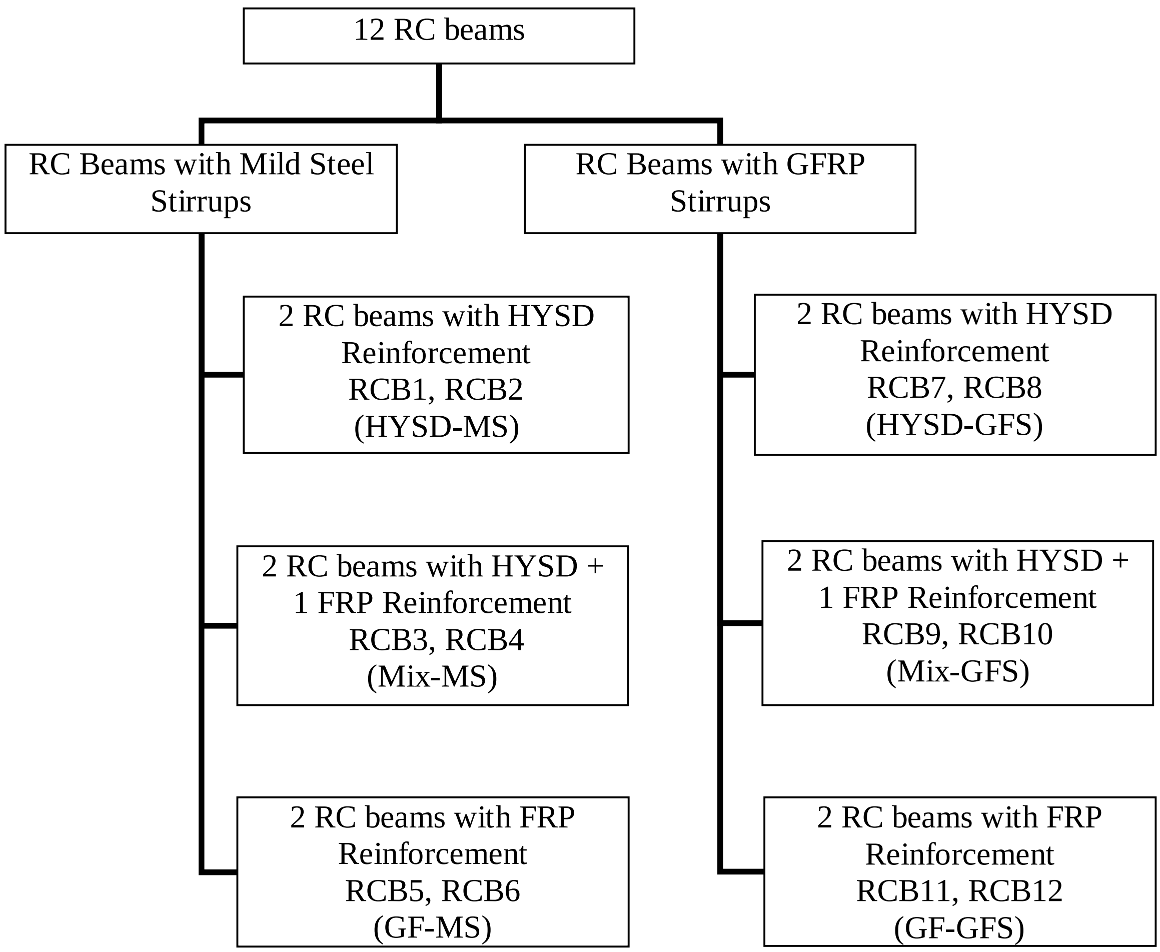

Fig. 1.9 Details of Reinforced Concrete Beams

Following parameters are required to be studied based upon measurement of various observations during experiment.

- Comparative study in terms of flexural behavior of RC beams reinforced with only HYSD bars, combination of HYSD bars and FRP bars and with only FRP bars.
- Comparative study on shear behavior of RC beams by reinforced with different types of tension reinforcement as suggested above and by varying type of stirrups.
- Study on change in type of main reinforcement on performance of RC beams.
- Study on influence of type of reinforcement on behaviour in terms of rupture, failure and crack patterns for RC beams.
- Comparison of experimental and theoretical results for RC beams

1.6 Organization of Major Project

This study is related to RC beams using FRP Reinforcement. Report of major project entitled “Enhancement of Flexural and Shear behavior RC beams using FRP Reinforcement” has been divided into eight chapters. Overview of each chapter and relevant contents has been explained briefly as follows.

- Chapter 1 deals with introduction, application, properties and features of FRP reinforcement. Characteristics of FRP material and its innovativeness in civil engineering field have been discussed. Properties and behavior of FRP reinforcement are explained. History and advantages of using FRP reinforcement have been covered. Objective and Scope of work for complete major project has been explained in this chapter.
- Chapter 2 discusses literature review. Many researchers have worked to improve flexure strength and shear strength of RC beams using FRP reinforcement. Like many researchers have further tried to study different parameters related to FRP reinforcement. All such detail are included in this chapter. Details of codal provisions of RC elements using FRP reinforcement have been discussed.
- Chapter 3 explains theoretical work conducted in this project. Calculations are made using code for design of RC beams using different type

reinforcement. It discusses method for calculate moment capacity of RC beams reinforced with combined use of HYSD and FRP reinforcement.

- Chapter 4 covers details related to how experimental work conducted. Compressive strength test performed for concrete cubes has been discussed. Tension test of FRP reinforcement, Test specimens and Formwork, Test setup and testing procedure, Instrumentation during entire experimentation has been discussed.
- Chapter 5 gives all results related to RC specimens like deflection, strain measurement, failure loads etc. Results have been in tabular form in a systematic way in this chapter.
- Chapter 6 incorporates discussing of results which have been obtained from testing of specimen. Comparison of different chart has been shown like deflection, strain, failure load, moment capacity etc. have been presented in form of charts and graphs.
- Chapter 7 gives details related to initiation of corrosion in RC beams. It also discusses about process of corrosion, experimental program to induce corrosion, establishment or circuitry for implantation or impressed current technique, Results and discussion etc.
- Chapter 8 consists of summary, concluding remarks and recommendation for future scope of work on basis of work conducted in major project.

2. LITERATURE REVIEW

2.1 General

Recent years have seen rapidly growing interests in application of advanced fiber-reinforced polymer (FRP) reinforcements in civil engineering field around the world, in terms of research activities and practical implementations both. It has been suggested by many researchers that "FRP reinforcements are a new generation of construction materials following steel." Deterioration observed in marine structures and bridges due to corrosion is a major problem throughout world today. To counteract such problem uses of FRP reinforcement is matter of interest among researchers globally.

2.2 Literature Review

Extensive literature review has been conducted using available resources from national and international journals, proceedings and codes. Information from literature has been classified in form of different types of different types of properties and different types of behaviour related to FRP reinforcement in this chapter as follows

1. Flexural strength
2. Shear strength
3. Analytical work
4. Behaviour of FRP reinforced beams
5. Deflection
6. Tensile test
7. Temperature and Fire performance
8. Bond test
9. Design provisions from relevant code of practice

2.2.1 Flexural strength

Alsayed [1] measured load-deflection relationship for 12 concrete beams reinforced using steel or glass fiber reinforced plastic (GFRP) bars. Numerical part of the study was conducted using, (i) computer model which accounted for actual properties of composite constituents, (ii) ACI load-deflection model, and (iii) modified load-deflection model available in the literature for beams reinforced by FRP bars. Error in prediction of service load deflection and ultimate flexural strength was less than 10% and 1%, respectively. For GFRP reinforced beams, service load deflection predicted by ACI model is in error by 70%. On the other hand, error predicted by modified model is in error by less than 15%.

Sarazin and Newhook [2] suggested that current design codes specify a minimum amount of flexural reinforcement for design of a RC beam. Minimum value for a RC beam is calculated by adjusting ultimate moment of section above concrete cracking moment. Unlike steel reinforcement, FRP does not yield and is linear elastic until failure. At low reinforcement ratios, failure of RC section is controlled by rupture of FRP and hence is considered to be more brittle than ductile failure of a steel reinforced section.

2.2.2 Shear strength

Stratford and Burgoyne [3] suggested that design of steel-reinforced concrete relies on lower-bound plasticity theory. This is of benefit in shear design due to complexity of shear-transfer and recommended use of where simplified models like truss analogy as shown in Fig.2.1.

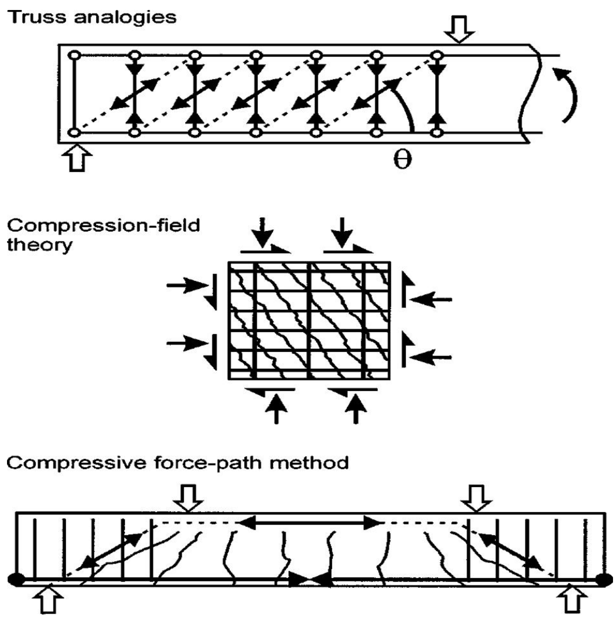

Fig. 2.1 Simplified models of equilibrium in shear span of reinforced concrete beam [3]

Further, lower-bound plasticity theory cannot be applied when brittle reinforcement like FRP is used in concrete. Study has been made on compatibility, equilibrium, and material constitutive laws of FRP-reinforced beam subjected to shear. A crack-based analysis is carried out to model shear failure in a beam with brittle reinforcement. Such analysis is found useful to illustrate importance of satisfying compatibility requirements.

Matta et al. [4] investigated 04 large-scale concrete beams reinforced with GFRP bars in flexure and shear. It was observed that concrete shear strength was strongly affected by size effect. With respect to strength reduction of 24% has been observed in beams with effective depth of 880 mm. FRP reinforcement ratio of 0.59% and 0.89% has commonly encountered in practice due to relatively small axial modulus of GFRP bars. Negligible difference on concrete shear strength was evaluated in sections with increased amount of shear reinforcement.

El sayed et al. [5] suggested theoretical equation for prediction of shear strength. They proposed modification to ACI 440.1R-03[23] shear design equation. Proposed equation was verified against experimental shear strengths of 98 specimens tested to date, and calculated values are shown to compare well. In addition, proposed equation was compared to major design provisions using available test results. Better and consistent predictions were obtained using proposed equation.

2.2.3 Analytical work

Gravina and Smith [6] proposed a local deformation model for RC beams reinforced with FRP bars. A detailed theoretical investigation was conducted by applying the model to continuous beams reinforced with FRP bars in order to predict bending moment distribution, progressive formation of flexural cracks, associated crack spacing and crack widths respectively. From use of analytical procedure of different reinforcement bars on bond properties on ductility and moment distribution was successfully investigates.

Lawrence [7] explained in detail structural design of RC elements using FRP reinforcement. FRP applications, products and properties of FRP materials for use in structural design have been explained. Design of flexural member also has been discussed in detail. Strengthening work related to masonry and concrete members is also covered.

Gangarao et al. [8] explained design of concrete structures reinforced with FRP reinforcement as a substitute for steel reinforcements. Information related to design and behaviour of concrete structures using FRP reinforcement as internal reinforcements, development length serviceability with Deflection and crack-width have been discussed in detail by author.

Krishnaraju [9] covered strain compatibility method evaluate true moment capacity of beams.

Shah and Karve [10] given complete reference for design of RC beam using Indian standard code of practice IS-456:2000. Other details regarding analysis are also covered in this book.

2.2.4 Behaviour of FRP reinforced beams

Pecce et al. [11] investigated three simply supported beams reinforced with FRP bars. Span was 340 cm, width and height of beam cross section were 50 and 18.5 cm, respectively. Beams were tested under two point loads. Two different amount of longitudinal reinforcement in tension were used in type F1 and F3 beams with 7Φ2.7 mm (889 mm^2) and type F2 with 4Φ2.7 mm (508 mm^2). For all beams compression reinforcement kept as 2Φ2.7-mm FRP bars uniformly. Design models at ultimate and serviceability conditions were discussed. It was observed that a linear analysis is reliable to control stresses of concrete and FRP rebars. Concrete stress was very high even with a low percentage of ultimate load and assumption of a reduced value of concrete working stress resulted in uneconomical use of FRP reinforcement.

Grace et al. [12] investigated seven rectangular beams and seven continuous T-beams. Reinforcing bars and stirrups were made of steel, carbon, and glass fiber reinforced polymer (GFRP). Use of FRP reinforcement in continuous beams increases deformation. This increase remained small and acceptable at service load level, but deformation increases significantly near failure. Ratio of absorbed energy to total energy was used as a measure of ductility. Based on this definition, a classification at failure ductile, semi-ductile, and brittle behavior was suggested. Theoretical results obtained using suggested method was substantiated experimentally. Continuous beams experienced higher "energy ratios" compared to simple beams.

2.2.5 Deflection

Abdalla [13] developed simple approaches in estimating deflection of FRP reinforced concrete members subjected to flexural stresses. Predictions of these approaches were compared with experimental results obtained by testing seven concrete beams reinforced with GFRP and CFRP bars respectively. Proposed analytical methods further substantiated by experimental results available in literature of eight concrete slabs reinforced with conventional steel, GFRP and CFRP bars.

Toutanji and Yong [14] suggested that concrete beams reinforced with FRP bars exhibited higher deflections and larger crack widths compared to concrete beams reinforced with steel due to lesser modulus of elasticity of FRP bars. Verification of ACI 440 methods for predicting deflections and crack widths for GFRP reinforced RC beams were presented. Improvement for crack width equation was suggested to account for two layers of reinforcement. Six RC beams reinforced with different GFRP reinforcement ratios were tested. Measured deflections and crack widths were analyzed and compared with those predicted by proposed models.

Sunna et al. [15] presented deflection results of a testing program of FRP RC beams and examined the ACI provisions of deflection in detail. Form of the equation for *Ie* (effective moment of inertia) is not fundamentally sound and cannot be used to predict deflections of FRP RC beams in all cases. More appropriate form is proposed involving reinforcement ratio and elastic properties of rebar.

2.2.6 Tensile Test

Kocaoz [16] performed tensile characterization of GFRP reinforcement. Total 32 no of bars from one manufacturer were investigated. Instead of a polymeric resin-based anchor, a steel pipe filled with expansive cementitious grout was

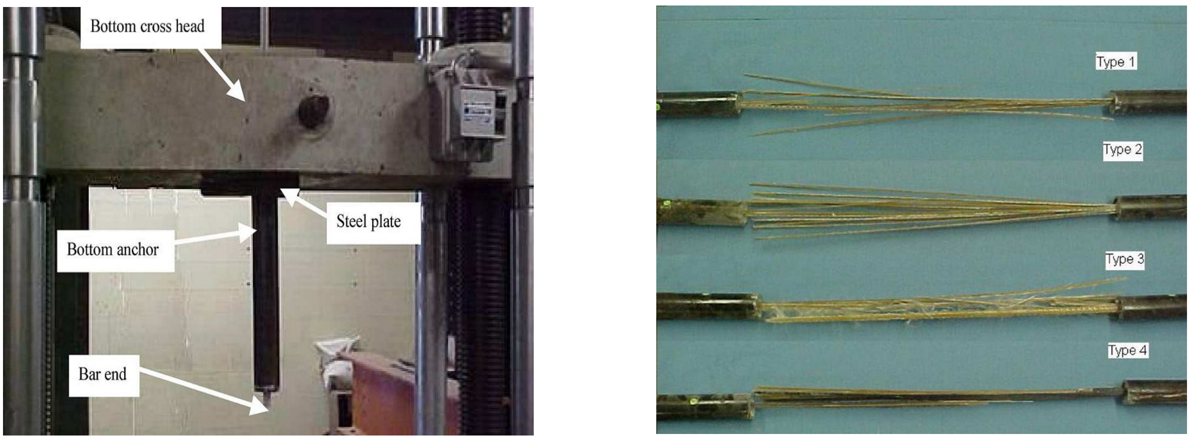

(a) Testing setup (b) Rupture of FRP rebars

Fig. 2.2 Special type of testing setup for tensile test of FRP rebars [16] used as the end restrainers as shown in Fig 2.2. An experiment based on a randomized complete block design was conducted to obtain data for statistical analysis. Analysis was carried out using a commercially available data analysis software program. Failure shape of different FRP bars has been presented in Fig.2.2.

Castro [17] carried out exploratory study to support development of standard test methods for FRP bars for use as concrete reinforcement. Principal objectives were to develop a system to permit tensile loading of bars in a universal test machine; to evaluate tensile strength; and to explore potential of measuring elastic modulus using available non-destructive test methods. Ends of a bar were embedded in steel tubes using a high-strength gypsum cement mortar. Different types of grip-fittings for tensile testing of FRP rebars as shown in Fig. 2.3. Bars were loaded by gripping tubes in conventional wedge friction grips of a tensile testing machine. Dynamic modulus of elasticity was determined using two stress-wave propagation methods, e.g. ultrasonic pulse velocity and resonant frequency. Dynamic values compared favourably with static values obtained from tensile stress-strain curves.

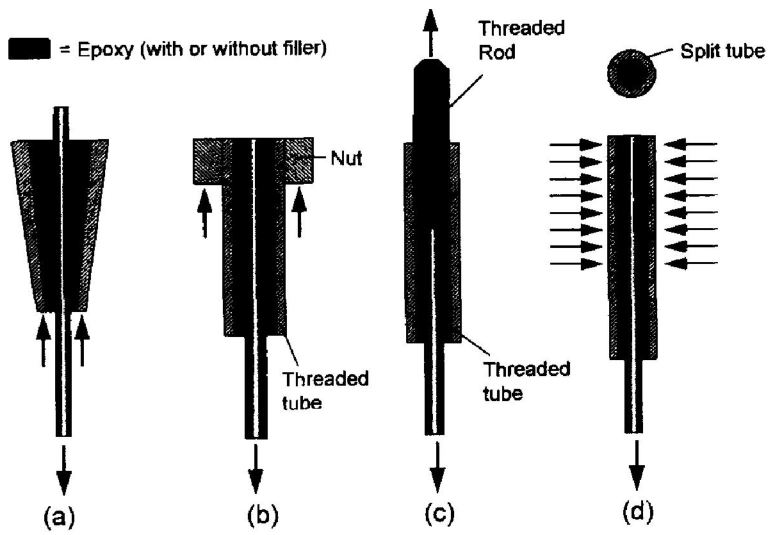

Fig. 2.3 Tensile test fittings for FRP bars used by various researchers [17]

2.2.7 Temperature and Fire Performance

Katz [18] has evaluated about bond properties of FRP reinforcing bars at temperatures ranging from room temperature (20 ^{O}C) to high temperatures up to (200 ^{O}C) accompanied by changes in pullout load-slip behaviour. A semiempirical model was developed in order to describe extent of reduction in bond strength as temperature rises. Model is based on following parameters: glass transition temperature of polymer layer at surface of rod; polymer's degree of cross-linking; residual bond strength at high temperature after polymer of external layer of rebar ceased to contribute to bond. Parameters of rods that were tested for pullout at various temperatures were introduced into model. Output curves of bond vs. temperature relationships showed good agreement with test results.

Nadjai [19] analyzed behaviour of concrete beams reinforced with hybrid FRP and steel reinforcements at elevated temperatures. Slice approach model was used and validated against experimental data for reinforced concrete beams with FRP from literature. Test setup for pullout test has been presented in Fig. 2.4. Good agreement with experimental results has been obtained at room temperature as well as at elevated temperatures.

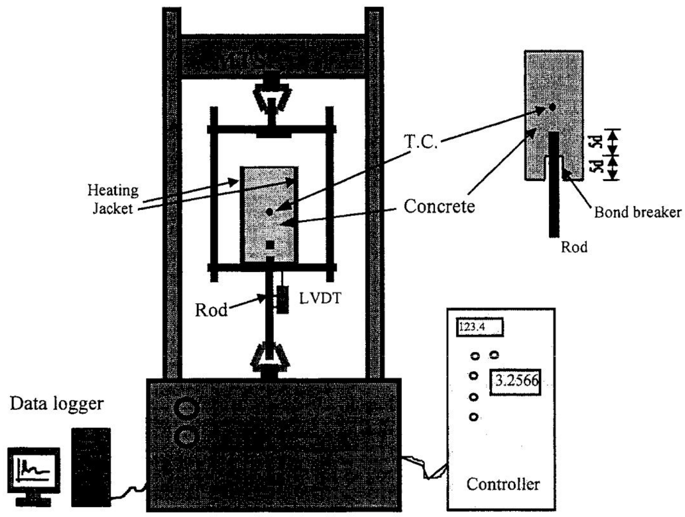

Fig. 2.4 Test setup for pullout test [19]

Galati et al. [20] conducted analysis of bond between FRP bars and concrete under thermal loads taking into account available data on bond–slip relationships and thermal behaviour from other literature. An experimental investigation was carried out on concrete specimens reinforced with a FRP bar and subjected to thermal cycles with a maximum temperature value of 70 ^{o}C. After thermal treatment, pull-out tests were performed at room temperature and higher temperature. Untreated specimens were further tested for comparison. Results were discussed to investigate degradation of concrete-reinforcement interface under thermal treatment and, as a consequence, its effect on bond-slip laws. A significant degradation induced by exposure to relatively high temperatures was observed.

2.2.8 Bond Test

Won et al. [21] evaluated effects of synthetic and steel fibers on bond of high-strength concrete and FRP reinforcing bars. Direct bond tests (Fig. 2.5) were performed to evaluate bond performance of 9mm £ CFRP and 13mm £ GFRP reinforcing bars in three types of high-strength concrete with varying amounts of steel (20 and 40 kg/m^3) and synthetic fiber (4.55 and 9.1 kg/m^3). Bond strength increased with compressive strength of high-strength concrete. Type and amount of fiber also affected bond strength. Specimens with 40 kg/m^3 steel fibers showed highest bond strength. As diameter of FRP bars large, it's exhibited stronger bonds regardless of strength of concrete, type and amount of fibers. Relative bond strength was evaluated to analyze effect of type and amount of fibers. Bond strength increased with more addition of fiber.

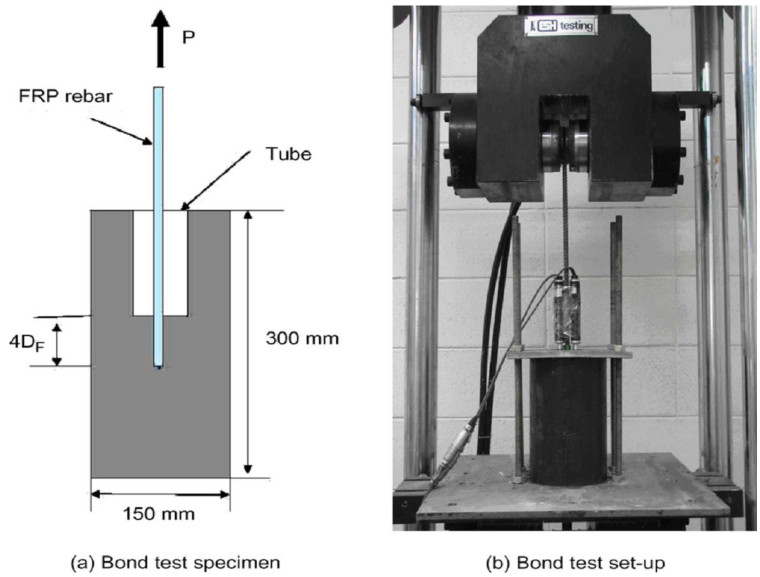

Fig. 2.5 Test setup for bond test [21]

Tighiouart et al. [22] investigated bond strength of FRP rebars and compared with that of steel rebars. Total 64 concrete beams reinforced with two types of FRP rebars were tested. Four nominal diameters of FRP and steel rebars 12.7mm, 15.9mm, 19.1mm and 25.4 mm, and three embedment lengths, 6, 10 and 16 times rebar diameters were used. Moreover, three concrete depths of 200mm, 600mm and 1000 mm were investigated in 18 pullout specimens. Test results indicated that applied tensile load approached tensile strength of rebars as embedment length increased. GFRP rebars showed lesser bond strength compared to that of steel rebars. Average maximum bond strength of FRP rebars varied from 5.1 MPa to 12.3 MPa depending on diameter and embedment length.

2.2.9 Design provisions from relevant code of practice

ACI 440.1 [23] is a report from ACI Committee 440. Details of history, properties, application and uses of FRP reinforcement have discussed. Criteria for design of flexure members alongwith solved examples also have been included.

IS 456 [24] different codal provisions for Plain or RCC concrete design have been given. Codal provisions for RC beam design have been used in this study from this standard. Mix design concept has also been followed from the code.

2.3 Summary

From literature review, some of important points have been summarized as follows.

- Dimensions of beam section have been decided on basis of literature and codal parameters.
- RC beam design has been conducted on basis of IS 456[23] provisions.
- Concept of strain compatibility method for evaluation of true moment capacity has been considered taken from Krishnaraju [9].
- General idea, properties and understanding of behaviour of FRP reinforcement have been understand from literature.
- Test setup, test data and scope of work finalization have been decided based on literature review.
- Design of RC flexure member with FRP reinforcement has been conducted on the basis on minimum reinforcement criteria from literature and ACI 440.1[22] design provisions.

3. DESIGN OF RC BEAMS

3.1 General

Reinforced Concrete has become most popular now-a-days. For all RC sections concrete is providing compressive strength and reinforcing material has been provided tensile strength.

Experiment has been performed on RC beams in present study. Total three categories of beams have been planned to be cast and tested as given below:

1. RC beams with only HYSD as main reinforcement.
2. RC beams with only FRP as main reinforcement.
3. RC beams with combination of HYSD+FRP as main reinforcement.

Therefore, design of RC beams with each of above combination of reinforcement has to be conducted as per codal provisions. Discussion pertaining to above has been given in this chapter with relevant calculations. For true moment capacity of RC beams with combination of HYSD and FRP as main reinforcement strain compatibility method has been described. Detailing drawing has been prepared for beams on the basis of design.

3.2 Design of Beams

Design of RC beams with steel reinforcement and FRP reinforcement has been present in this section.

3.2.1 RC beams with HYSD reinforcement (RCB1, RCB2)

This example has been calculated using codal parameters of IS 456[24] and Shah and Karve [10].

Span of beam (L) = 2100 mm

Other parameters of assumed section are as follows,

Width (b)	= 150 mm
Overall depth (D)	= 200 mm
Clear cover (d’)	= 30 mm
Effective Depth (d)	= 170 mm

Loads which have been acting on a simply supported beam have been assumed and from that ultimate load is calculated.

Assuming slab thickness as 120mm and wall thickness as 150mm

Load from Slab = 0.12 x 25	=	3.00	kN/m
Self wt. of Beam = 2 x 0.15 x (0.2-0.03) x 25	=	1.28	kN/m
Live Load (Assumed)	=	4.00	kN/m
Load from Wall = 20 x 3 x 0.15	=	9.00	kN/m
Total Working Load W	=	(13.28+4)	kN/m

Total Ultimate Load W_u= 1.5 x W = 1.5 x 17.28 ≈ 26 kN/m

Design Moment= $M_u = \frac{W_u \times L^2}{8}$ = 14.33 kNm ... (3.2.1.1)

For M25 grade of concrete and Fe 415 grade of steel

Ru_{max} = 3.45 and %age of reinforcement P_{tmax} = 1.2%

(Ref. Shah and Karve [10])

Moment of Resistance $Mu_{rmax} = Ru_{max} \times b \times d^2$ ... (3.2.1.2)

$= 3.45 \times 150 \times 170^2$

= 14.96 kN/m > M_u

$$A_{st} = \frac{0.5 \times f_{ck}}{f_y}\left[1-\left(\sqrt{1-\frac{4.6 \times M_u}{f_{ck} \times b \times d^2}}\right)\right] \times b \times d \quad \text{... (3.2.1.3)}$$

= 287.3 mm^2

Provide 3-#12mm diameter HYSD bars as main reinforcement

Thus, $Ast_{provided}$ = 339 mm^2 > 287.3 mm^2 (OK)

Assuming maximum %age of reinforcement as 1.2 and calculating main reinforcement,

$$A_{st} = \frac{P_t \times b \times d}{100} = \frac{1.2 \times 150 \times 170}{100} = 326 \text{ mm}^2 \quad \text{... (3.2.1.4)}$$

Provided area for beam is also satisfying from provision of max % of reinforcement also.

So after providing above said reinforcement,

By putting $A_{stprovied}$ value in equation (3.2.1.1), maximum moment capacity has been obtained as M_u = 16.21 kNm.

Here assuming 2-#10mm diameter bars as compression reinforcement

$$V_u = \frac{w \times l}{2} = \frac{26 \times 2.1}{2} = 27.3 \text{ kN} \qquad \text{...(3.2.1.5)}$$

$$\tau_v = \frac{V_u}{b \times d} = \frac{27.3 \times 10^3}{150 \times 170} = 1.07 \quad \text{N/mm}^2 \qquad \text{(Cl. 40.1, IS 456[24])}$$

$$P_t = \frac{100 A_{st}}{b \times d} = \frac{100 \times 339}{150 \times 170} = 1.33\% \quad \text{For M-25}$$

τ_c = 0.72 (Table-19, IS 456[24])

Here, τ_v > τ_c so, required to design the shear reinforcement

V_{us} = V_u - τ_c x b x d (Cl. 40.4, IS 456 [24])

= 27.3 x 10^3 – 0.72 x 150 x 170

= 8940 N

Consider, 2-legged, 6 mm-Ø, mild steel having f_y = 250 N/mm^2 vertical stirrups

$$S_v = \frac{0.87 \times f_y \times A_{sv} \times d}{V_{us}} \qquad \text{... (3.2.1.6)}$$

$$= \frac{0.87 \times 250 \times 56.55 \times 170}{8940}$$

= 233.88 mm

(Cl. 26.5.1.6, IS 456[24])

(i) 0.75 x d = 0.75 x 200 = 150 mm

(ii) 300 mm

(iii) $$S_v = \frac{0.87 \times f_y \times A_{sv}}{0.4 \times b} \qquad \text{... (3.2.1.7)}$$

$$= \frac{0.87 \times 250 \times 56.55}{0.4 \times 170}$$

= 180.87 mm

So provided, 2-legged, 6 mm-Ø, vertical stirrups used at 180 mm c/c. Detail of test specimen are summarized in Fig. 3.1.

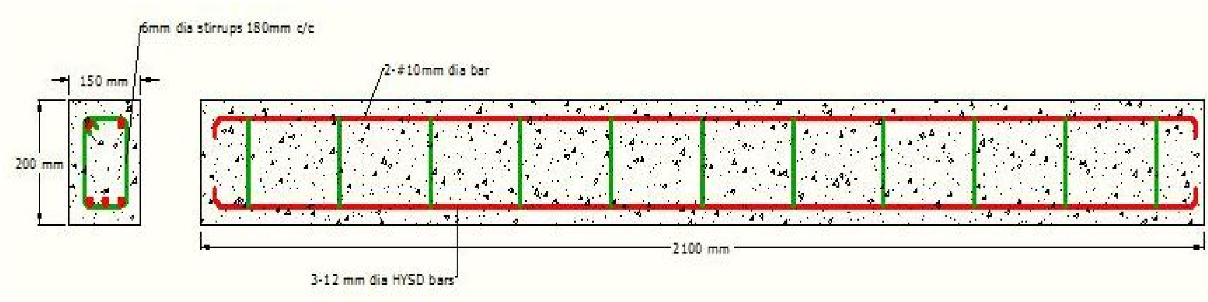

Fig. 3.1 Details of HYSD reinforced beams (RCB1, RCB2)

3.2.2 RC beam with FRP reinforcement

This example has been solved using codal parameters of ACI 440.1 [23].

Step-1 Estimation of appropriate c/s dimensions of the beam:

$$h = \frac{L}{16} = \frac{2100}{16} = 131.25 \qquad \text{ACI 440.1[23]}$$

Assume h = 0.20 m and assuming b = 0.15 m

Our section is of 150mm x 200mm x 2100mm

Step-2 Computation of factored load

Load from Slab = 0.12 x 25	=	3.00 kN/m
Self wt. of Beam = 2 x 0.15 x 0.2 x 25	=	1.28 kN/m
Live Load (Assumed)	=	4.00 kN/m
Load from Wall = 20 x 3 x 0.15	=	9.00 kN/m
Total Working Load	=	(13.28 + 4) kN/m

Total Ultimate Load $= 1.4 x W_{DL} + 1.7 x W_{LL} = 1.4 x 13.28 + 1.7 x 4$

$= 25.39$ kN/m

$$\text{Design Moment} = M_u = \frac{W_u \times L^2}{8} = 14.00 \text{ kNm}$$

Step-3 Computation of design rupture stress for FRP bars

Design tensile strength $f_{fu} = C_E \times f_{fu}^*$ ...(3.2.2.1)

= 0.8 x 690.6

= 552.5 MPa

Here, C_E is Environmental reduction factor (Ref. Table 7.1, ACI 440.1[23]) and f_{fu}^* = Guaranteed tensile strength of GFRP bar from manufacturer

Step-4 calculation of area of GFRP bars for required flexural strength

$$\rho_f = \frac{A_f}{b \times d} \quad \text{... (3.2.2.2)}$$

Assuming an initial amount of FRP reinforcement as 3-#3 bars

$$= \frac{3 \times 84.32}{150 \times 170} = 0.0099$$

Computation of balanced FRP reinforcement ratio as per (eq. 8.3) ACI 440.1[23]

$$\rho_{fb} = \frac{0.85 \times f_c'}{f_{fu}} \times \beta_1 \times \frac{E_f \times \varepsilon_{cu}}{E_f \times \varepsilon_{cu} + f_{fu}} \quad \text{... (3.2.2.5)}$$

$$= \frac{0.85 \times 31.25}{552.5} \times 0.85 \times \frac{40800 \times 0.003}{(40800 \times 0.003) + 552.5} = 0.0074$$

$\rho_f > \rho_{fb}$,

Stress in FRP reinforcement in tension, as per eq. (8.4d) ACI 440.01[23],

$$f_f = \sqrt{\frac{E_f \times \varepsilon_{cu}}{4} + \frac{0.85 \times f_{ck} \times \beta_1}{\rho_f} \times E_f \times \varepsilon_{cu}} - 0.5 \times E_f \times \varepsilon_{cu} \quad \text{... (3.2.2.3)}$$

$$= \sqrt{\frac{(40800 \times 0.003)^2}{4} + \frac{0.85 \times 0.85 \times 31.25}{0.0099} \times 40800 \times 0.003} - 0.5 \times 40800 \times 0.003$$

= 470.68 MPa

Nominal moment capacity, as per (eq.8.5) ACI 440.01[23]

$$Mn = \rho_f \times f_f \times (1 - 0.59 \times \frac{\rho_f \times f_f}{f_c'}) \times b \times d^2 \quad \text{----------(3.2.3.4)}$$

$$= 0.0099 \times 470.68 \times (1 - 0.59 \frac{0.0099 \times 470.68}{1.25 \times 25}) \times 150 \times 170^2$$

= 18.42 kN.m

Step-5 Computation of strength reduction factor

$$\Phi = \frac{\rho_f}{2 \times \rho_{fb}} = 0.7 \quad \text{... (3.2.2.6)}$$

$\Phi M_n = 0.7 \times 18.42 = 12.89 \text{ kNm} \leq M_u$

Step-6 Design for Shear

$$V_u = \frac{W_u \times L}{2} - W_u \times d \qquad = \frac{26 \times 2.1}{2} - 26 \times 0.17 = 22.88 \text{ kN}$$

$$V_{cf} = \frac{\rho_f \times E_f \times \sqrt{f_c'}}{90 \times \beta_1 \times f_c' \times 6} \times b \times d \qquad \text{(Ref. ACI 440.1[23], eq. 9.1)} \qquad \ldots (3.2.2.7)$$

$$= \frac{0.0099 \times 40800 \times \sqrt{31.25}}{90 \times 0.85 \times 31.25 \times 6} \times 150 \times 170 = 4.01 \text{ kN}$$

$$f_{fb} = \left(0.05 \times \frac{r_b}{d_b} + 0.3\right) \times f_{fu} = \left(0.05 \times \frac{3 \times 6}{6} + 0.3\right) \times 470.68 = 211.8 \text{ MPa}$$

$$s = \frac{\phi \times A_{fv} \times f_{fv} \times d}{V_u - \phi \times V_{cf}} = \frac{0.85 \times 2 \times 33.23 \times 81.6 \times 170}{22880 - 0.85 \times 4018} = 87.02 \text{mm} \qquad \ldots (3.2.2.8)$$

Compression reinforcement has been kept similar to that adopted for Design of RC beams with HYSD reinforcement. Type amount and spacing of stirrups also has been kept similar to that of RC beams reinforced with HYSD bars. Fig.3.2 show the reinforcement details for FRP reinforced beams as discussed.

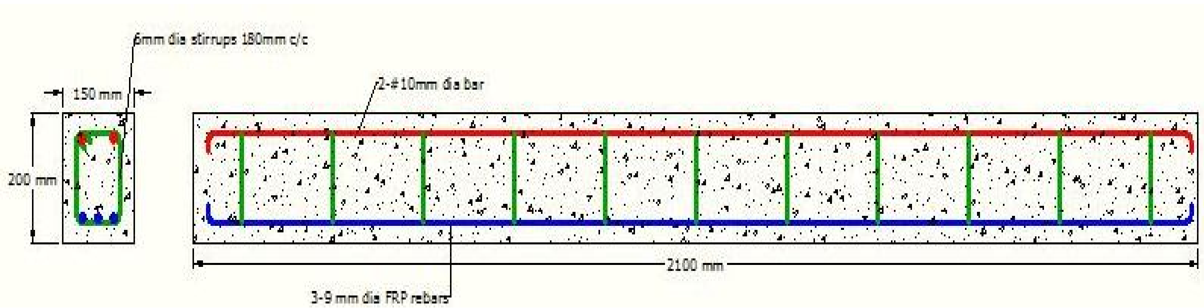

Fig. 3.2 Details of FRP reinforced concrete beams

3.3 Strain Compatibility Method for RC beams with Combined Reinforcement

For evaluating true moment capacity of Hybrid (HYSD+FRP) reinforced beams, Strain Compatibility Method has been used. Design example based on this method has been given here. Load-Strain diagram of tension reinforcements is required for necessary calculations. Therefore, a 12mm diameter HYSD TMT bar as well as 9.5 mm diameter FRP bar has been tested in the laboratory. From which results in terms of Load-strain curve is plotted as shown below.

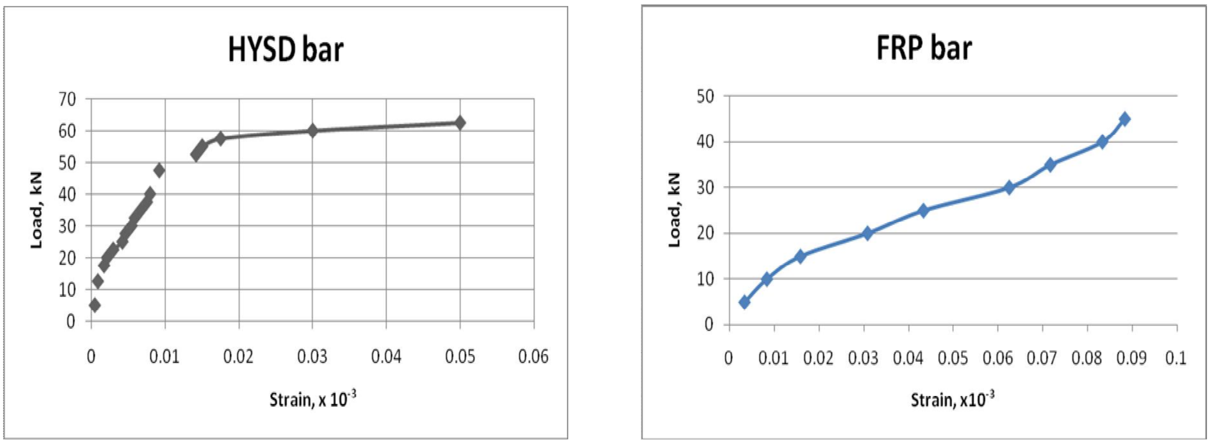

Fig. 3.3 Plot of load-strain curve for HYSD and FRP bar

Section of beam = 150mm x 200mm

Assumed design of beam with HYSD and FRP as main reinforcement

Area of steel in Compression = 2-10mm diameter bars = 157 mm^2

Area of steel in Tension = 2-12mm diameter bars = 226 mm^2

+ 1-9.5mm diameter FRP bar = 84.32 mm^2

Considering strain in concrete block (ε_{cu}) = 0.0035 and

= 0.003 (in case of FRP)

and neutral axis X_u = 93.35 mm

Here value of neutral axis has been assumed

From Load-strain diagram strain in steel,

$$\varepsilon_{su} = \frac{\varepsilon_{cu} \times (d - x_u)}{x_u} = \frac{0.0035 \times (170 - 93.35)}{93.35} = 0.002874 \qquad ...(3.3.1)$$

Now, from (Fig. 3.3) load-strain curve taking values for 12mm diameter bars, and from load-strain curve of FRP bar taking values of 9.5mm diameter bars,

Corresponding force in each bar = 56.73 kN

Corresponding forced in each FRP bar = 11.74 kN

Tension T = (2 x 56.73) + (1 x 11.74) = 125.2 kN

Compression C = 0.36 x f_{ck} x b x X_u ...(3.3.2)

= 0.36 x 25 x 150 x 93.35/1000 =126.02 kN

Ultimate Moment M_u = 0.87 x f_y x A_{st} x (d-0.416 x X_u) ...(3.3.3)

$= 0.87 \times 415 \times 226 \times (170 - 0.416 \times 93.35)$

$= 10.7$ kNm

$$\rho_f = \frac{A_f}{b \times d} = \frac{84.32}{150 \times 170} = 0.0033 \qquad \text{...(3.3.4)}$$

As per ACI 440.01R-03 eq. (8.4d), stress in FRP reinforcement in tension

$$f_f = \sqrt{\frac{E_f \times \varepsilon_{cu}}{4} + \frac{0.85 \times f_c' \times \beta_1}{\rho_f} \times E_f \times \varepsilon_{cu}} - 0.5 \times E_f \times \varepsilon_{cu} \qquad \text{...(3.3.5)}$$

$$= \sqrt{\frac{(40800 \times 0.003)^2}{4} + \frac{0.85 \times 0.85 \times 31.25}{0.0033} \times 40800 \times 0.003} - 0.5 \times 40800 \times 0.003$$

$= 854$ MPa

As per ACI 440.01 (eq.8.5), nominal moment capacity

$$Mn = \rho_f \times f_f \times \left(1 - 0.59 \times \frac{\rho_f \times f_f}{f_c'}\right) \times b \times d^2 \qquad \text{...(3.3.6)}$$

$$= 0.0033 \times 854 \times \left(1 - 0.59\,\frac{0.0033 \times 854}{1.25 \times 25}\right) \times 150 \times 170^2$$

$= 11.56$ kNm

True moment capacity = 22.26 kNm

In above approach X_u value has been assumed. Hence trials are to be made evaluating values of tension and compression at same level.

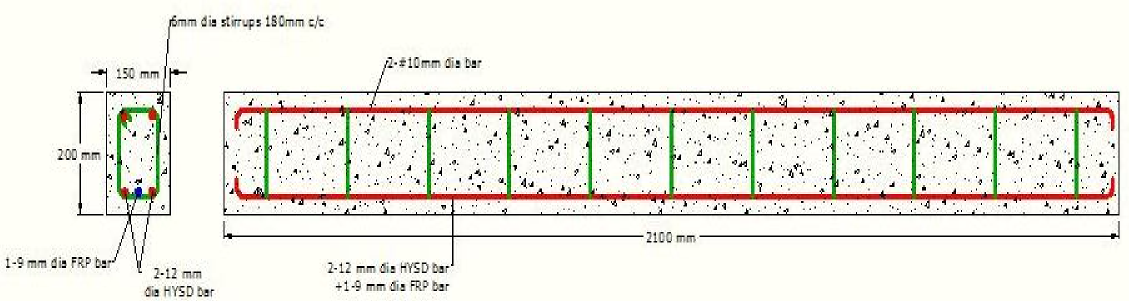

Fig .3.4 Details of combined reinforced concrete beams

3.4 Theoretical Computation of Different Parameters

3.4.1 Failure load

Calculation of theoretical failure load has been predicted from various

For RC beam with HYSD reinforcement (RCB1, RCB2, RCB7, RCB8)

Theoretical moment capacities

Theoretical moment capacity = 16.2 kNm

$M_u = \frac{W_u \times l}{6}$, (1.5 x 16.2) $= \frac{W_u \times 1.8}{6}$, W_u = 81 kN

For RC beam with FRP reinforcement (RCB 5, RCB 6, RCB 9, RCB 10)

Theoretical moment capacity = 18.42 kNm

$M_u = \frac{W_u \times l}{6}$, 18.42 $= \frac{W_u \times 1.8}{6}$, W_u = 61.4 kN

For RC beam with combination reinforcement (RCB 3, RCB 4, RCB 11, RCB 12)

Theoretical moment capacity = (11.56+10.7) kNm

$M_u = \frac{W_u \times l}{6}$, 27.61 $= \frac{W_u \times 1.8}{6}$, W_u = 92 kN

3.4.2 Deflection

3.4.2.1 RC beams with HYSD reinforcement (RCB1, RCB2)

For simply supported beam subjected to two point loading, deflection has been worked out as follows.

$$\Delta = \frac{23 \times P \times l^3}{648 \times E \times I_e} \qquad \text{... (3.4.2.1)}$$

P = Load applied from jack

l = Effective length of specimen

E = Modulus of Elasticity of Concrete

= $5000\sqrt{f_{ck}}$ = 25000 N/mm^2

I_e = Moment of Inertia of section

$$= \frac{b \times d^3}{12} = \frac{150 \times 170^3}{12} = 61.41 \times 10^6 \qquad \text{... (3.4.2.2)}$$

Assuming for 10 kN load from jack,

deflection $\Delta = \frac{23 \times 10 \times 10^3 \times (1.8 \times 1000)}{648 \times 25000 \times 61.41 \times 10^6}$

Δ = 1.35 mm

3.4.2.2 RC beams with GFRP reinforcement (RCB 5, RCB 6)

For simply supported beam subjected to two point loading, deflection has been worked out as follows.

$$\Delta = \frac{P \times x}{48 \times E_c \times I_e}\left(3 \times l^2 - 4 \times x^2\right) \qquad ...(3.4.2.3)$$

P = Load applied from jack

l = Effective length of specimen

x= Distance between the support

E_c = Modulus of elasticity of concrete

here, f_c' has been considered as 1.25 times cube strength

= $4560\sqrt{fc'}$ = 27360 N/mm^2

Now. for I_e

$$I_e = \left[\left(\frac{M_{cr}}{M_{DL+LL}}\right)^3 \times \beta_d \times I_g\right] + \left[\left[1 - \left(\frac{M_{cr}}{M_{DL+LL}}\right)^3\right] \times I_{cr}\right] \qquad ...(3.4.2.4)$$

So, for solution of above equation,

I_g= Gross Moment of Inertia = $\frac{150 \times 200^3}{12}$ = 100 x 10^6 mm^4

f_r = $0.62 \times \sqrt{f_{ck}}$ = 3.47 MPa

M_{cr} = $\frac{2 \times f_r \times I_g}{h}$ = (2 x 3.47 x 100 x 10^6)/200 = 3.47 kN.m ...(3.4.2.5)

$$I_{cr} = \left(\frac{b \times d^3}{3}\right) \times K^3 + n_f \times A_f \times (1 - K)^2 \qquad ...(3.4.2.6)$$

$$k = \sqrt{2 \times \rho_f \times n_f + (\rho_f \times n_f)^2} - (\rho_f \times n_f) \qquad ...(3.4.2.7)$$

n_f = E_f /E_c , =40800/(4560 x $\sqrt{(1.25 \times 25)}$) = 1.46 ...(3.4.2.8)

k = 0.161

I_{cr} = 7.51+e06

$\beta_d = \alpha_b \times \left[\frac{E_f}{E_c} + 1\right] = 0.602$ ...(3.4.2.9)

$P_{DL+LL} = 16.675$

$M_{DL+LL} = (P_{DL+LL} \times l^2)/8 = 9.2$ kN.m

By putting above different values in equation (3.4.2.4)

$I_e = 10.47 \times 10^6$ mm^4,

l=1.8 m, x=0.6 m

For P = 10 kN,

$$= \frac{10\times10^3\times(0.6\times1000)}{48\times25492\times10.47\times10^6}\left(3\times1800^2 - 4\times600^2\right) = 3.88 \text{ mm}$$

3.4.3 Shear Strength

RC beam with HYSD reinforcement and mild-steel stirrups (RCB1, RCB2)

$V_c = \tau_c \times b \times d = 0.72 \times 150 \times 170 = 18.36$ kN ... (3.4.3.1)

$$V_{us} = \left(\frac{0.87\times f_y \times A_{sv} \times d}{S_v}\right) = \left(\frac{0.87\times250\times56.55\times170}{180}\right) = 11.62 \text{ kN} \quad \text{... (3.4.3.2)}$$

$V_s = V_c + V_{us} = 18.36+11.62 \approx 30$ kN ,

for ultimate shear strength = (1.5 x 30) = 45 kN

RC beam with GFRP reinforcement and GFRP stirrups (RCB11, RCB12)

$$V_c = (2/5)\times k \times \sqrt{f_c'} \times b \times d \text{ and } V_f = \left[\frac{A_{fv}\times f_{fv}\times d}{s_f}\right] \quad \text{... (3.4.3.3)}$$

here, k = $\sqrt{2\times\rho_f\times n_f + (\rho_f\times n_f)^2} - (\rho_f\times n_f) = 0.1629$ ... (3.4.3.4)

$V_c = (2/5)\times 0.1629\times\sqrt{31.25}\times150\times170 = 9.29$kN

$$V_f = \left(\frac{A_{fv}\times f_{fv}\times d}{S_v}\right) = (2 \times 33.23 \times 81.6 \times 170)/180 = 5.12 \text{ kN} \quad \text{... (3.4.3.5)}$$

$V_s = V_c + V_f = 14.41$ kN

3.5 Summary

Summary of computations related to RC beams with HYSD reinforcement and FRP reinforcement has been presented in Table 3.1:

Table 3.1 Design results of RC beams

Type of beam	Compression reinforcement	Tension reinforcement	Moment capacity (kNm)	Failure loads (kN)	Maximum Theoretical Deflection (mm)	Shear-strength (kN)
Design of RC beam with HYSD reinforcement	2-#10mm HYSD bars	3-#12mm HYSD bars	16.2	81	13.48	30
Design of RC beam with GFRP reinforcement	2-#10mm HYSD bars	3-#9.5mm FRP bars	18.42	61.4	34.9	14.41
Design of RC beam with Combined reinforcement	2-#10mm HYSD bars	2-#12mm HYSD bars + 1-#9.5mm FRP bar	22.26	92	-	-

Above Table 3.1 has been summarized on calculations computed. As per Table 3.1 RC beam with combined reinforcement show higher moment capacity as well as failure load capacity compared to other beams. In case of deflection RC beam with GFRP reinforcement has been observed higher compared to RC beam with HYSD reinforcement.

4. EXPERIMENTAL PROGRAMME

4.1 General

Description about test setup, methods to be employed for conducting experiment, Reinforcement details for different category of beams have been discussed in this chapter. Details regarding appropriate selection of method out of various available methods have been described.

4.2 Test Specimen

It has been planned to test beams for 2-point loads at loading frame. Geometry of beams has been decided on basis of literature survey. Dimensions have been decided using relevant codal provisions. Total 12 beams have been cast in entire investigation. Total beams have been divided into six categories with different configuration as discussed in scope of work and in Fig.1.9 in chapter 1. Each category of beam consists of two beams and average results from both beams are to be considered. Corresponding calculation for RC beams based on different codal provisions have been presented in chapter 3. Their details have been presented as follows:

1] RC beams with HYSD Reinforcement [RCB1, RCB2, RCB7, and RCB8]

Details of reinforcement for RCB1 and RCB2 have been given in Fig. 3.1. Other details of beams RCB7 and RCB8 remain same. Mild steel stirrups have been replaced by FRP stirrups in RCB7 and RCB8. However, spacing of both category of stirrups has been kept same for all four beams. Reinforcement cage for above beams have been presented in Fig. 4.1.

a) Reinforcement cage for specimen with HYSD reinforcement and mild steel stirrups

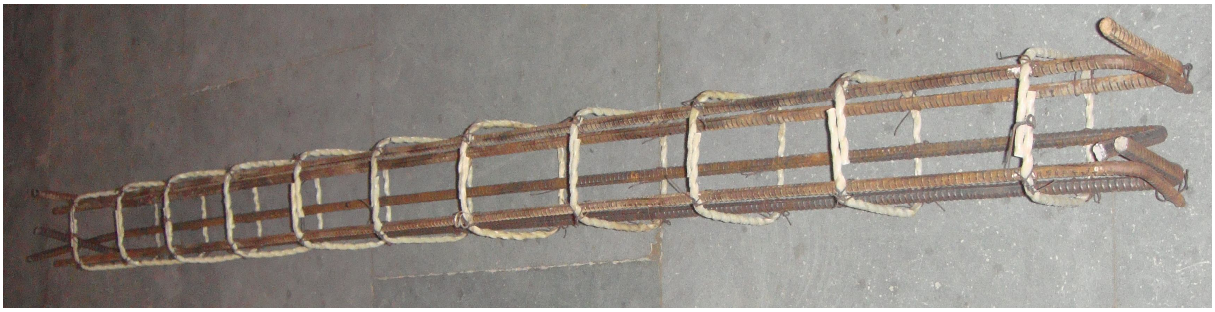

b) Reinforcement cage for specimen with HYSD reinforcement and GFRP stirrups

Fig. 4.1 RC beams with HYSD reinforcement

2] RC beam with both HYSD and FRP reinforcement [RCB3, RCB4, RCB9, RCB10]

Detailing of reinforcement for beams RCB3 and RCB4 have been presented in Fig. 4.2. These beams have been designed with an assumption that one HYSD reinforcement from main reinforcements has been replaced by GFRP reinforcement partially. Details of beams RCB9 and RCB10 remains same except the stirrups type change to FRP stirrups have been used in beams RCB9 and RCB10 in place of mild steel stirrups used for RCB3 and RCB4 respectively.

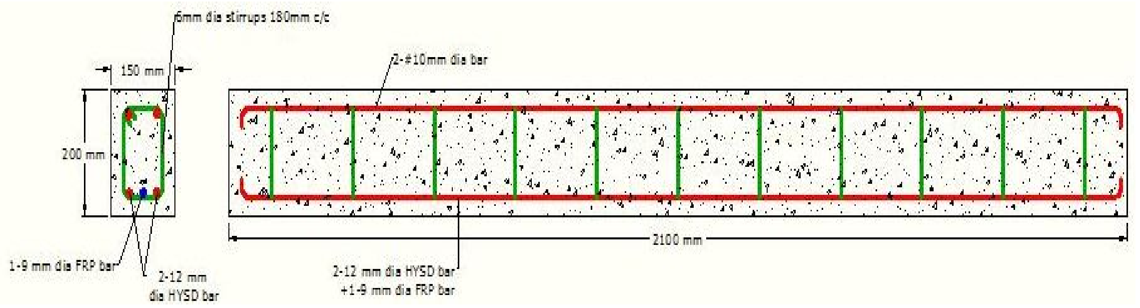

Fig. 4.2 RC beam with HYSD and FRP reinforcement

3] RC beam with FRP Reinforcement [RCB5, RCB6, RCB11, RCB12]

Design of RC beams using ACI 440.1[23] codal provision has been conducted. Detailing of reinforcement in beams RCB5 and RCB6 has been presented in Fig. 3.2. Compression reinforcement is of HYSD bar on the other hand tension reinforcement has been replaced by GFRP reinforcement. Keeping all other configuration same, beam RCB11 and RCB12 have been cast using FRP stirrups. Reinforcement cage for above beams have been presented in Fig.4.3.

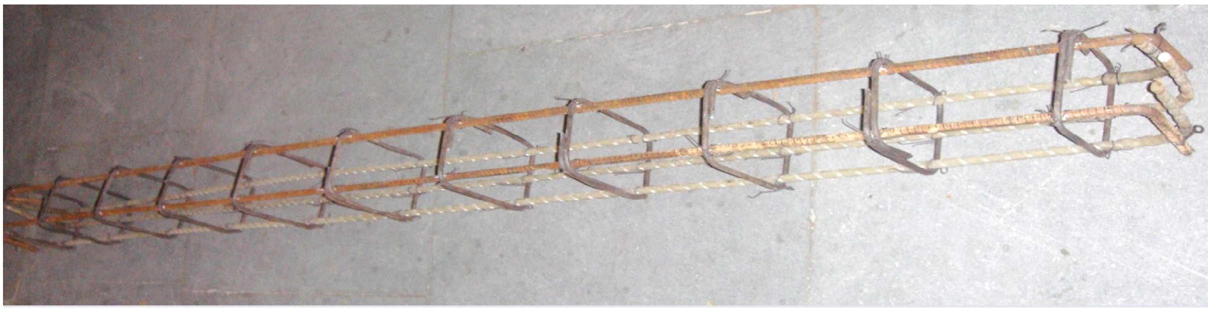

a) Specimen with GFRP as tension reinforcement and mild steel stirrups

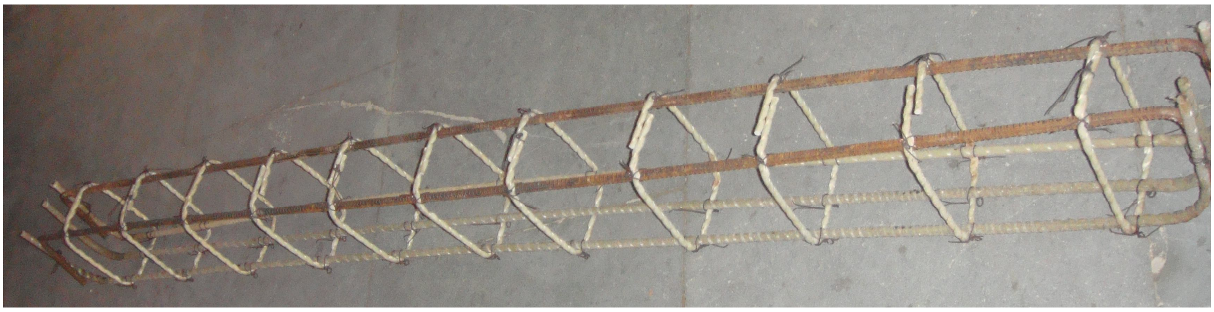

b) Specimen with GFRP as tension reinforcement as well as stirrups

Fig. 4.3 RC beam with FRP reinforcement

4.3 Concrete Mix Proportion

IS code method of concrete mix design has been used. Calculation of mix proportion of concrete for casting of specimens has been made. RC beams have been cast with M25 grade concrete. Details of concrete constituents use for casting of RC beams have been given in Table 4.1.

Table 4.1 Mix proportion for M25 grade concrete

Cement	Sand	Aggregate		Water
1	1.27	2.26		0.45
		20 mm	10 mm	
		1.49	0.77	

4.4 Casting of Beams

Twelve RC beams have been cast to study flexural and shear behaviour of beams at Structures Laboratory, Civil Engineering Department, Nirma University. Available test setup for casting of pre-tensioned PSC beam in laboratory as given in Fig. 4.4 has been used for this purpose. Existing setup is for 3m maximum span of beams. Hence to facilitate casting of 2.1m span modifications are required to be made in setup. Therefore, plates have been fabricated as per details given in Fig. 4.5. Arrangements have been made in such a way that simultaneous casting of two beams is possible.

a) Form-work with modifications

b) concreting of beams in progress

Fig. 4.4 Modified formwork and concreting

Casting of all beams has been conducted M25 grade concrete mix. Mix every batch design of M25 concrete has been prepared in machine of concrete mixture of half bag capacity. Casting of each beam has been conducted in three separate batches. Concrete is placed in layers into moulds as shown in Fig. 4.5.

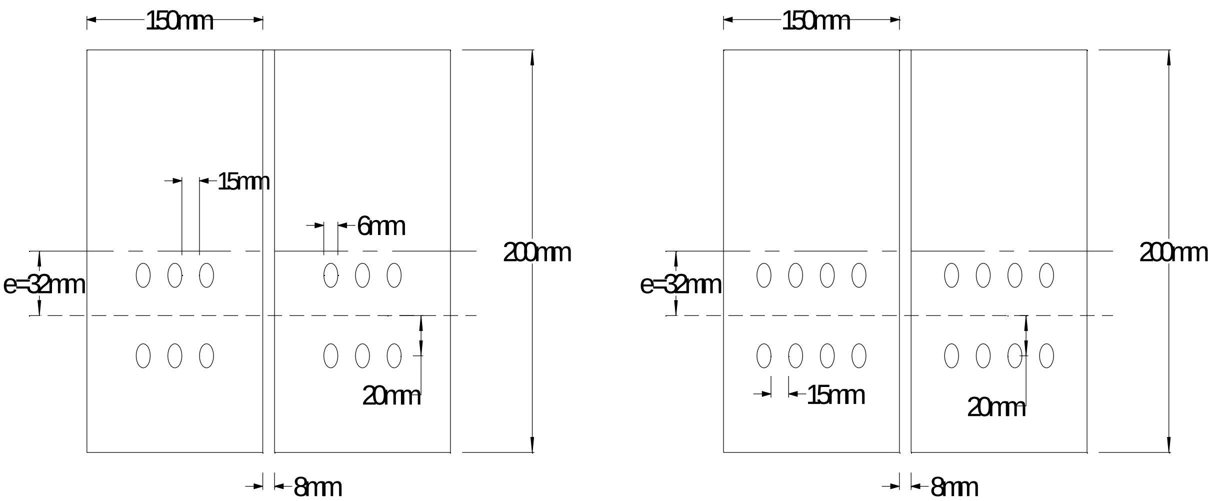

Fig. 4.5 Details of plate fabricated

Thus, total eighteen batches of concreting has been conducted. Three cubes also have been cast to measure compressive strength of concrete during casting of each batch of concrete.

4.4.1 Compressive Strength of Concrete

150mm x 150mm x 150mm cubes have been tested in compression at different ages at the time of actual testing of RC beams. Cubes have been tested at 14 days and at 28 days respectively. Results of concrete compressive strength of concrete have been given in Table 4.2. Curing of concrete cubes and testing under CTM has been presented in Fig. 4.6. Details of compressive strength of concrete cubes have been presented in Fig. 4.7.

a) Curing of concrete cubes

b) Testing of concrete cube in progress

Fig. 4.6 Curing and test setup for concrete cube

Results of concrete compressive strength of concrete have been given in Table 4.2. Curing of concrete cubes and testing under CTM has been presented in Fig.4.6. Compressive strength development of concrete beam is shown as graph in Fig. 4.7.

Table 4.2 Compressive strength of concrete cubes

Beam mark	Compressive strength, (MPa)	
	14 days	28 days
RCB1, RCB2	15.28	28.44
RCB3,RCB4	16.89	29.78
RCB5, RCB6	16.48	28.89
RCB7, RCB8	16.18	29.07
RCB9, RCB10	17.78	31.11
RCB11, RCB12	17.33	30.2

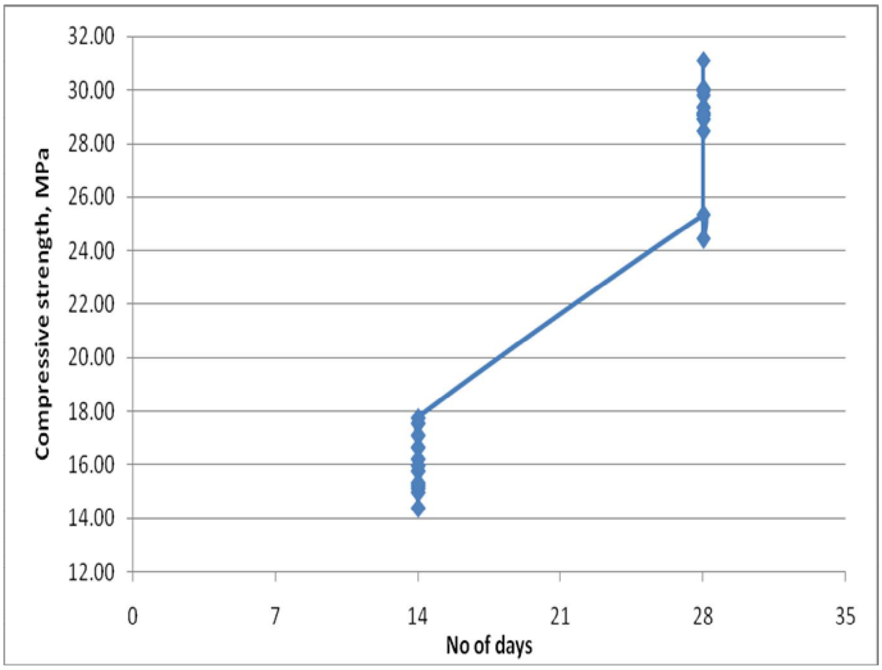

Fig. 4.7 Compressive strength of concrete

4.5 Tension test

Tension test on HYSD and FRP reinforcement has been conducted on Universal Testing Machine at Nirma University.

4.5.1 Objective of test

1. To evaluate Load- strain relationship for HYSD and FRP reinforcements for applying strain compatibility method for beams with combined reinforcement.

2. To compare tensile strength of FRP bars experimentally with value given by a manufacturer.

4.5.2 Specimen and test setup

Test specimen of specified dimensions is required to be prepared for necessary tensile testing. Two bars of HYSD and two bars of FRP have been tested in laboratory. Length of bars has been kept as 600 mm. marking at every 100 mm length has been made. Around 100 mm length of bar has been considered as sufficient to be provided on both sides for proper grip of the specimens. Tensile test setup for FRP reinforcement has been presented in Fig. 4.8 (a).

a) Test setup

b) Extensometer

Fig. 4.8 Tensile test-setup for FRP reinforcement

Extensometer has been used to measure extension as shown in Fig. 4.8 (b). Load has been applied at every 5kN interval and readings on extensometer are recorded. Extensometer has been removed after applying about 70% of expected ultimate load to avoid damages. Sudden failure of FRP reinforcement has been observed. Failure shape of FRP reinforcement has been given in Fig. 4.9. 12 mm diameter HYSD reinforcement also has been tested in the laboratory.

a) Initiation of cracks in specimen

b) Failed FRP bar

Fig. 4.9 Failure shape of FRP reinforcement

4.5.3 Load-strain curve

Load-strain curves both type of reinforcement have been presented has been shown in Fig. 4.10.

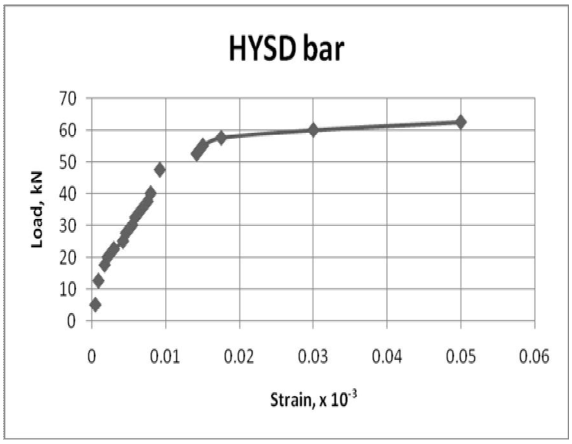

a) Load-strain relationship for HYSD bar

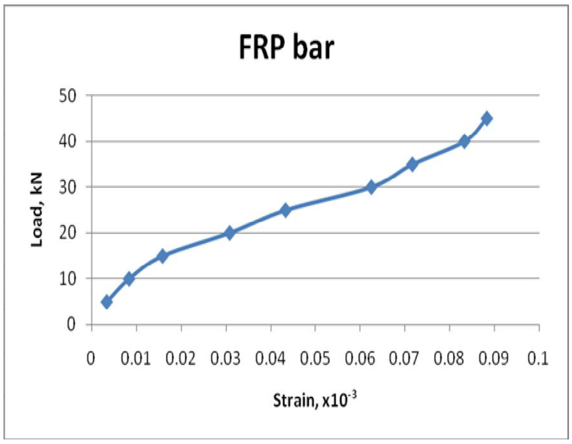

b) Load-strain relationship for FRP bar

Fig.4.10 Load-strain relationship

4.6 Test Setup

Beam specimens have been tested under 2-point loading at loading frame at structures laboratory. Test setup has been presented in Fig. 4.5. The beams have been tested using simple support on either side and are placed using support columns as shown in Fig. 4.11.

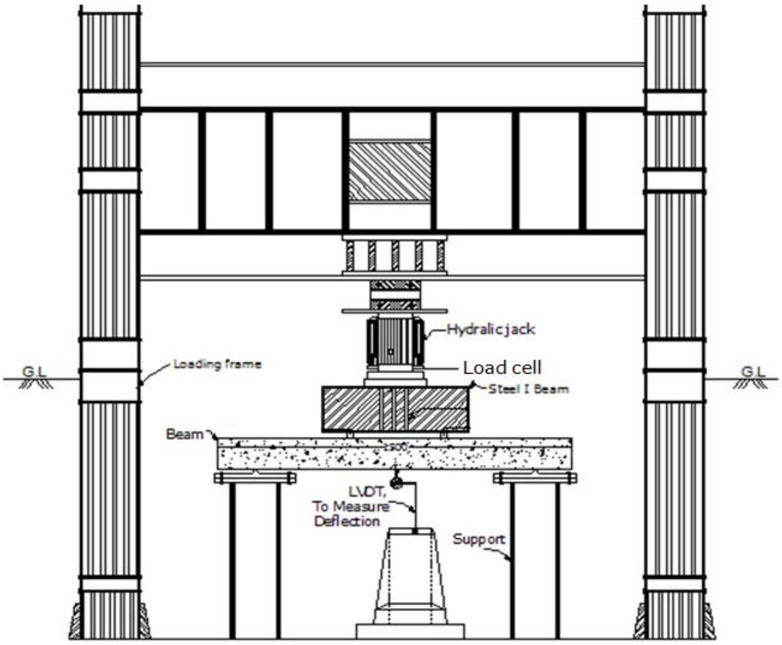

Fig. 4.11 Testing set-up

Following parameters during testing of each specimen:

- Deflection measurement
- Ultimate Failure Load
- Crack and failure patterns
- Strain Measurement

4.7 Instrumentation

To measure different parameters during experiments use of various type of instruments have been required. Different instruments used in experimental work have been as follows:-

1 Hydraulic Jack
2 Deflection dial gauge
3 LVDT (Linear Variable Differential Transducer)
4 Mechanical Strain Gauges

1) Hydraulic Jack

Hydraulic jack of capacity of 500 kN has been used. Jack has been based on Pascal's principle. Pressure is described, mathematically by a Force divided by Area. Therefore, if we assume two cylinders say one smaller and another larger has been connected together. Now, apply force to a smaller cylinder from larger cylinder, and at the end it would result in a given pressure. Hydraulic jack which has been used for the application of loads is given in Fig. 4.12 (a).

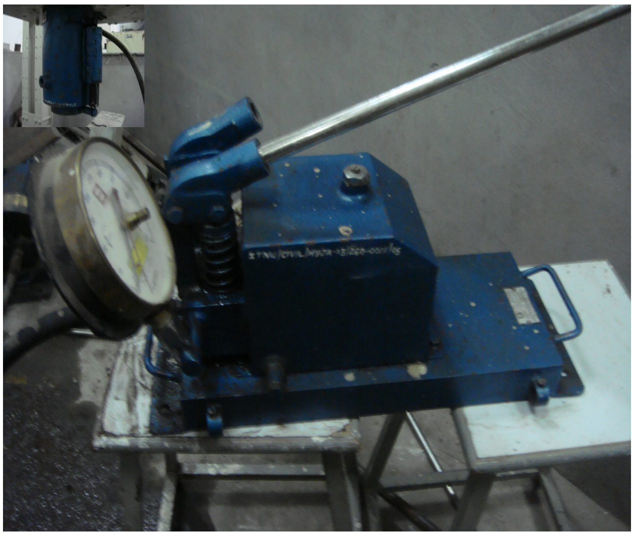

a) Hydraulic Jack

b) Deflection dial gauge

Fig. 4.12 Hydraulic jack and deflection dial gauge

2) Dial gauge

Dial gauge has been used to measure displacement of a beam during load application on it. It has been fitted in such a way that it touched point at which measure of deflection is required. Dial gauge used for above application has been shown in Fig.4.12 (b).

3) LVDT (Linear Variable Differential Transducer)

LVDT has been used to evaluate displacement for RC Beam during application of load on it. LVDT has been attached at a position where deflection is required to be measured for beam. LVDT sensor's principle is that there is no electrical contact across transducer. Position of sensing element is to be set from where user of sensor means to get data, it has infinite resolution and a very long life.

a) LVDT

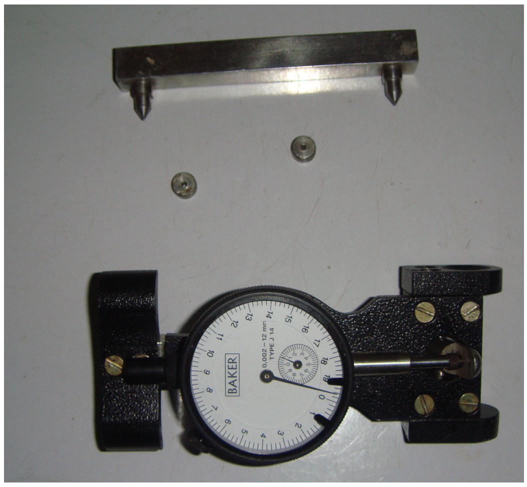

b) Mechanical strain gauge

Fig 4.13 LVDT and Mechanical strain gauge instrument

4 Mechanical Strain Gauges

Mechanical strain gauges which are also known as DEMEC (Demountable Mechanical) strain gauges. DEMEC gauges consist of an analogue dial gauge attached to an Invar bar. A fixed conical point is mounted at one end of bar. A moving conical point is mounted on a knife edge pivot at opposite end. Pivoting movement of second conical point is measured by dial gauge. A setting out bar is used to position pre-drilled stainless steel discs attached to beam using a suitable adhesive. In this way, strain changes in beam are converted into a change in reading on dial gauge. Instruments of mechanical strain gauge setup have been given in Fig. 4.13(b).

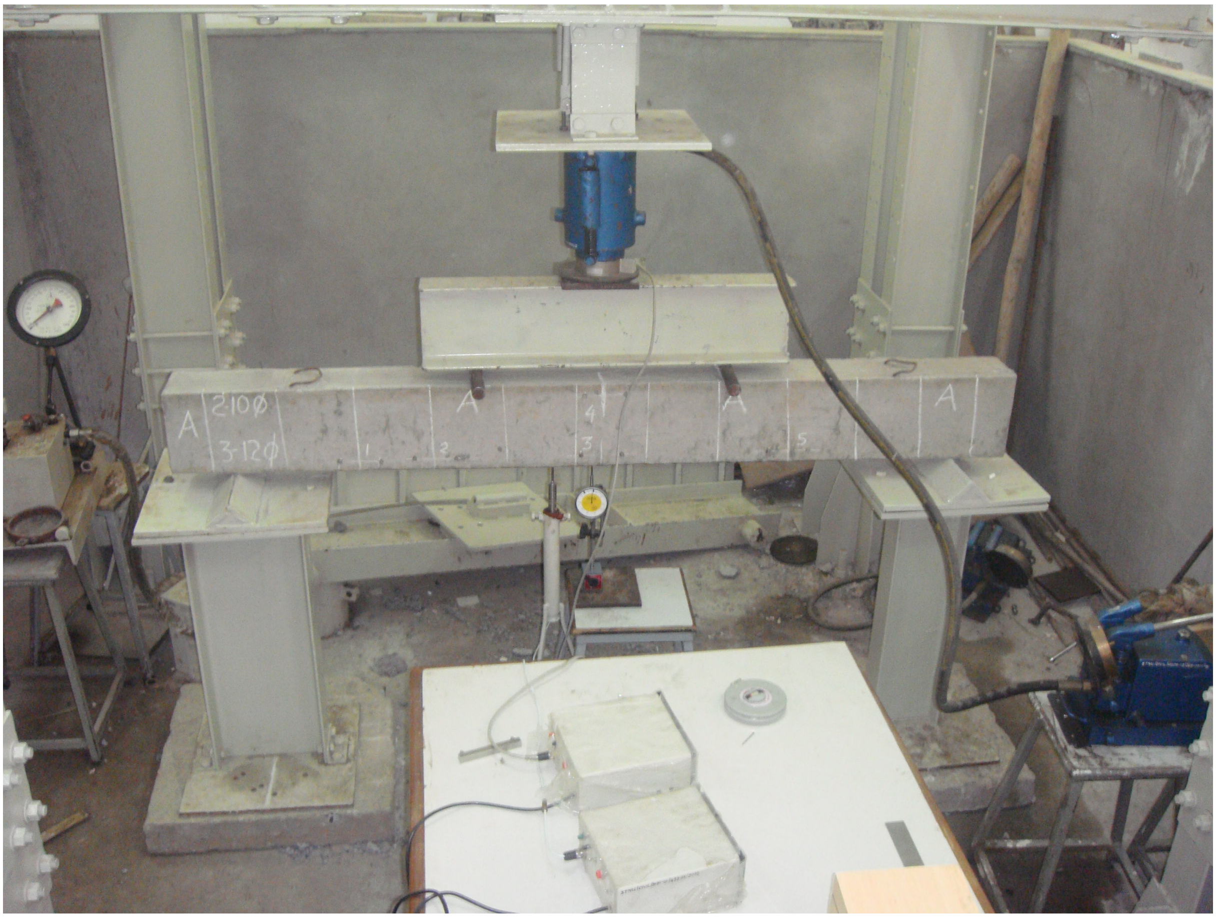

Fig. 4.14 Complete test Setup with RC beam.

Complete test-setup with RC beam placed on supporting steel column has been presented in Fig. 4.14.

5. RESULTS OF EXPERIMENT

5.1 General

Results obtained and observations made during testing of beams under two point load has been discussed in this chapter. All beams have been subjected to two point loading. Different results have been recorded as follow.

- Failure load
- Deflection
- Strain at different positions
- Shear strength

These parameters are essential to understand behaviour of RC beams having different types of reinforcements. Bending and deflection can be clearly visible during testing of specimens.

5.2 Failure Load

Table 5.1 gives the values of failure loads for all specimens; it shows average experimental failure load. Experimental failure loads have been measured from hydraulic jack dial gauge.

Table 5.1- Failure load for all beam specimens

Specimen No.	Specimen Type	Experimental Failure Load (kN)	Avg. Experimental Load (kN)
RCB1	HYSD-MS	108	106
RCB2	HYSD-MS	104	
RCB3	Mix-MS	144	135
RCB4	Mix-MS	126	
RCB5	GFRP-MS	100	96
RCB6	GFRP-MS	92	
RCB7	HYSD-GFS	124	120
RCB8	HYSD-GFS	116	
RCB9	Mix-GFS	148	145
RCB10	Mix-GFS	142	
RCB11	GFRP-GFS	94	93
RCB12	GFRP-GFS	92	

5.3 Moment Capacity

Moment capacity has been calculated using experimentally obtained failure loads as follows

W= (Avg. failure load/2)

l = Length of RC beam = 2.1 m

1. RC beam reinforced with HYSD reinforcement and mild steel stirrups (RCB1 and RCB2, HYSD-MS)

   As average failure load (2W) = 106 kN, Therefore W= 53 kN.

   Moment capacity = (W x l)/6

   = (53 x 2.1)/6

   = 18.55 kNm

2. RC beam using combined reinforcement and mild steel stirrups (RCB3 and RCB4, Mix-MS)

   As average failure load (2W) = 135 kN, Therefore W= 67.5 kN.

   Moment capacity = (W x l)/6

   = (67.5 x 2.1)/6

   = 23.63 kNm

3. RC beam using FRP reinforcement and mild steel stirrups (RCB5 and RCB6, GFRP-MS)

   As average failure load (2W) = 96 kN, Therefore W= 48 kN.

   Moment capacity = (W x l)/6

   = (48 x 2.1)/6

   = 16.80 kNm

4. For RC beam reinforced with HYSD reinforcement and GFRP stirrups (RCB7 and RCB8, HYSD-GFS)

   Average failure load (2W) = 120 kN, Therefore W= 60 kN.

   Moment capacity = (W x l)/6

   = (60 x 2.1)/6

   = 21.00 kNm

5. RC beam using combined reinforcement and GFRP stirrups (RCB9 and RCB10, Mix-GFS)

Average failure load (2W) = 145 kN. Therefore W= 72.5 kN.

Moment capacity = (W x l)/6

= (72.5 x 2.1)/6

= 25.38 kNm

6. RC beam using FRP reinforcement and GFRP stirrups (RCB11 and RCB12, GFRP-MS)

Average failure load (2W) = 93 kN. Therefore W= 46.5 kN.

Moment capacity = (W x l)/6

= (46.5 x 2.1)/6

= 16.28 kNm

Moment capacities for all specimens have been summarized in Table 5.2

Table 5.2 Moment capacities for all beams

Specimen no.	Specimen Type	Moment capacity from experimental loads (kNm)
RCB1, RCB2	HYSD-MS	18.55
RCB3, RCB4	Mix-MS	23.63
RCB5, RCB6	GFRP-MS	16.80
RCB7, RCB8	HYSD-GFS	21.00
RCB9, RCB10	Mix-GFS	25.38
RCB11, RCB12	GFRP-GFS	16.28

5.4 Shear Strength

Shear strength of RC beams have been computed as per experimental load has been shown in below Table 5.3

Table 5.3 Shear strength for all beam specimens

Specimen no.	Specimen Type	Shear strength from experimental loads (kN)
RCB1, RCB2	HYSD-MS	53
RCB3, RCB4	Mix-MS	67.5
RCB5, RCB6	GFRP-MS	48
RCB7, RCB8	HYSD-GFS	60
RCB9, RCB10	Mix-GFS	72.5
RCB11, RCB12	GFRP-GFS	46.5

5.5 Deflection

Table 5.4 Load-deflection relationship for all beams

Load	RCB1	RCB2	RCB3	RCB4	RCB5	RCB6	RCB7	RCB8	RCB9	RCB10	RCB11	RCB12
	HYSD-MS	HYSD-MS	Mix-MS	Mix-MS	GFRP-MS	GFRP-MS	HYSD-GFS	HYSD-GFS	Mix-GFS	Mix-GFS	GFRP-GFS	GFRP-GFS
0	0.00	0.00	0.00	0.00	0.00	0.00	0.00	0.00	0.00	0.00	0.00	0.00
5	0.22	0.20	0.80	0.68	1.28	0.40	0.36	0.31	0.24	0.33	0.42	0.53
10	0.41	0.67	1.74	1.10	4.45	2.05	0.69	0.70	0.42	0.95	2.40	1.10
15	0.73	1.29	2.10	1.80	6.74	3.75	1.29	1.04	0.73	1.30	5.92	2.77
20	1.14	1.80	2.80	2.92	8.15	7.10	1.64	1.50	1.17	1.84	9.66	6.25
25	1.74	2.49	3.51	3.32	9.95	10.8	2.20	2.05	1.76	2.26	12.79	9.10
30	2.20	3.04	4.15	3.88	15.00	14.6	2.62	2.59	2.20	2.99	15.00	12.90
35	3.48	3.78	5.00	4.44	17.14	18.4	3.29	3.11	2.78	3.54	17.29	18.68
40	4.11	4.32	5.60	5.78	18.90	21.00	3.87	3.86	3.48	4.94	22.30	20.75
45	4.83	4.74	6.24	6.72	21.70	23.10	4.36	4.44	4.11	5.21	23.65	21.52
50	5.55	5.73	7.34	7.96	24.35	27.40	5.01	4.96	4.83	5.58	29.95	24.10
55	6.12	6.68	8.60	9.23	26.70	29.61	5.67	5.64	5.55	7.27	31.38	27.40
60	6.64	7.27	11.21	11.30	29.22	32.59	6.44	6.26	6.12	8.45	34.20	30.54
65	7.27	8.13	13.50	14.42	31.74	35.58	6.95	7.96	6.64	9.80	37.27	33.38
70	8.05	8.83	15.81	17.32	34.25	38.56	7.63	8.90	7.27	10.90	40.34	36.21
75	8.95	10.99	17.74	21.33	36.77	41.55	8.31	10.01	8.05	11.29	43.41	39.05
80	9.94	11.10	18.44	23.55	39.29	44.53	9.20	10.79	8.95	12.52	46.49	41.89
85	11.40	12.35	19.38	28.42	41.80	47.52	10.40	11.30	9.94	13.22	49.56	44.73
90	12.75	13.11	21.19	28.50	44.32	50.50	11.08	12.94	10.40	13.65	-	-
95	14.80	15.70	22.22	28.61	-	-	13.53	13.00	10.75	14.48	-	-
100	18.95	17.40	23.25	28.72	-	-	14.00	13.29	11.45	15.32	-	-
105	-	-	24.57	30.42	-	-	14.03	14.03	12.09	16.16	-	-
110	-	-	25.88	32.13	-	-	14.76	14.76	12.72	17.00	-	-
115	-	-	27.20	33.83	-	-	15.50	15.50	13.35	17.83	-	-
120	-	-	28.51	35.54	-	-	16.24	16.24	13.98	18.67	-	-
125	-	-	29.82	-	-	-	16.98	16.98	14.61	19.51	-	-
130	-	-	31.14	-	-	-	17.71	17.71	15.24	20.35	-	-

Details of corresponding deflection with respect to measured load for all beams have been presented in Table 5.4

5.6 Strain

Strain at various positions for reinforced concrete beams has been measured using mechanical strain gauges. Strain has been measured at various positions as presented in Fig. 5.1. Strain gauges have been fixed at different positions on beam surfaces described below using quick setting hardener as explained below.

1. Shear tension zone of point load 1 (at stirrup no. 3) – Position 1
2. Near point load 1 in tension zone (at stirrup no. 4) – Position 2
3. At center of span in tension zone – Position 3
4. At center of span in compression zone – Position 4
5. Near point load 2 in tension zone (at stirrup no. 8) – Position 5
6. Shear tension zone of point load 2 (at stirrups no. 9) – Position 6

Values of strain measured for all above positions have been presented in Tables 5.5, 5.6, 5.7, 5.8, 5.9 and 5.10 respectively.

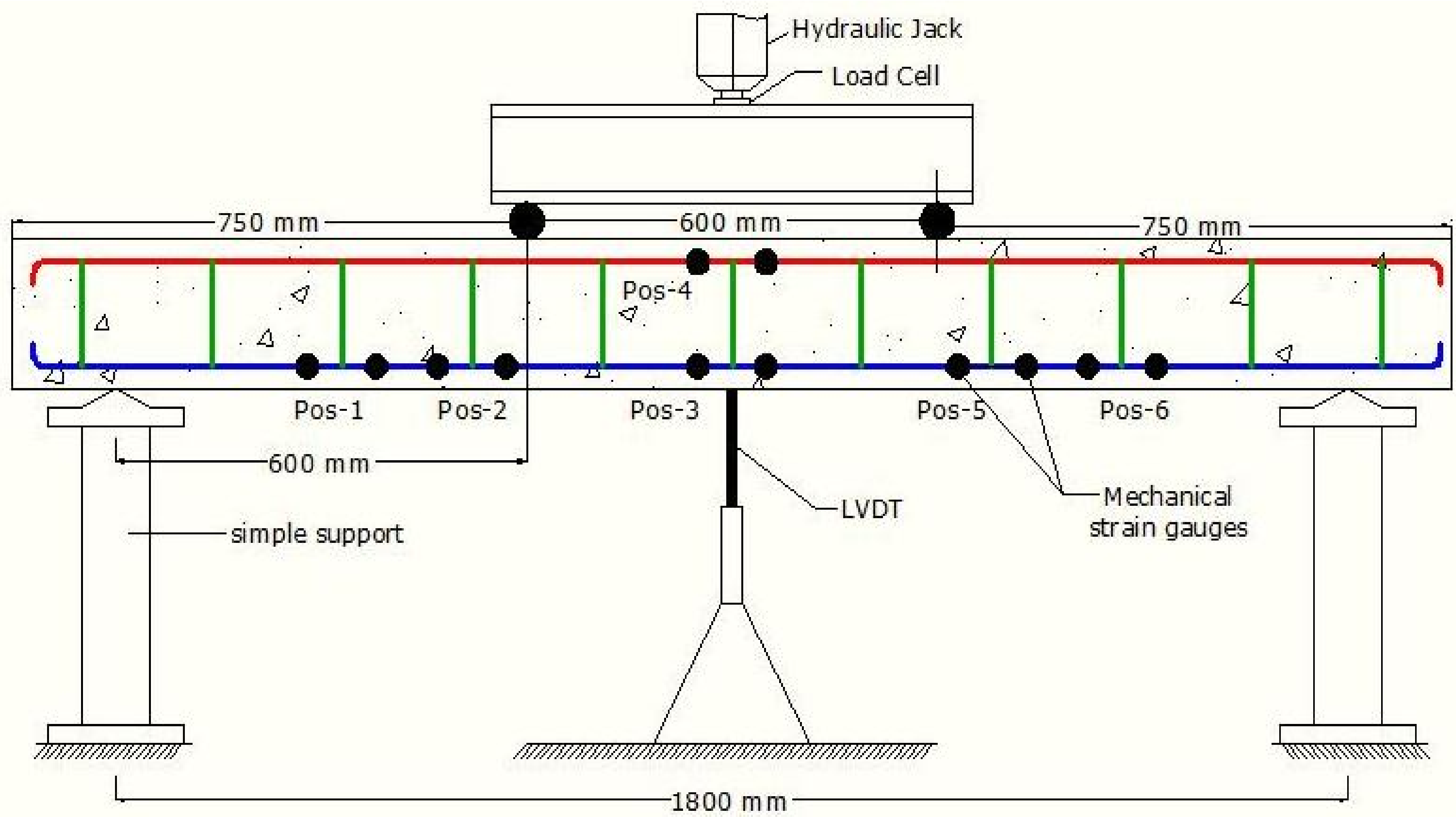

Pos- Position

Fig. 5.1 Position of strain gauges

Table 5.5 Strain position 1 (shear tension zone of point load 1 at stirrup no. 3)

Load	RCB1	RCB2	RCB3	RCB4	RCB5	RCB6	RCB7	RCB8	RCB9	RCB10	RCB11	RCB12
(kN)	HYSD-MS	HYSD-MS	Mix-MS	Mix-MS	GFRP-MS	GFRP-MS	HYSD-GFS	HYSD-GFS	Mix-GFS	Mix-GFS	GFRP-GFS	GFRP-GFS
0	0.0000	0.0000	0.0000	0.0002	0.0000	0.0000	0.0000	0.0002	0.0000	0.0000	0.0006	0.0010
5	0.0000	0.0000	0.0002	0.0006	0.0004	0.0002	0.0012	0.0004	0.0002	0.0000	0.0022	0.0022
10	0.0000	0.0002	0.0002	0.0010	0.0008	0.0006	0.0022	0.0010	0.0004	0.0008	0.0034	0.0038
15	0.0000	0.0002	0.0004	0.0016	0.0012	0.0012	0.0018	0.0014	0.0010	0.0020	0.0038	0.0064
20	0.0002	0.0004	0.0006	0.0020	0.0020	0.0020	0.0022	0.0016	0.0010	0.0022	0.0042	0.0070
25	0.0004	0.0006	0.0008	0.0022	0.0040	0.0028	0.0028	0.0018	0.0024	0.0022	0.0044	0.0072
30	0.0004	0.0014	0.0012	0.0030	0.0070	0.0036	0.0032	0.0020	0.0038	0.0030	0.0068	0.0076
35	0.0006	0.0006	0.0012	0.0038	0.0076	0.0046	0.0032	0.0024	0.0054	0.0034	0.0088	0.0098
40	0.0010	0.0014	0.0016	0.0044	0.0080	0.0054	0.0036	0.0034	0.0062	0.0032	0.0100	0.0114
45	0.0010	0.0012	0.0018	0.0050	0.0088	0.0062	0.0032	0.0038	0.0064	0.0034	0.0118	0.0118
50	0.0016	0.0022	0.0020	0.0060	0.0106	0.0067	0.0032	0.0040	0.0076	0.0040	0.0130	0.0124
55	0.0018	0.0028	0.0020	0.0068	0.0118	0.0075	0.0036	0.0048	0.0074	0.0042	0.0138	0.0144
60	0.0024	0.0040	0.0034	0.0078	0.0130	0.0082	0.0044	0.0060	0.0076	0.0046	0.0151	0.0156
65	0.0026	0.0050	0.0036	0.0084	0.0142	0.0090	0.0048	0.0072	0.0086	0.0054	0.0164	0.0168
70	0.0026	0.0074	0.0044	0.0096	0.0154	0.0097	0.0066	0.0082	0.0092	0.0060	0.0176	0.0180
75	0.0028	0.0076	0.0040	0.0110	0.0166	0.0105	0.0084	0.0090	0.0100	0.0062	0.0189	0.0191
80	0.0030	0.0082	0.0036	0.0112	0.0178	0.0112	0.0110	0.0096	0.0106	0.0068	0.0201	0.0203
85	0.0030	0.0078	0.0044	0.0115	0.0191	0.0119	0.0114	0.0100	0.0108	0.0074	0.0214	0.0215
90	0.0032	0.0074	0.0048	0.0123	0.0203	0.0127	0.0106	0.0103	0.0114	0.0076	-	-
95	0.0034	0.0068	0.0051	0.0130	0.0215	0.0134	0.0112	0.0109	0.0129	0.0080	-	-
100	0.0042	-	0.0054	0.0137	0.0227	0.0142	0.0119	0.0115	0.0136	0.0084	-	-
105	-	-	0.0057	0.0145	-	-	0.0125	0.0122	0.0143	0.0088	-	-
110	-	-	0.0060	0.0152	-	-	0.0132	0.0128	0.0151	0.0093	-	-
115	-	-	0.0063	0.0159	-	-	0.0139	0.0134	0.0158	0.0097	-	-
120	-	-	0.0066	0.0166	-	-	0.0145	0.0141	0.0165	0.0101	-	-
125	-	-	0.0069	-	-	-	0.0152	0.0147	-	-	-	-
130	-	-	0.0072	-	-	-	0.0158	-	-	-	-	-

Table 5.6 - Strain position 2 (Near point load 1 in tension zone at stirrup no. 4)

Load	RCB1	RCB2	RCB3	RCB4	RCB5	RCB6	RCB7	RCB8	RCB9	RCB10	RCB11	RCB12
(kN)	HYSD-MS	HYSD-MS	Mix-MS	Mix-MS	GFRP-MS	GFRP-MS	HYSD-GFS	HYSD-GFS	Mix-GFS	Mix-GFS	GFRP-GFS	GFRP-GFS
0	0.0000	0.0000	0.0002	0.0002	0.0000	0.0000	0.0000	0.0000	0.0000	0.0002	0.0000	0.0008
5	0.0002	0.0000	0.0010	0.0006	0.0000	0.0008	0.0006	0.0002	0.0002	0.0002	0.0004	0.0018
10	0.0004	0.0002	0.0016	0.0010	0.0004	0.0014	0.0016	0.0002	0.0002	0.0006	0.0012	0.0022
15	0.0006	0.0002	0.0022	0.0012	0.0004	0.0026	0.0004	0.0012	0.0008	0.0010	0.0016	0.0030
20	0.0008	0.0000	0.0042	0.0014	0.0008	0.0032	0.0004	0.0006	0.0010	0.0012	0.0028	0.0040
25	0.0014	0.0000	0.0054	0.0016	0.0016	0.0038	0.0008	0.0012	0.0014	0.0014	0.0034	0.0048
30	0.0018	0.0002	0.0072	0.0020	0.0020	0.0039	0.0014	0.0032	0.0028	0.0020	0.0042	0.0058
35	0.0020	0.0012	0.0078	0.0028	0.0024	0.0043	0.0020	0.0046	0.0036	0.0028	0.0054	0.0060
40	0.0028	0.0008	0.0092	0.0032	0.0028	0.0054	0.0040	0.0046	0.0048	0.0030	0.0062	0.0068
45	0.0032	0.0016	0.0096	0.0038	0.0036	0.0054	0.0044	0.0046	0.0052	0.0030	0.0076	0.0070
50	0.0036	0.0012	0.0102	0.0044	0.0038	0.0065	0.0044	0.0060	0.0062	0.0040	0.0085	0.0076
55	0.0046	0.0018	0.0110	0.0050	0.0042	0.0071	0.0044	0.0062	0.0068	0.0044	0.0090	0.0088
60	0.0052	0.0012	0.0122	0.0056	0.0046	0.0078	0.0064	0.0080	0.0068	0.0048	0.0099	0.0075
65	0.0054	0.0006	0.0126	0.0060	0.0050	0.0084	0.0066	0.0084	0.0074	0.0054	0.0108	0.0082
70	0.0062	0.0024	0.0140	0.0070	0.0055	0.0090	0.0072	0.0110	0.0082	0.0064	0.0117	0.0089
75	0.0066	0.0024	0.0146	0.0080	0.0059	0.0096	0.0080	0.0130	0.0086	0.0068	0.0125	0.0096
80	0.0082	0.0026	0.0158	0.0086	0.0063	0.0103	0.0100	0.0132	0.0092	0.0080	0.0134	0.0103
85	0.0090	0.0034	0.0170	0.0085	0.0068	0.0109	0.0096	0.0132	0.0100	0.0090	0.0143	0.0110
90	0.0102	0.0040	0.0186	0.0090	0.0072	0.0115	0.0101	0.0141	0.0102	0.0085	-	-
95	0.0122	0.0048	0.0192	0.0096	0.0076	0.0121	0.0108	0.0150	0.0113	0.0090	-	-
100	-	-	0.0202	0.0101	0.0080	0.0128	0.0114	0.0159	0.0120	0.0095	-	-
105	-	-	0.0212	0.0106	-	-	0.0121	0.0168	0.0126	0.0101	-	-
110	-	-	0.0222	0.0112	-	-	0.0127	0.0177	0.0133	0.0106	-	-
115	-	-	0.0232	0.0117	-	-	0.0134	0.0186	0.0139	0.0111	-	-
120	-	-	0.0243	0.0122	-	-	0.0140	0.0195	0.0145	0.0116	-	-
125	-	-	0.0253	-	-	-	0.0146	0.0205	-	-	-	-
130	-	-	0.0263	-	-	-	0.0153	-	-	-	-	-

Table 5.7 Strain position 3 (at center of span in tension zone)

Load	RCB1	RCB2	RCB3	RCB4	RCB5	RCB6	RCB7	RCB8	RCB9	RCB10	RCB11	RCB12
(kN)	HYSD-MS	HYSD-MS	Mix-MS	Mix-MS	GFRP-MS	GFRP-MS	HYSD-GFS	HYSD-GFS	Mix-GFS	Mix-GFS	GFRP-GFS	GFRP-GFS
0	0.0000	0.0000	0.0000	0.0004	0.0008	0.0000	0.0000	0.0002	0.0000	0.0008	0.0001	0.0006
5	0.0000	0.0000	0.0002	0.0010	0.0012	0.0008	0.0006	0.0002	0.0000	0.0004	0.0002	0.0014
10	0.0000	0.0004	0.0002	0.0014	0.0012	0.0012	0.0016	0.0004	0.0000	0.0016	0.0012	0.0016
15	0.0002	0.0000	0.0008	0.0018	0.0018	0.0014	0.0024	0.0008	0.0002	0.0028	0.0024	0.0028
20	0.0004	0.0002	0.0012	0.0020	0.0018	0.0022	0.0036	0.0016	0.0004	0.0036	0.0020	0.0032
25	0.0008	0.0006	0.0018	0.0022	0.0018	0.0028	0.0046	0.0028	0.0008	0.0042	0.0026	0.0036
30	0.0016	0.0016	0.0032	0.0030	0.0022	0.0026	0.0048	0.0030	0.0016	0.0048	0.0030	0.0040
35	0.0016	0.0014	0.0038	0.0038	0.0022	0.0036	0.0050	0.0032	0.0016	0.0058	0.0032	0.0052
40	0.0018	0.0022	0.0050	0.0044	0.0028	0.0047	0.0051	0.0042	0.0018	0.0060	0.0036	0.0052
45	0.0022	0.0022	0.0054	0.0050	0.0030	0.0052	0.0054	0.0042	0.0022	0.0064	0.0038	0.0056
50	0.0028	0.0022	0.0062	0.0058	0.0032	0.0056	0.0062	0.0046	0.0028	0.0068	0.0046	0.0064
55	0.0030	0.0022	0.0066	0.0068	0.0034	0.0061	0.0074	0.0046	0.0030	0.0076	0.0049	0.0070
60	0.0038	0.0026	0.0076	0.0074	0.0037	0.0067	0.0086	0.0050	0.0038	0.0082	0.0053	0.0076
65	0.0044	0.0032	0.0082	0.0080	0.0039	0.0073	0.0086	0.0054	0.0038	0.0088	0.0058	0.0082
70	0.0046	0.0038	0.0090	0.0088	0.0041	0.0078	0.0090	0.0058	0.0044	0.0096	0.0062	0.0088
75	0.0060	0.0046	0.0100	0.0100	0.0044	0.0084	0.0096	0.0064	0.0046	0.0100	0.0067	0.0093
80	0.0066	0.0054	0.0110	0.0120	0.0046	0.0090	0.0100	0.0066	0.0060	0.0106	0.0071	0.0099
85	0.0084	0.0046	0.0124	0.0112	0.0048	0.0095	0.0104	0.0074	0.0066	0.0112	0.0076	0.0105
90	0.0102	0.0042	0.0136	0.0119	0.0051	0.0101	0.0116	0.0078	0.0084	0.0121	-	-
95	0.0124	0.0052	0.0134	0.0126	0.0053	0.0107	0.0122	0.0083	0.0073	0.0127	-	-
100	-	-	0.0141	0.0133	0.0056	0.0112	0.0128	0.0087	0.0077	0.0133	-	-
105	-	-	0.0149	0.0140	-	-	0.0134	0.0091	0.0082	0.0140	-	-
110	-	-	0.0157	0.0147	-	-	0.0140	0.0096	0.0086	0.0146	-	-
115	-	-	0.0165	0.0154	-	-	0.0147	0.0100	0.0091	0.0152	-	-
120	-	-	0.0172	0.0161	-	-	0.0153	0.0105	0.0095	0.0159	-	-
125	-	-	0.0180	-	-	-	0.0159	0.0109	-	-	-	-
130	-	-	0.0188	-	-	-	0.0165	-	-	-	-	-

Table 5.8 Strain position 4 (at center of span in compression zone)

Load (kN)	RCB1 HYSD-MS	RCB2 HYSD-MS	RCB3 Mix-MS	RCB4 Mix-MS	RCB5 GFRP-MS	RCB6 GFRP-MS	RCB7 HYSD-GFS	RCB8 HYSD-GFS	RCB9 Mix-GFS	RCB10 Mix-GFS	RCB11 GFRP-GFS	RCB12 GFRP-GFS
0	0.0000	0.0006	0.0000	0.0000	0.0000	0.0000	0.0000	0.0000	0.0002	0.0000	-0.0008	-0.0004
5	0.0000	0.0006	0.0000	-0.0002	0.0000	-0.0008	-0.0002	0.0000	0.0002	-0.0002	-0.0014	-0.0012
10	-0.0004	0.0008	-0.0002	-0.0002	-0.0004	-0.0008	0.0000	-0.0008	-0.0004	-0.0006	-0.0016	-0.0036
15	-0.0008	0.0008	0.0004	0.0002	-0.0004	-0.0002	0.0004	-0.0004	-0.0008	-0.0014	-0.0016	-0.0032
20	-0.0008	0.0004	0.0008	0.0006	-0.0004	0.0000	-0.0004	-0.0010	-0.0008	-0.0012	-0.0010	-0.0032
25	-0.0006	0.0004	0.0008	0.0006	-0.0012	-0.0008	-0.0004	-0.0004	-0.0006	-0.0010	-0.0018	-0.0012
30	-0.0006	0.0000	0.0000	0.0004	-0.0012	-0.0008	-0.0004	-0.0008	-0.0008	-0.0014	-0.0026	-0.0020
35	-0.0006	-0.0004	-0.0004	0.0000	-0.0014	-0.0010	0.0000	-0.0006	-0.0008	-0.0016	-0.0030	-0.0012
40	-0.0008	-0.0002	-0.0008	-0.0002	-0.0014	-0.0014	-0.0004	-0.0014	-0.0010	-0.0020	-0.0038	-0.0022
45	-0.0018	-0.0004	-0.0008	-0.0004	-0.0018	-0.0020	0.0004	-0.0016	-0.0014	-0.0022	-0.0034	-0.0032
50	-0.0018	-0.0008	-0.0010	-0.0008	-0.0020	-0.0023	0.0000	-0.0004	-0.0018	-0.0018	-0.0036	-0.0052
55	-0.0014	-0.0008	-0.0008	-0.0008	-0.0023	-0.0025	-0.0006	-0.0008	-0.0014	-0.0020	-0.0044	-0.0077
60	-0.0008	-0.0006	-0.0014	-0.0016	-0.0025	-0.0028	-0.0012	-0.0010	-0.0008	-0.0024	-0.0047	-0.0085
65	-0.0014	-0.0010	-0.0018	-0.0024	-0.0027	-0.0031	-0.0008	-0.0010	-0.0012	-0.0020	-0.0051	-0.0094
70	-0.0016	-0.0012	-0.0022	-0.0034	-0.0029	-0.0033	-0.0016	-0.0018	-0.0016	-0.0022	-0.0054	-0.0103
75	-0.0018	-0.0014	-0.0028	-0.0048	-0.0032	-0.0036	-0.0016	-0.0020	-0.0018	-0.0026	-0.0058	-0.0111
80	-0.0016	-0.0014	-0.0036	-0.0060	-0.0034	-0.0039	-0.0013	-0.0018	-0.0016	-0.0030	-0.0061	-0.0120
85	-0.0016	-0.0012	-0.0040	-0.0054	-0.0036	-0.0041	-0.0013	-0.0022	-0.0016	-0.0036	-0.0065	-0.0129
90	-0.0016	-0.0016	-0.0046	-0.0059	-0.0038	-0.0044	-0.0020	-0.0025	-0.0016	-0.0035	-	-
95	-0.0014	-0.0020	-0.0043	-0.0063	-	-	-0.0021	-0.0026	-0.0023	-0.0037	-	-
100	-0.0012	-	-0.0046	-0.0068	-	-	-0.0023	-0.0028	-0.0024	-0.0039	-	-
105	-	-	-0.0049	-0.0073	-	-	-0.0025	-0.0029	-0.0025	-0.0040	-	-
110	-	-	-0.0053	-0.0078	-	-	-0.0026	-0.0031	-0.0027	-0.0042	-	-
115	-	-	-0.0056	-0.0082	-	-	-0.0028	-0.0032	-0.0028	-0.0044	-	-
120	-	-	-0.0059	-0.0087	-	-	-0.0029	-0.0034	-0.0029	-0.0046	-	-
125	-	-	-0.0062	-	-	-	-0.0031	-0.0035	-	-	-	-
130	-	-	-0.0065	-	-	-	-0.0032	-	-	-	-	-

Table 5.9 Strain position 5 (near point load 2 in tension zone, at stirrup no. 8)

Load	RCB1	RCB2	RCB3	RCB4	RCB5	RCB6	RCB7	RCB8	RCB9	RCB10	RCB11	RCB12
(kN)	HYSD-MS	HYSD-MS	Mix-MS	Mix-MS	GFRP-MS	GFRP-MS	HYSD-GFS	HYSD-GFS	Mix-GFS	Mix-GFS	GFRP-GFS	GFRP-GFS
0	0.0000	0.0000	0.0000	0.0000	0.0008	0.0004	0.0004	0.0002	0.0000	0.0002	0.0014	0.0002
5	0.0006	0.0004	0.0004	0.0000	0.0038	0.0014	0.0010	0.0004	0.0008	0.0000	0.0032	0.0008
10	0.0018	0.0006	0.0004	0.0002	0.0020	0.0020	0.0012	0.0004	0.0018	0.0004	0.0044	0.0014
15	0.0008	0.0006	0.0008	0.0006	0.0010	0.0026	0.0024	0.0006	0.0010	0.0010	0.0050	0.0024
20	0.0012	0.0010	0.0014	0.0008	0.0052	0.0038	0.0032	0.0010	0.0012	0.0014	0.0060	0.0034
25	0.0006	0.0018	0.0018	0.0010	0.0072	0.0046	0.0044	0.0010	0.0006	0.0020	0.0084	0.0040
30	0.0018	0.0022	0.0022	0.0018	0.0104	0.0058	0.0052	0.0012	0.0018	0.0024	0.0106	0.0048
35	0.0022	0.0024	0.0024	0.0020	0.0136	0.0068	0.0056	0.0012	0.0022	0.0032	0.0116	0.0060
40	0.0032	0.0026	0.0030	0.0028	0.0136	0.0074	0.0066	0.0014	0.0032	0.0034	0.0132	0.0068
45	0.0034	0.0028	0.0034	0.0038	0.0146	0.0086	0.0066	0.0018	0.0034	0.0032	0.0142	0.0072
50	0.0034	0.0034	0.0038	0.0046	0.0177	0.0089	0.0070	0.0018	0.0034	0.0036	0.0172	0.0080
55	0.0038	0.0038	0.0044	0.0056	0.0197	0.0098	0.0074	0.0026	0.0038	0.0040	0.0179	0.0090
60	0.0050	0.0046	0.0056	0.0068	0.0216	0.0108	0.0078	0.0028	0.0050	0.0040	0.0195	0.0098
65	0.0054	0.0050	0.0062	0.0078	0.0235	0.0117	0.0080	0.0030	0.0052	0.0048	0.0210	0.0106
70	0.0058	0.0058	0.0072	0.0090	0.0254	0.0126	0.0080	0.0036	0.0054	0.0050	0.0225	0.0114
75	0.0056	0.0058	0.0082	0.0104	0.0273	0.0135	0.0082	0.0044	0.0058	0.0050	0.0241	0.0123
80	0.0070	0.0062	0.0086	0.0099	0.0292	0.0144	0.0102	0.0054	0.0056	0.0054	0.0256	0.0131
85	0.0102	0.0066	0.0086	0.0107	0.0311	0.0153	0.0108	0.0054	0.0070	0.0054	0.0272	0.0139
90	0.0106	0.0072	0.0094	0.0114	0.0331	0.0163	0.0114	0.0052	0.0102	0.0058	-	-
95	0.0112	0.0078	0.0098	0.0122	0.0350	0.0172	0.0120	0.0056	0.0085	0.0066	-	-
100	-	-	0.0103	0.0129	0.0369	0.0181	0.0126	0.0059	0.0090	0.0069	-	-
105	-	-	0.0109	0.0137	-	-	0.0132	0.0062	0.0095	0.0073	-	-
110	-	-	0.0115	0.0144	-	-	0.0138	0.0065	0.0099	0.0076	-	-
115	-	-	0.0120	0.0152	-	-	0.0144	0.0069	0.0104	0.0079	-	-
120	-	-	0.0126	0.0159	-	-	0.0150	0.0072	0.0109	0.0083	-	-
125	-	-	0.0132	-	-	-	0.0156	0.0075	-	-	-	-
130	-	-	0.0137	-	-	-	0.0162	-	-	-	-	-

Table 5.10 Strain position 6 (shear tension zone of point load 2, at stirrups no. 9)

Load	RCB1	RCB2	RCB3	RCB4	RCB5	RCB6	RCB7	RCB8	RCB9	RCB10	RCB11	RCB12
(kN)	HYSD-MS	HYSD-MS	Mix-MS	Mix-MS	GFRP-MS	GFRP-MS	HYSD-GFS	HYSD-GFS	Mix-GFS	Mix-GFS	GFRP-GFS	GFRP-GFS
0	0.0000	0.0000	0.0000	0.0002	0.0008	0.0000	0.0000	0.0008	0.0002	0.0000	0.0008	0.0002
5	0.0002	0.0002	0.0004	0.0006	0.0024	0.0004	0.0002	0.0012	0.0004	0.0000	0.0014	0.0006
10	0.0006	0.0002	0.0004	0.0012	0.0032	0.0004	0.0004	0.0012	0.0006	0.0002	0.0016	0.0014
15	0.0012	0.0004	0.0008	0.0016	0.0048	0.0012	0.0008	0.0024	0.0016	0.0006	0.0008	0.0018
20	0.0014	0.0004	0.0010	0.0018	0.0066	0.0032	0.0012	0.0022	0.0020	0.0010	0.0010	0.0026
25	0.0002	0.0008	0.0014	0.0020	0.0132	0.0062	0.0012	0.0036	0.0024	0.0010	0.0022	0.0034
30	0.0002	0.0016	0.0018	0.0026	0.0164	0.0086	0.0014	0.0050	0.0038	0.0012	0.0040	0.0046
35	0.0028	0.0020	0.0022	0.0030	0.0184	0.0098	0.0018	0.0052	0.0048	0.0018	0.0050	0.0058
40	0.0034	0.0022	0.0028	0.0036	0.0224	0.0108	0.0024	0.0064	0.0054	0.0020	0.0060	0.0074
45	0.0036	0.0022	0.0030	0.0040	0.0276	0.0148	0.0032	0.0068	0.0058	0.0020	0.0085	0.0086
50	0.0042	0.0028	0.0032	0.0048	0.0290	0.0154	0.0042	0.0076	0.0064	0.0022	0.0085	0.0090
55	0.0050	0.0032	0.0038	0.0056	0.0321	0.0172	0.0046	0.0076	0.0070	0.0026	0.0095	0.0100
60	0.0050	0.0038	0.0044	0.0062	0.0353	0.0190	0.0048	0.0082	0.0074	0.0030	0.0104	0.0109
65	0.0054	0.0038	0.0048	0.0074	0.0385	0.0208	0.0048	0.0088	0.0082	0.0038	0.0114	0.0119
70	0.0060	0.0044	0.0052	0.0084	0.0416	0.0226	0.0052	0.0094	0.0092	0.0042	0.0124	0.0129
75	0.0068	0.0046	0.0060	0.0096	0.0448	0.0244	0.0056	0.0096	0.0094	0.0044	0.0134	0.0138
80	0.0078	0.0060	0.0060	0.0100	0.0479	0.0262	0.0060	0.0104	0.0104	0.0048	0.0143	0.0148
85	0.0086	0.0066	0.0064	0.0100	0.0511	0.0279	0.0060	0.0112	0.0118	0.0052	0.0153	0.0158
90	0.0094	0.0084	0.0074	0.0106	0.0543	0.0297	0.0069	0.0111	0.0124	0.0053	0.0163	0.0167
95	0.0102	0.0102	0.0073	0.0112	0.0574	0.0315	0.0073	0.0117	0.0127	0.0056	-	-
100	0.0112	-	0.0077	0.0119	0.0606	0.0333	0.0077	0.0124	0.0134	0.0059	-	-
105	-	-	0.0081	0.0125	-	-	0.0081	0.0130	0.0141	0.0062	-	-
110	-	-	0.0085	0.0131	-	-	0.0085	0.0137	0.0148	0.0065	-	-
115	-	-	0.0090	0.0138	-	-	0.0089	0.0143	0.0155	0.0069	-	-
120	-	-	0.0094	0.0144	-	-	0.0094	0.0150	0.0161	0.0072	-	-
125	-	-	0.0098	-	-	-	0.0098	0.0156	0.0168	-	-	-
130	-	-	0.0102	-	-	-	0.0102	-	-	-	-	-

Results of failure loads, Load – deflection, Load- strain relationship evaluated during testing and obtained by calculations subsequently have been tabulated as discussed for different RC beams in this chapter. Graphical variations using available readings have been presented in Chapter 6.

6. DISCUSSION OF RESULTS

6.1 General

Discussion of all results related RC beams tested have been given in present Chapter. This Chapter deals with comparison of results in terms of failure loads and displacement induced for RC beams. Theoretical and experimental results have been compared to understand accuracy of adopted method of analysis and design. Comparison of strain has been presented along with graphical representation for load versus strain curve for all RC beams. Behaviour of RC beams have been compared in terms of failure shape, crack pattern etc.

6.2 Comparison of Results

Here in this section results for different parameters have been compared for RC beams. In different sub-heads following parameters have been covered

1. Failure Load
2. Load-Deflection relationship
3. Load-strain relationship

6.2.1 Failure load

Experimental as well as theoretical average values of failure loads for all RC beams have been presented in Table 6.1.

It has been observed that theoretical and experimental values have significant amount of variations. Experimentally observed failure loads have been increases upto 30.86%, 46.74%, 56.35%, 48.15%, 57.61%, 51.47% in all series of beams as shown in Table 6.1 compared to capacity of beams evaluated theoretically in all beams.

From comparison of failure loads for all beams, it has been clearly observed that compared to RC beams with HYSD reinforcement (RCB1, RCB2) load carrying capacity increases upto 27.36% in Mix-MS (RCB3, RCB4), 13.21% in HYSD-GFS (RCB7, RCB8), 36.79% in Mix-GFS (RCB9, RCB10) respectively. It has been observed in GFRP-MS (RCB5, RCB6) and GFRP-GFS(RCB11, RCB12) capacity decreases upto 9.43% and 12.26% respectively. RC beam with combined reinforcement have highest load capacity (RCB3, RCB4, RCB9, RCB10) compared to other beams.

RC beams HYSD-GFS and Mix-GFS (RCB7 to RCB10) have higher load capacity compared to RC beams HYSD-MS and Mix-MS (RCB1 to RCB4). GFRP-MS (RCB5, RCB6) show higher load capacity compared to GFRP-GFS (RCB11, RCB12) stirrups.

Table 6.1- Comparison for failure loads

Specimen No.	Specimen Type	Theoretical Failure Load (kN)	Average Experimental Failure Load (kN)	% increase compared to theoretical failure load	% increase compared to HYSD-MS beams	% increase with GFRP stirrups compared to mild-steel stirrups
RCB 1, RCB 2	HYSD-MS	81	106	30.86	-	-
RCB 3, RCB 4	Mix-MS	92	135	46.74	27.36	-
RCB 5, RCB 6	GFRP-MS	61.4	96	56.35	-9.43	-
RCB 7, RCB 8	HYSD-GFS	81	120	48.15	13.21	13.21
RCB 9, RCB 10	Mix-GFS	92	145	57.61	36.79	7.41
RCB 11, RCB 12	GFRP-GFS	61.4	93	51.47	-12.26	-3.13

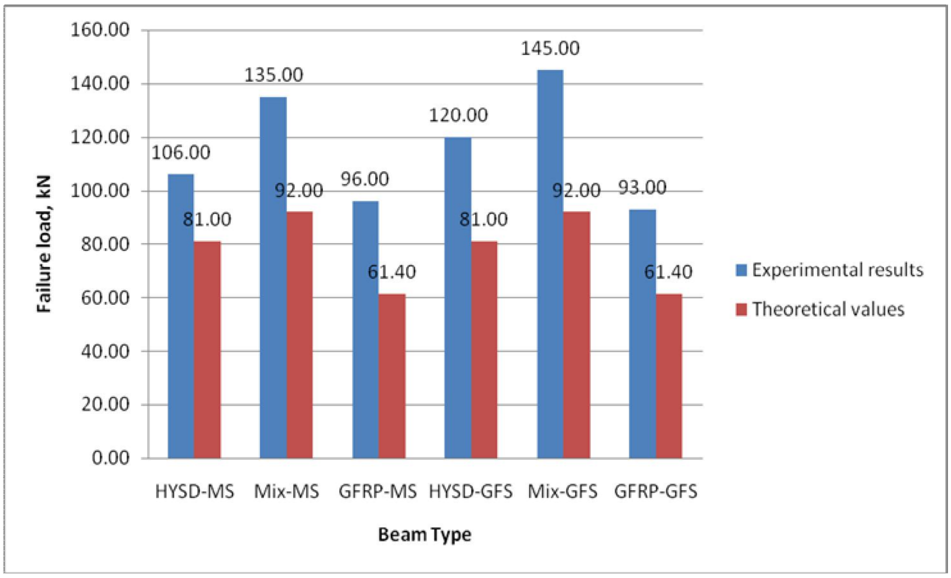

Fig. 6.1 Experimental vs. Theoretical values for failure loads

6.2.3 Load-Displacement

Maximum displacements at time of failure for all beams have been presented in Table-6.2. These are observed maximum displacements at the centre span for all beam specimens during testing. All experimental deflections have been taken from section 5.3 of Chapter 5. Theoretical deflections have been presented here from section 3.4.2 of Chapter 3. Comparative variation of load versus displacement at centre for all beam specimens has been presented in Figure 6.2.

It has been observed from Fig. 6.2 that with change in type of reinforcement in beams, magnitude of deflection for beams also changes.

Table 6.2- Maximum Displacement for various specimens

Specimen No.	Specimen Type	Maximum Displacement form Experiment (mm)	Theoretical Max. Displacement (mm)
RCB 1,2	HYSD-MS	18.18	13.48
RCB 3,4	Mix-MS	33.34	-
RCB 5,6	GFRP-MS	47.41	34.90
RCB 7,8	HYSD-GFS	17.71	13.48
RCB 9,10	Mix-GFS	17.80	-
RCB 11,12	GFRP-GFS	47.14	34.90

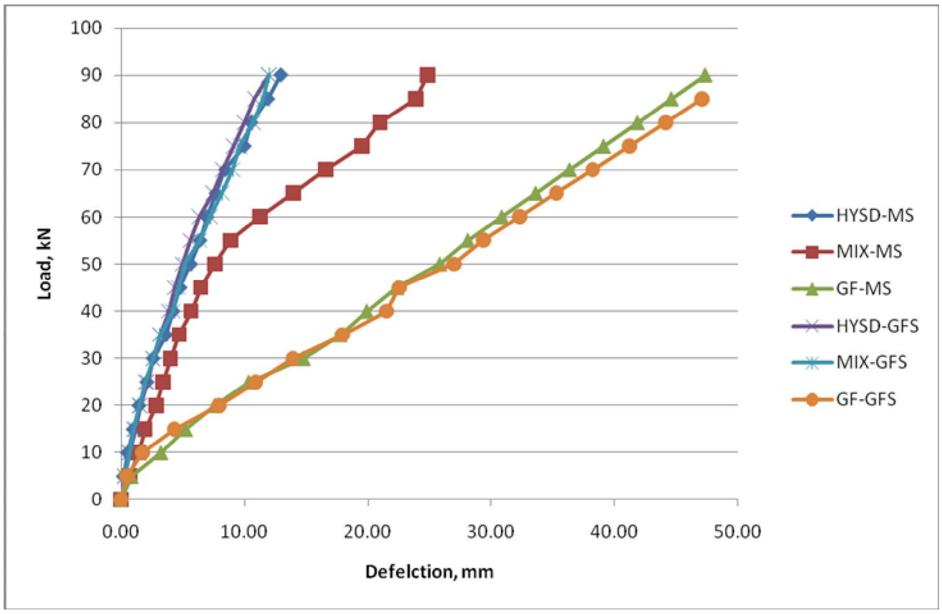

Fig. 6.2 Load-Deflection relationship

It has been observed from Table 6.2 that compared to RC beams with HYSD reinforcement (RCB1, RCB2, RCB7, RCB8), Other beams have much higher displacement in both experimental results and theoretical computations. Maximum displacement is visible in GFRP-MS (RCB5, RCB6) and GFRP-GFS (RCB11, RCB12) beam specimens. Least displacement has been observed for HYSD-GFS, Mix-GFS and HYSD-MS specimens.

It has been observed that with change in type of stirrups, deflection of beams also changes. RC beams with mild steel stirrups (RCB1 to RCB6) gives higher displacement compared to RC beams with GFRP stirrups(RCB7 to RCB12).

6.4.4 Load-strain behaviour

Load-strain behaviour for RC beams have been presented in form of graphical variation in Fig. 6.4 to 6.9 respectively. Strain gauges have been attached to six different positions on surface of beams as discussed in chapter-5. All positions have been presented in Fig. 6.3. All graphs have been prepared from average results for identical type of beams. Results have been taken from Tables 5.4, 5.5, 5.6, 5.7, 5.8 and 5.9 of strain at different position as given in Chapter-5.

Strain position 1(shear zone of point load 1 in bottom portion, stirrup-3) has been shown in Fig. 6.3. Strain variation for beam has been shown in Fig. 6.4. It has been observed that GFRP-GFS beams (RCB11, RCB12) show higher strain compared to other specimen. HYSD-MS beams (RCB1, RCB2) shows least strain. RC beams with GFRP stirrups(RCB 7 to RCB12) shows higher strain compared to RC beams with mild-steel stirrups(RCB1 to RCB6).

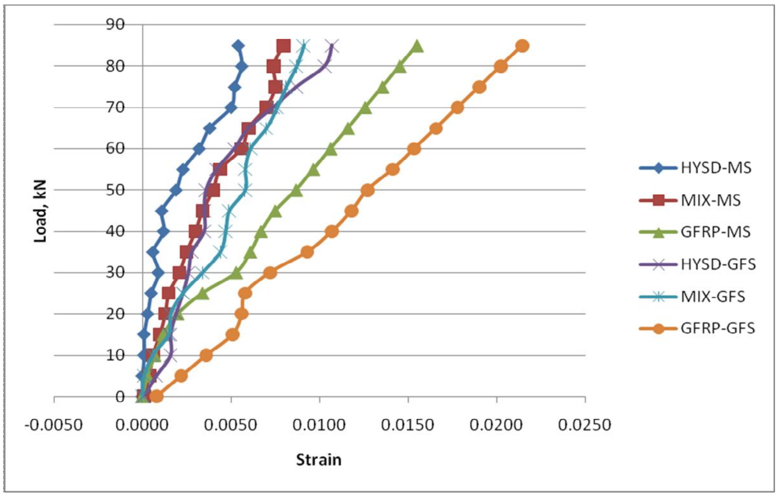

Fig. 6.4 Load strain behaviour for strain position -1

Strain position 2 (near point load 1 in bottom portion, stirrup-4) has been shown in Fig. 6.3. Graphical variation of strain for beams have been shown in Fig. 6.5. It has been observed that GFRP-GFS (RCB11, RCB12) beams as well as Mix-MS (RCB3, RCB4) beams show higher strain compared to other beams. HYSD-MS (RCB1, RCB2) beams show least strain. RC beams with GFRP stirrups (RCB7 to RCB12) show higher strain compared to RC beams with mild-steel stirrups (RCB1 to RCB6). Mix-GFS beams (RCB9, RCB10) show lesser strain compared to Mix-MS beams (RCB3, RCB4).

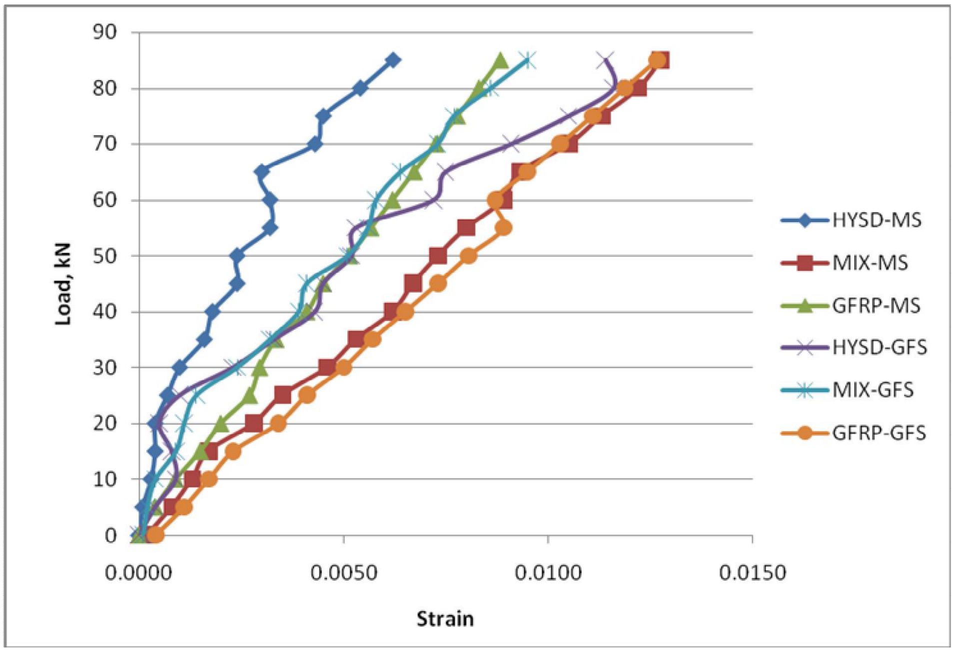

Fig. 6.5 Load strain behaviour for strain position-2

Strain position 3 (at mid-point in bottom portion) has been shown in Fig. 6.3. It has been observed that Mix-MS beams (RCB3, RCB4) show higher strain compared to other beam specimens. HYSD-MS beams (RCB1, RCB2) show least strain. RC beams with GFRP stirrups (RCB7 to RCB12) show higher strain compared to RC beams with mild-steel stirrups (RCB1 to RCB6). Mix-GFS beams (RCB9, RCB10) show lesser strain compared to Mix-MS beams (RCB3, RCB4).

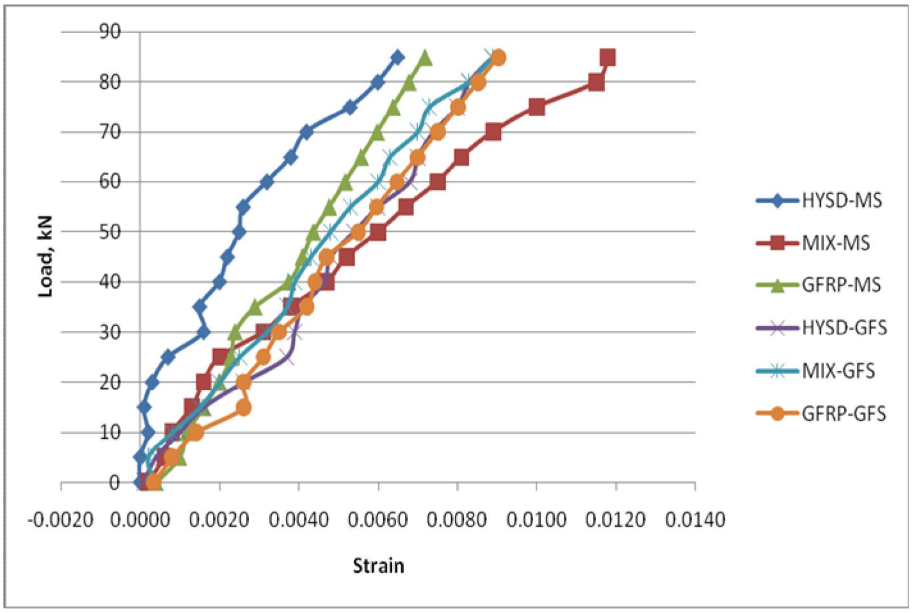

Fig. 6.6 Load strain behaviour for strain position-3

Strain position 4 (at mid-point in top portion) has been shown in Fig. 6.3. It has been observed that HYSD-MS beams (RCB1, RCB2) show higher strain compared to other beam specimen. GFRP-GFS beams (RCB11, RCB12) show least strain. RC beams with GFRP stirrups (RCB7 to RCB12) show lesser strain compared to RC beams with mild-steel stirrups (RCB1 to RCB6). Mix-GFS beams (RCB9, RCB10) show leser strain compared to Mix-MS beams (RCB3, RCB4).

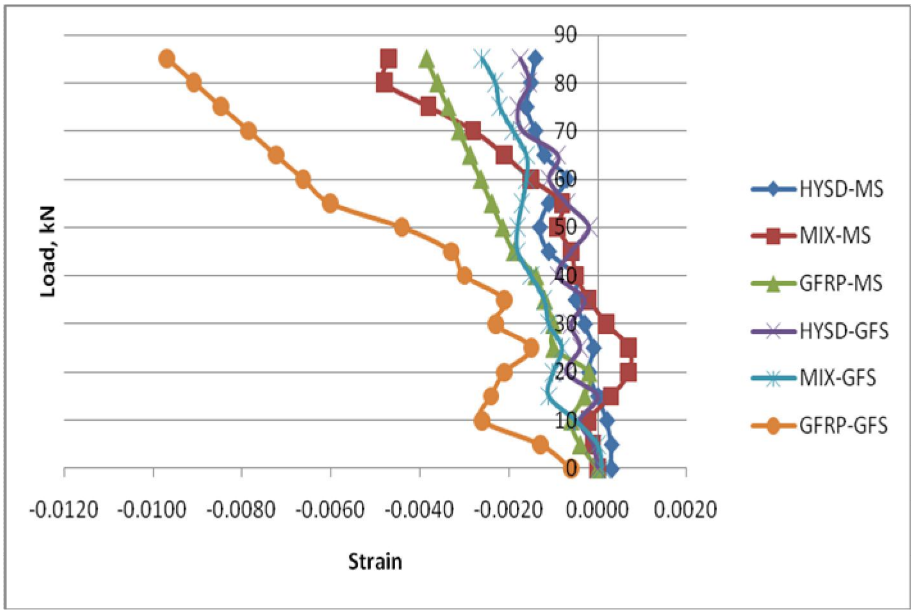

Fig. 6.7 Load strain behaviour for strain position-4

Strain position 5 (near point load 2 in bottom portion, stirrup-8) has been shown in Fig. 6.3. It has been observed that GFRP-MS beams (RCB5, RCB6) show higher strain compared to other beam specimen. HYSD-GFS beams (RCB 7, RCB8) show least strain. RC beams with GFRP stirrups (RCB7 to RCB12) show lower strain compared to RC beams with mild-steel stirrups (RCB1 to RCB6).

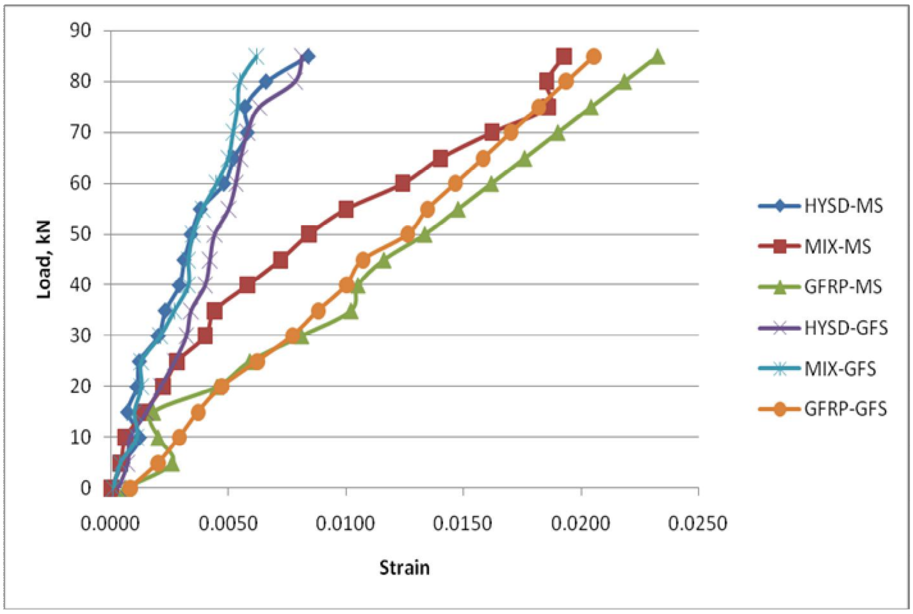

Fig. 6.8 Load-strain behaviour for strain position-5

Strain position 6 (Shear zone of point load 1 in bottom portion, stirrup-9) has been shown in Fig. 6.3. It has been observed that GFRP-MS beams(RCB5, RCB6) show higher strain compared to other beam specimen. Mix-GFS beams (RCB7, RCB8) show least strain. RC beams with GFRP stirrups (RCB7 to RCB12) show lower strain compared to RC beams with mild-steel stirrups (RCB1 to RCB6).

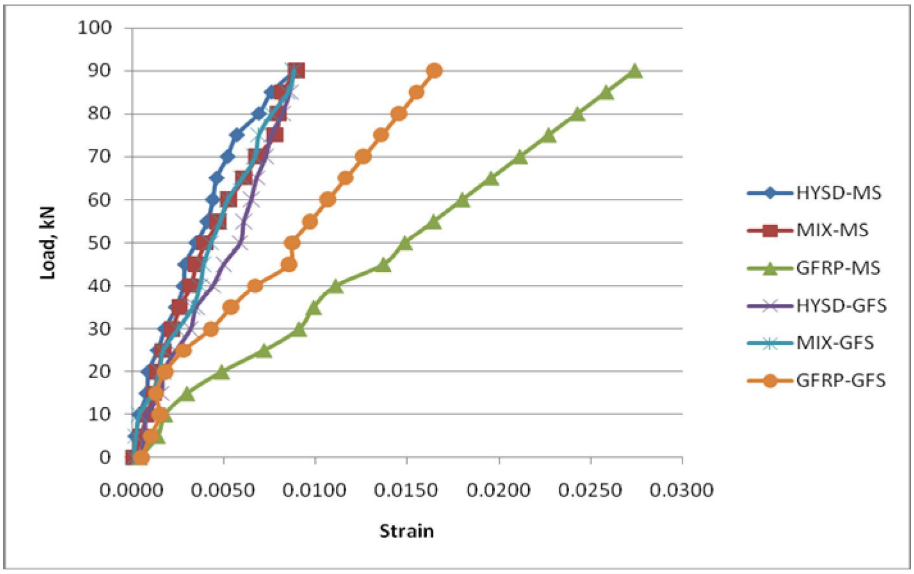

Fig. 6.9 Load-strain behaviour for strain position-6

6.3 Moment Capacity of RC Beams

Theoretical Moment capacities of RC beams reinforced with different type of reinforcement have been calculated in Chapter 3. Moment capacities evaluated from experimental results have been calculated in Chapter 5. These details in comparative form have been given in Table 6.3.

Table 6.3 Moment capacity of RC beams

Beam mark	Specimen Type	Moment Capacity from theoretical results (kNm)	Moment Capacity from experimental results (kNm)
RCB1, RCB2	HYSD-MS	16.2	18.55
RCB3, RCB4	Mix-MS	22.26	23.63
RCB5, RCB6	GFRP-MS	18.42	16.80
RCB7, RCB8	HYSD-GFS	16.2	21.00
RCB9, RCB10	Mix-GFS	22.26	25.38
RCB11, RCB12	GFRP-GFS	18.42	16.28

It has been observed From Table 6.3 that for all specimens theoretical and experimental moment capacities are in close agreement. Higher moment capacity has been observed in all RC beams other than HYSD-MS beams (RCB1, RCB2). However, GFRP-GFS (RCB11, RCB12) beams are exception in this case due to their lesser failure load. Mix-GFS beams (RCB9, RCB10) show highest moment capacity. Higher moment capacities of RC beams with GFRP stirrups have been observed compared to RC beams with mild-steel stirrups.

6.4 Comparison of Failure Modes and Crack Patterns

For both HYSD-MS beams first crack has observed after load of 40 and 35 kN respectively. Several minor flexure cracks have been visible at later stages for both beams as shown in Fig. 6.10 and 6.11 respectively. Flexure failure after completion of application of ultimate load using Hydraulic jack has been presented in Fig. 6.11(a). Cover failure in compression zone of beam also has been clearly visible in Fig. 6.10 and 6.11.

a) Flexure cracks after initiation of failure

b) Flexure failure after ultimate load

Fig. 6.10 Crack patterns and Failure shape observed for RCB1

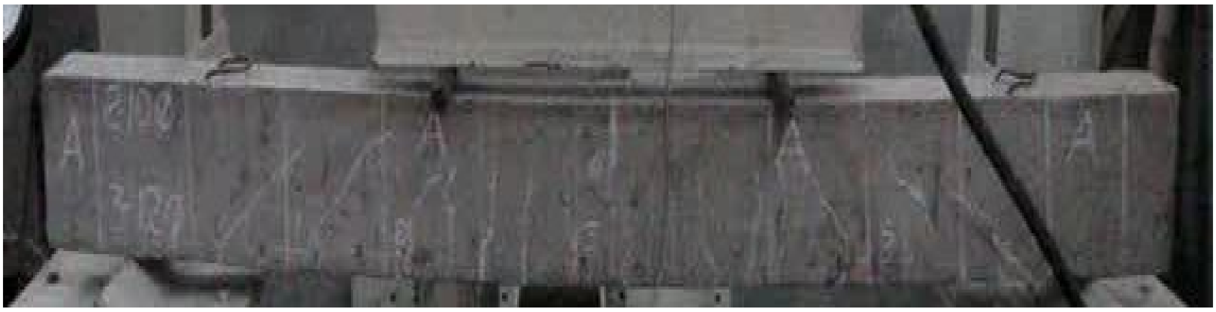

a) Flexure cracks after initiation of failure

b) Flexure failure after ultimate load

Fig. 6.11 Crack patterns and Failure shapes observed for RCB2

For beams RCB3 and RCB4 HYSD and FRP reinforcement have been provided in tension zone. First crack has been observed at 55-60 kN load for these beams. Crack propagation and failure shape for both beams have been given in Fig. 6.12 and Fig. 6.13 respectively. Opposite behaviour has been observed for RCB3 and RCB4. Shear failure for RCB3 and flexure behavior for RCB4 has been observed. Concrete crushing has been visible in shear failure of RCB3. In specimen RCB4, a bending has been observed.

a) Flexure cracking after initiation of cracks

b) Shear failure at ultimate load

Fig. 6.12 Crack propagation and Failure pattern for RCB3

a) Flexure and shear cracks

b) Flexure failure with bending

Fig. 6.13 Failure type and crack pattern for RCB4

GFRP reinforcement has been used as tension reinforcement and mild-steel stirrups are used for RCB5 and RCB6 beams. First crack has been observed at 30kN and 34kN load respectively for both beams. Several minor flexure cracks have been visible for RCB5 and RCB6 respectively in Fig. 6.14 and in Fig. 6.15. Shear failure has been observed at maximum load for both beams. Sudden failure of FRP reinforcement and compete rupture has been observed. FRP rupture in closer view also has been presented in Fig. 6.16 (a) and (b) for more understanding.

a) Flexure cracks

b) Shear failure at ultimate load

Fig. 6.14 cracks and failure pattern for RCB5

a) Minor cracks and bending of beam

b) Shear failure at ultimate load

Fig. 6.15 Failure pattern and initiation of cracks for RCB6

(a) Failure observed for RCB5

(b) Failure observed for RCB6

Fig. 6.16 Closer View of GFRP reinforcement failure at ultimate load

For specimens RCB7 and RCB8, GFRP stirrups have been used. First crack has been observed at 45kN and 49kN respectively for both beams. Minor flexure cracks and shear failure at maximum load have been visible as shown in Fig. 6.17 for both beams. Braking down of GFRP stirrups has been observed.

a) Shear cracks

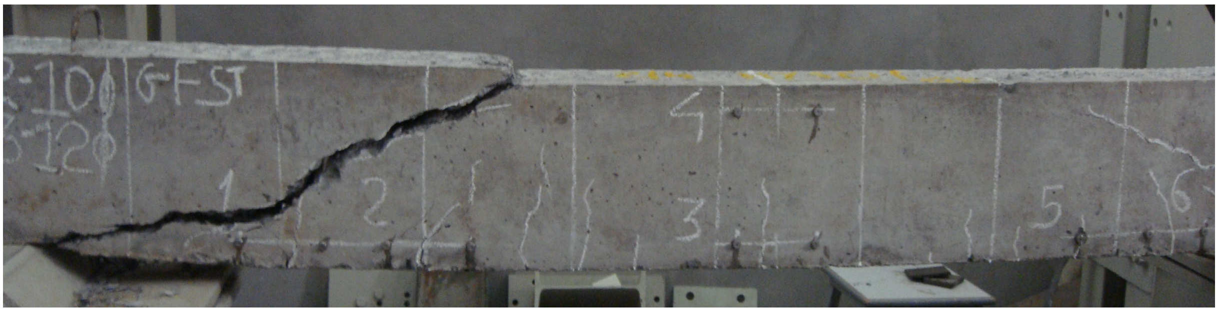

b) Shear failure

c) Shear failure

Fig. 6.17 Behaviour of beams RCB7 and RCB8

For RCB9 and RCB10, combined reinforcement and GFRP stirrups have been used. First crack has been observed at 55kN and 61kN load respectively for both beams. Several flexure cracks have been visible as shown in Fig. 6.18 and in Fig. 6.19 for both beams at later stage. Shear failure at maximum load has been observed for both beams. Failure of GFRP stirrups has been observed due to shear failure of beams. Failure of GFRP stirrups has been presented in Fig. 6.20.

a) Flexure and shear cracks

b) Shear failure

Fig. 6.18 Crack pattern and failure type for RCB9

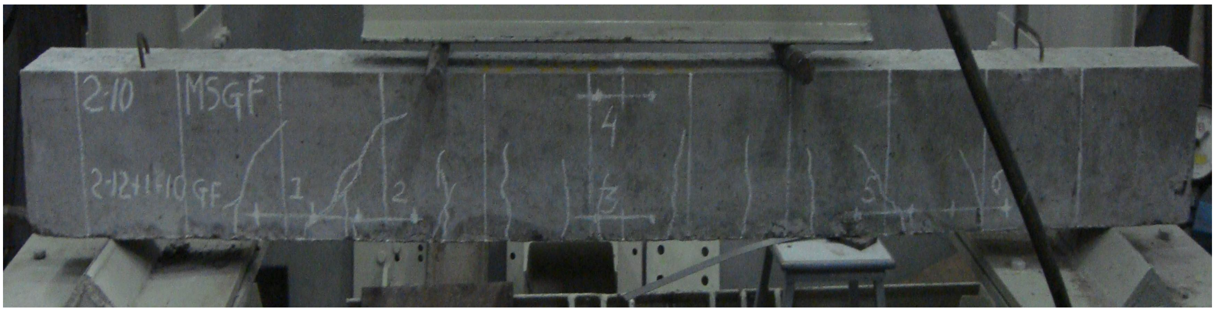

a) Flexure and shear cracks

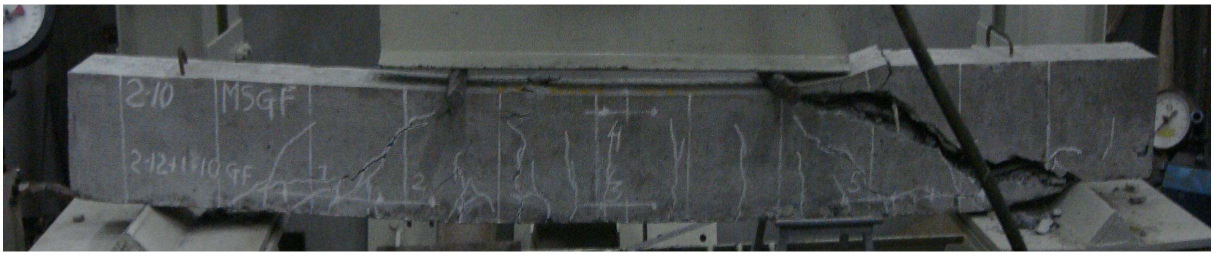

b) Shear failure

Fig. 6.19 Crack pattern and failure type for RCB10

a) Breaking of stirrup for RCB9

b) Breaking of two stirrups for RCB10

Fig. 6.20 Breaking of GFRP stirrups when used in Hybrid Reinforced beams

First crack has been observed at 34 kN and 36 kN load respectively for RCB11 and RCB12. Number of minor flexure cracks have been visible for both beams as given in Fig. 6.21 and 6.22 respectively. Shear failure has been observed at maximum load. No damage to GFRP reinforcement has been observed during failure of these beams. Failure of GFRP stirrups has been given in Fig. 6.23.

a) Larger Shear cracks

b) Shear failure with falling of cover

Fig. 6.21 Failure shape and crack pattern for RCB11

a) Minor shear and flexure cracks

b) Shear failure with falling of cover

Fig. 6.22 Failure shape and crack pattern for RCB12

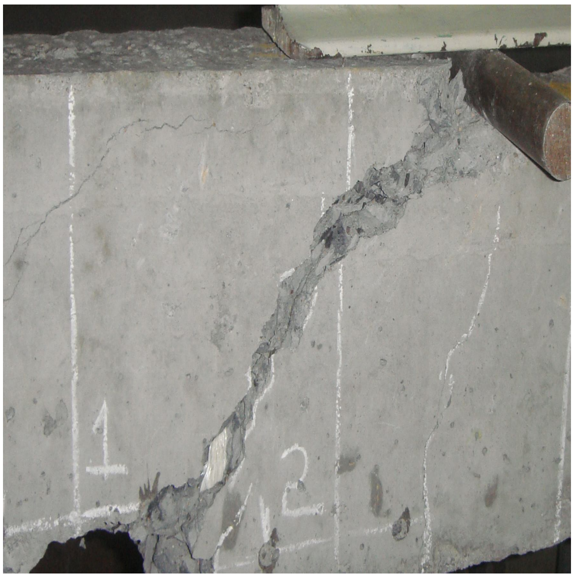

a) Stirrup failure for RCB11 b) Bottom view after failure for RCB12

Fig. 6.23 Failure of stirrups in GFRP reinforced beams(GFRP-GFS)

Thus for all categories of beams tested during experiment, loading and other relevant parameters evaluated during experiment and their theoretical comparison in detail have been discussed in this chapter. Important research findings have been summarized in Chapter 8.

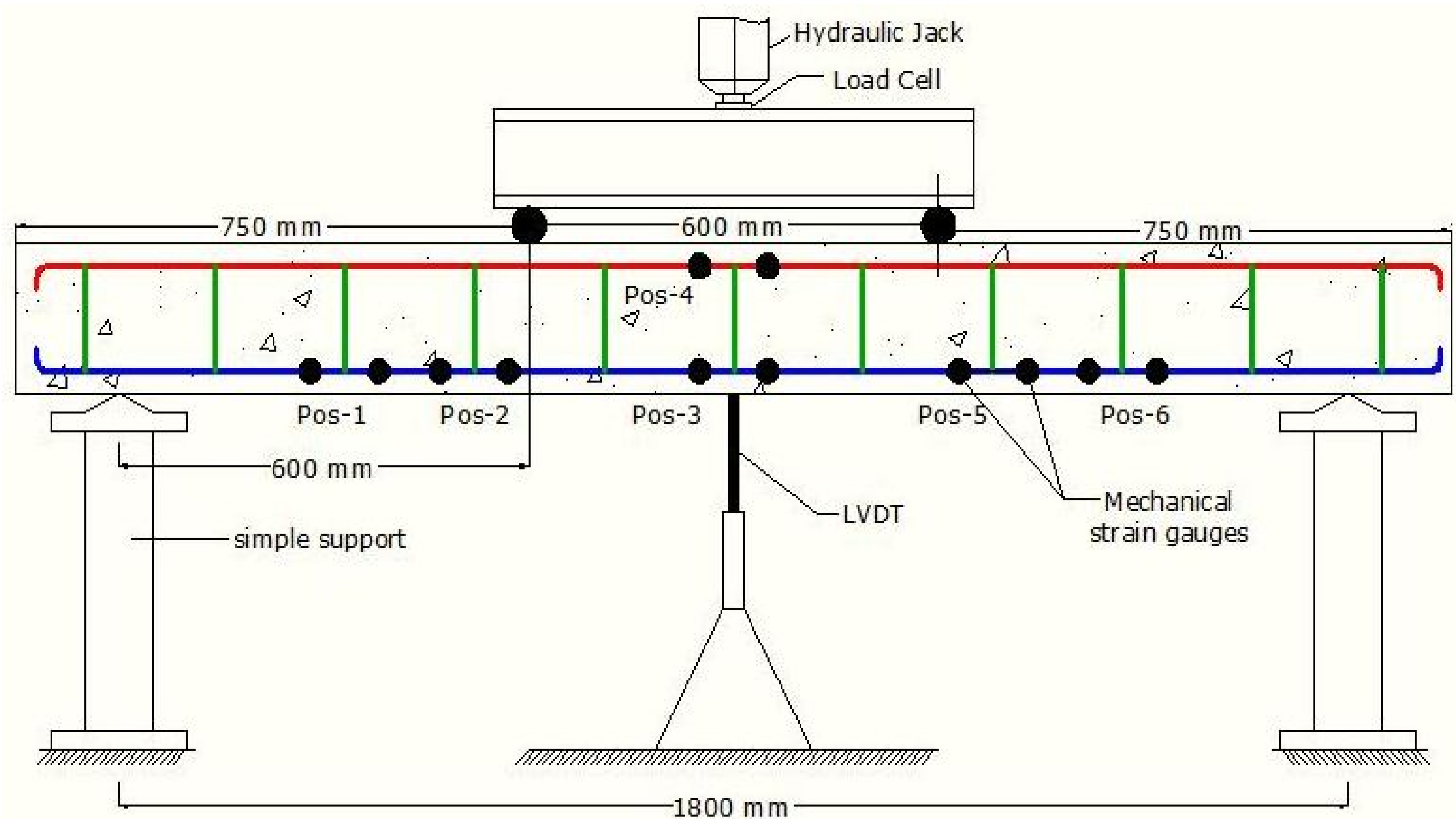

Fig. 6.3 Position of strain gauges

7. INITIATION OF CORROSION IN RC CYLINDERS

7.1 General

Corrosion has been defined as the rust of metal. As per ASTM G 15 “Corrosion is the electrochemical reaction between a material usually a metal and its environment that produces deterioration of material and its properties”.
Corrosion of steel in concrete has become a considerable durability problem in mild as well as severe climatic conditions since last many decades worldwide. The process by which a refined metal reverts back to its natural state by oxidation reaction with non metallic environment is called corrosion. This is an interaction between a material and its environment that results in a degradation of physical, mechanical, or even esthetic properties of that material.

More specifically, corrosion is usually associated with a change in oxidation state of a metal, oxide, or semiconductor. Corrosion of steel in concrete is an electrochemical process. A electrochemical cell is set up when, there is a difference in electrical potential along the steel reinforcement in concrete. In steel, one part becomes anode, and another part becomes cathode. Both of these parts are connected by an electrolyte in form of pore water in hardened cement paste. Positively charged ferrous ion Fe^{++} at anode passes in to solution. Negatively charged free electron e^- passes through steel into cathode where they are absorbed by constituent of electrolyte and combine with water and oxygen to form hydroxyl ions.

7.1.1 Effects of corrosion

Reinforced concrete uses steel to provide tensile properties that are required for structural concrete. It prevents failure of concrete structures, which are subjected to tensile and flexural stresses due to traffic, winds, dead loads and thermal cycling.

Basic problem associated with deterioration of conventional reinforced concrete due to corrosion of embedded reinforcement is that products of corrosion exert stresses within concrete which cannot be supported by limited plastic deformation of concrete and hence concrete cracks. Final stage of deterioration of conventional reinforced concrete from corrosion of reinforcing steel in RC structure include cracks reaching surface of, and causing disintegration of concrete cover. This phenomenon leads to problems regarding structural soundness, to discomfort, and to cosmetic problems. However, when reinforcements corrode, formation of rusts leads to loss of bonds between steel and concrete and subsequent delamination and spalling take place. If left unchecked integrity of structure has been affected. Reduction in cross sectional area of steel reduces its strength capacity. This is detrimental to performance of tensioned strands in prestressed concrete. Detrimental effects of corrosion on both RC as well as steel structures have been presented in Fig. 7.1.

(a) Bhopal Event (b) San Francisco Bridge

Fig. 7.1 Different Effects of Corrosion

As per one American report, $150 billion worth of corrosion damage only on their interstate highway bridges is due to de-icing and sea salt induced corrosion.

In UK, the Highway Agency’s estimate of salt induced corrosion damage is a total of £616.5 million on motorway and trunk road bridges in England and Wales alone. Similar type of damage statistics have been there from Asian countries and as well as Australia.

7.2 Mechanism of corrosion

Reinforcement corrosion mechanism has been attributed to three predominant processes, namely, chemical, electro-chemical and physical.

1. Chemical

Rebar corrosion is a chemical process in the sense that alkalinity of concrete can get reduced to a pH value less than 10.00 by ingress of carbon dioxide, or passivity of steel can be destroyed by ingress of chloride and thereby initiating corrosion in either case.

2. Electro-chemical process

Steel in concrete is usually in a non-corroding, passive condition. Once the passive layer breaks down, areas of rust start appearing on steel surface. When concrete corrodes, it dissolves in pore water and emits electrons:

$$\text{Anodic reaction:} \quad Fe \longrightarrow Fe^{2+} + 2e^{-} \qquad \text{... (7.1)}$$

Two electrons created in anodic reaction are to be consumed elsewhere on steel surface to preserve electrical neutrality. Therefore,

$$\text{Cathodic reaction:} \quad 2e^{-} + H_2O + ½ \, O2 \longrightarrow 2OH^{-} \qquad \text{... (7.2)}$$

Anodic and cathodic reactions are only the first step in process of creating rust. Full corrosion process has been explained as follows.

$$4Fe(OH)_2 + O_2 + 2H_2O \longrightarrow 4Fe(OH)_3 \longrightarrow \underset{\text{Rust}}{2Fe_2O_3.H_2O} + 4H_2O \qquad (7.3)$$

$$Fe^{2+} + 2OH^{-} \longrightarrow Fe(OH)_2 \qquad (7.4)$$

3. Physical process

Physical process of corrosion mainly consists of expansive forces caused by volume growth of corrosion products. Cracking occurs in concrete when stress induced by these forces exceeds tensile strength of concrete. A spalling has been observed in concrete with further progress in corrosion.

4. Corrosion due to environmental attacks

Embedded steel in reinforced concrete structure is exposed to corrosion due to reactions taking place between various components of atmosphere.
Some of these attacks have been listed as follows.

(a). Sulfate attack

The term sulphate attack denotes an increase in volume of mortar due to chemical action between products of hydration of cement and solution containing sulphates. Rate of sulphate attack increases with increase in strength of sulphate solution.

Most soils have been containing some sulphates in form of calcium, sodium, potassium and magnesium. They occur in soil and ground water. Ground water contains less of calcium sulphates. Ammonium sulphates have been present in agricultural soil and water from use of fertilizers, from sewage and industrial effluents. Sulphates enter into porous concrete and react with hydrated cement products.

(b). Alkali-aggregate reaction

Alkali aggregate reaction is basically a chemical reaction between hydroxyl ions in pore water within concrete with certain types of aggregate.

(c). Acid attack

Concrete is not fully resistant to acid. Certain acid such as oxalic acid and phosphoric acid are harmless. Concrete can be attacked by liquids with pH value less than 6.5. However, attack is severe at pH value below 5.5. At a pH below 4.5 attack is very severe.

(d). Carbonation

Carbonation of concrete is a process by which carbon dioxide from air penetrates in to concrete and react with calcium hydroxide to form calcium carbonate. Conversion of $Ca(OH)_2$ in to $CaCO_3$ by action of CO_2 results in shrinkage.

CO_2 changes into dilute carbonic acid which attacks concrete and reduces alkalinity of concrete.

$$CO_2 + H_2O \longrightarrow H_2CO_3 \qquad \text{... (7.5)}$$

$$H_2CO_3 + Ca(OH)_2 \longrightarrow CaCO_3 + 2H_2O \qquad \text{... (7.6)}$$

Rate of carbonation depends on the following.

- Level of pore water
- Grade of concrete

- Permeability of concrete
- Depth of cover
- Time

(e). Chloride attack

Chloride attack is one of the most important aspects related to durability of concrete. Chloride attack is a prime cause for corrosion of reinforcement.

- Sources of chloride
  - Addition of chloride set accelerators
  - Use of sea water in mix
  - Contaminated aggregates
- Chloride attack mechanism

  Chloride ion attacks passive layer of concrete. However, no drop in pH has been observed of concrete. Chloride act as catalyst to corrosion when it is opt sufficient concentration at rebar surface and capable enough to break down passive layer. Chlorides are not consumed in process, but help to break down passive layer of oxide on steel and allow corrosion process to aggravate further.

7.3 Literature Review

Broomfield [25] provided information on corrosion of steel in atmospherically exposed concrete structures. Clear idea of problems of corrosion, its causes and solutions were elaborately discussed. Condition evaluation and calculations related to corrosion of steel in concrete were also covered.

Bentur et al. [26] described mechanism of corrosion, field and laboratory methods of measurement for corrosion, corrosion control, protection methods, repair and rehabilitation of structures exposed to corrosion is also covered in it.

Maaddawy et al. [27] performed test on thirty two cylinders to induce corrosion with impressed current technique using different current densities. Corrosion was measured by mass loss formula given by faraday. For impressed current technique proper circuitry was required for constant supply of DC current. Steel reinforcement acted as anode while stainless steel acted as cathode. Results were achieved at faster rate when current capacity increases.

Maaddawy et al. [28] investigated actual degree of corrosion and concrete strain behavior experimentally. Such investigation was due to expensive corrosion products because of impressed current using electric power supplies to depassify the steel reinforcement. 5% NaCl was added by weight of cement to concrete mix. Using faradays law, mass loss was observed upto 7.27%. Increase in level of current density above 200 $\mu A/cm^2$ resulted in a significant increase in strain response and crack width due to corrosion of steel reinforcement.

Austin [29] found suitability of impressed current technique to model chloride-induced corrosion. Corrosion was investigated by examining electrochemical nature of test method.

Pruckner and Gjorv [30] described influence of level of chloride content in concrete on its electrical resistivity. It was observed that binding of chlorides in concrete is higher when $CaCl_2$ added in fresh concrete, compared to addition of NaCl. Effect of different chloride sources on concrete resistivity is not so well defined. Different mortars with OPC and 0.50 w/c were prepared to quantify effect of different types of chloride source on concrete corrosivity. Different amount of $CaCl_2$, NaCl and NaOH was added to fresh concrete mixtures. Corrosivity was primarily tested by measurements of electrical resistivity and acid capacity.

Andrade and Alonso [31] reviewed some of the methods published in literature with special attention to sensorized confinement of current. Finally, values of corrosion rate were measured in concrete specimens in laboratory and on-site suggestion were gives related to levels of risk regarding loss in rebar cross-section.

Veerachai leelarleikeit [32] employed half-cell potential measurement to estimate corrosion of reinforcing steel bars. Potential distribution and current flow from anodic region to cathodic region on rebars were analyzed by applying three-dimensional boundary element method (3D-BEM). Thus, influence of voids on potential distribution and current flow was investigated. Results of current flows revealed presence of macro-cell mechanism and generation of micro-cell mechanism. These mechanisms between cathodic and anodic regions conclude that half-cell potential measurement is not readily applicable to estimate corrosion near voids.

ACI 222 [33] is a ACI committee report. Mechanisms of corrosion of metals in concrete, protective measures for new concrete construction and remedial measures have been discussed in this report.

Significance, uses, apparatus of Half-cell potential, its calibration and procedure for use in practical have been explained in ASTM C 876:1991 [34].

7.4 Scope of Work

In addition to evaluation or enhancement in performance of RC beams using FRP reinforcement, an attempt is made to initiate and assess corrosion in cylinders in this project. The experimental work has been divided into two parts as follows.

1. Theoretical work

   Following work has been conducted.

   - Effects of corrosion phenomenon on RC structures has been studied.
   - Prevailing techniques for inducing accelerated corrosion in RC elements from literature has been studied.
   - A measurement technique of corrosion in RC elements from literature has been studied.

2. Laboratory Work

   Following work has been performed.

   - Cylinders have been cast by selecting dimensions of cylinder and deciding reinforcement position from literature.
   - Techniques of inducing corrosion using NaCl solution have been studied. Proper circuitry has been established between anode and cathode in specimens.
   - Half-cell potentiometer has been used for measurement of corrosion.
   - Plain concrete cylinders of grade of concrete M20 have been cast and compressive strength at 28 days has been measured.
   - Non destructive testing on RC cylinders has been conducted.

7.5 Experimental programme

1. Objectives of Experiment

To protect any structure from adverse effects of corrosion, initiation of corrosion in structure is very essential. It is obvious that corrosion is a natural process and takes years to occur in RC structures. Therefore, in laboratory to conduct investigations have been conducted related to corrosion in limited time duration to fulfill following objectives.

- To induce corrosion in reinforcement of concrete cylinders.
- To evaluate corrosion at certain time intervals for both types of reinforcement and compare results.

2. Details of specimen

It has been decided to cast total six concrete cylinders of size 150mm diameter and 300mm height. Variations in each type of cylinders have been presented in Table 7.1.

Table 7.1 Types of cylinders cast

Specimen no.	Specimen type	Concentration of chemicals (%)
1,2	Control	-
3,4	NaCl-cylinders	5%
5,6	$CaCl_2$-cylinders	5%

3. Material Properties

Portland pozzolana cement 53 grade of J K Lakshmi brand has been used. Two types of aggregates 20mm downsize and 10 mm downsize have been used. Fine sand of usual quality was used. To allow occurrence of corrosion at faster rate variations has been made as shown in table 7.1. Remaining two specimens have been cast with usual condition to serve as control specimens. One reinforcement of 12mm diameter and one stainless steel bar of 6mm diameter have been used for all the concrete cylinders. It has been assumed that stainless steel bar act as a cathode and current is anticipated to flow through concrete to steel reinforcing bars.

4. Mix Proportion for Concrete

IS Code Method used to carry Mix proportions of concrete for has been worked out casting of cylindrical specimens using IS method of concrete mix design. Details concrete mix proportion employed for cylinders have been given in Table 7.2.

Table 7.2 Concrete mix proportion

Cement	Sand	Aggregate		Water
		20 mm size	10 mm size	
1	1.73	2.49	1.24	0.5

5. Fabrication or moulds and curing of specimen

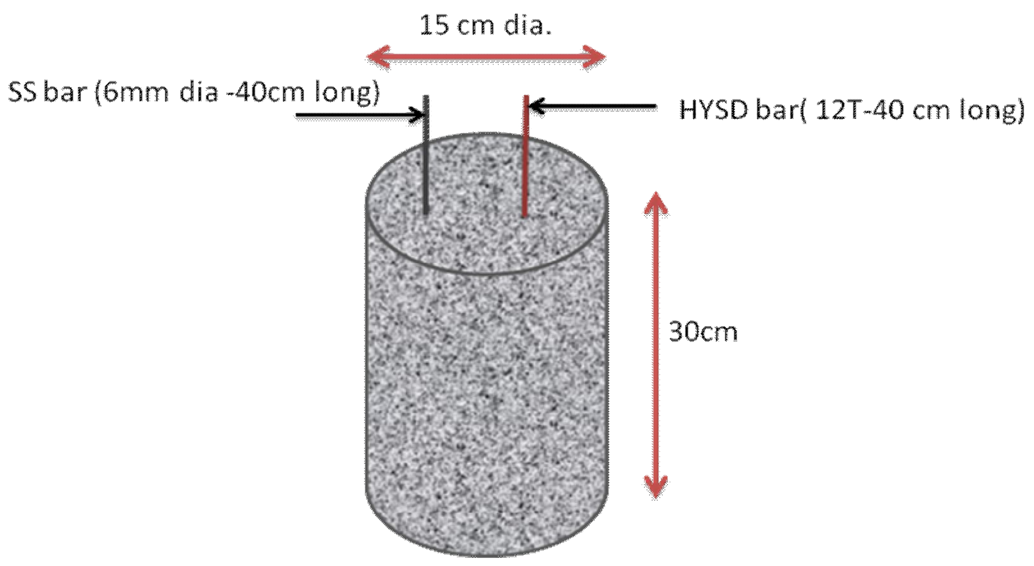

Fig 7.2 Test Specimen Details

Details of test specimen have been presented in Fig 7.2.

- All six specimens are of 150 mm diameter and 300 mm height. Both reinforcing bars have been extended upto 75-100 mm from top of cylinder and touching to bottom most part of the cylinder.
- Such positions of reinforcing bars have been employed to allow electrical connection required to impress the current.

Moulds of standard cylinder have been properly oiled. The specimens have been cast in two batches. Two specimens of first batch have been cast in normal way using hand-mixing procedure. Two specimens of second batch have been cast by adding 5% NaCL by weight of cement with hand mixing. Third batch two specimens have been cast by adding 5% $CaCl_2$ by weight of cement in concrete mix.

Fig. 7.3 Curing of Specimens

First two specimens have been placed in a container. Later specimens have been cured in regular manner suggested by IS 456[23].

6. Test Set-Up and Its Procedure

Test setup employed in experimentation has been as follows.

Direct current has been impressed on steel reinforcing bars by use of separate power units for each group of specimen to accelerate the corrosion. Power supply has been used such a manner each specimen has current density of 500 μA/cm^2. This power supply allow application of a constant current operation with automatic crossover. Therefore, non-constant parameters like current and power changes automatically in order to maintain voltage.

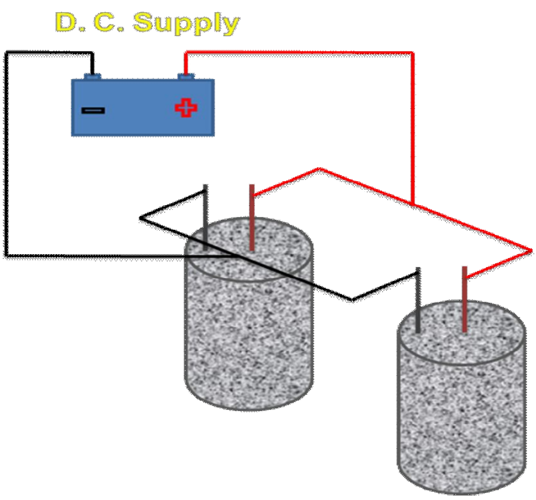

Fig 7.4 Circuit Diagram

A schematic diagram of corrosion circuit employed for both group of specimen has been presented in Fig. 7.4. The specimens of one group have been tied together in parallel circuit. Direction of current has been adjusted in such a way that steel bars act as anode and stainless steel bar act as cathode respectively.

For deciding exact current capacity and requirement of voltage, a trial experiment has been conducted in the Power System laboratory of Electrical Engineering Department, Nirma University. Test set up has been presented in Fig 7.5.(a) and (b) Current capacity of 225 mA and voltage requirement of 25-35 V has been adhered to during trial testing.

For direct current DC power supply is required. The circuit diagram for the same is as shown in Fig.7.6

a) Connection with DC supply

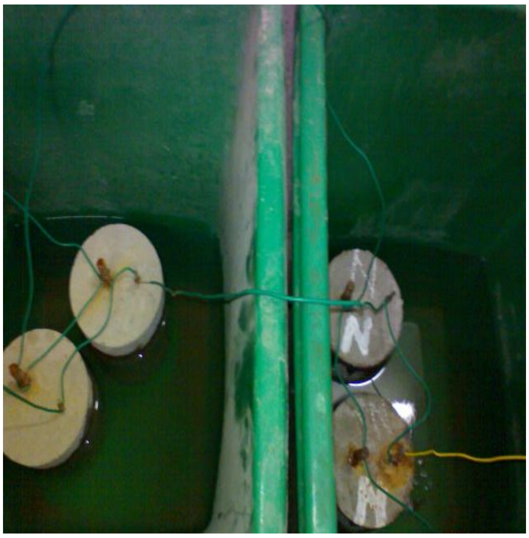

b) Internal connection between cylinders

Fig 7.5 Test Setup

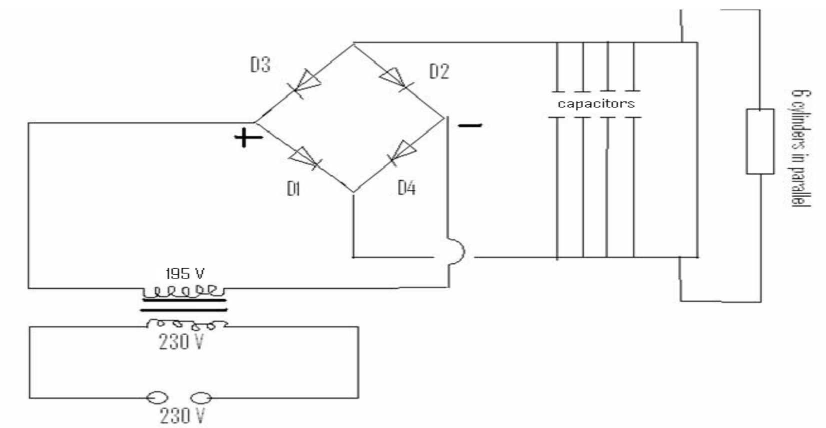

Fig. 7.6 Circuit Diagram of DC Power Supply

7. Measurement Techniques

Use of two non destructive testing equipments has been made to evaluate effect of applied corrosion to concrete cylinders. In terms of extent of active corrosion and compressive strength. Rebound hammer has been made to evaluate quality of concrete. Half cell potentiometer has been measure extent of corrosion in concrete cylinders. It has been decided to use these two equipments due to their easy operations and simple approach. It is convenient to handle and carry these equipments. Results have been provided in convenient terms by these equipments and are efficient for comparison. These equipments have been used several times to conduct testing.

7.6 Results and Discussion

1. Concrete with addition of NaCl

First cracks have been observed in a specimens subjecting to accelerated corrosion for 105 hours. Change in color of specimen has been observed. Color of specimens changed to orange red rust color. Change also has been observed in water and it becomes muddy due to mass loss of HYSD reinforcement in concrete. Initial signs of corrosion in the specimen with NaCl have been seen in Fig. 7.7 (a). Rust powder produced also is clearly visible. Cracks and change in color of specimen due to corrosion has been depicted in Fig. 7.7 (b).

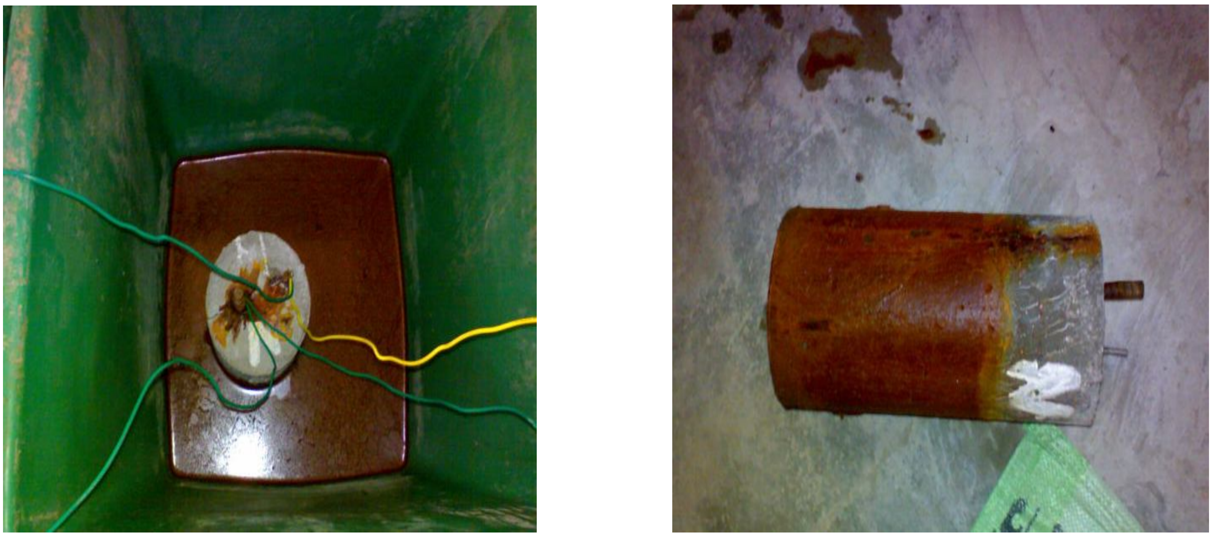

a) Initial signs of corrosion b) Change in Color & Cracks observed

Fig. 7.7 Corrosion Impact on Specimens with Addition of NaCl

2. Concrete with addition of $CaCl_2$

To evaluate effect of lime on reinforcement bars, 5% $CaCl_2$ has been added in two cylinders during casting. It has been observed that no changes in appearance of specimens are visible after 105 hours. The specimens are intact with no cracking and water is also clear.

First crack on cylinders was observed after completion of 200 hours. Only few cracks have been observed in specimens. No change in colur of water has been observed. Even no major change in appearance and colour of specimens has been observed. obviously no mass loss has been observed. The cracks have propagated mainly due to expansion of reinforcement bars.

Effect of accelerated corrosion on cylinders with addition of $CaCl_2$ has been presented in Fig. 7.8 (a) and (b). No physical signs of corrosion has been observed on specimen with $CaCl_2$ as given in Fig. 7.8 (a). However, signs of active corrosion have been visible on the same specimens after completion of 200 hours as presented in Fig. (b).

a) No initiation of corrosion till 105 hrs

b) Initial signs of corrosion

Fig. 7.8 Corrosion Effects on Concrete with Addition of $CaCl_2$

3. Plain Concrete

Effect of accelerated corrosion on control concrete cylinders also is studied. Hence, third group of specimens have been prepared without addition of any ingredient, to serve as control specimens. Therefore, normal concrete mix has been employed to cast specimen. Cracks have been visible in the specimens as per expectations. More deterioration after 150 hours has been observed in these specimens. Corrosion effects on concrete cylinders with plain concrete have been given in Fig. 7.9(a) and 7.9(b).

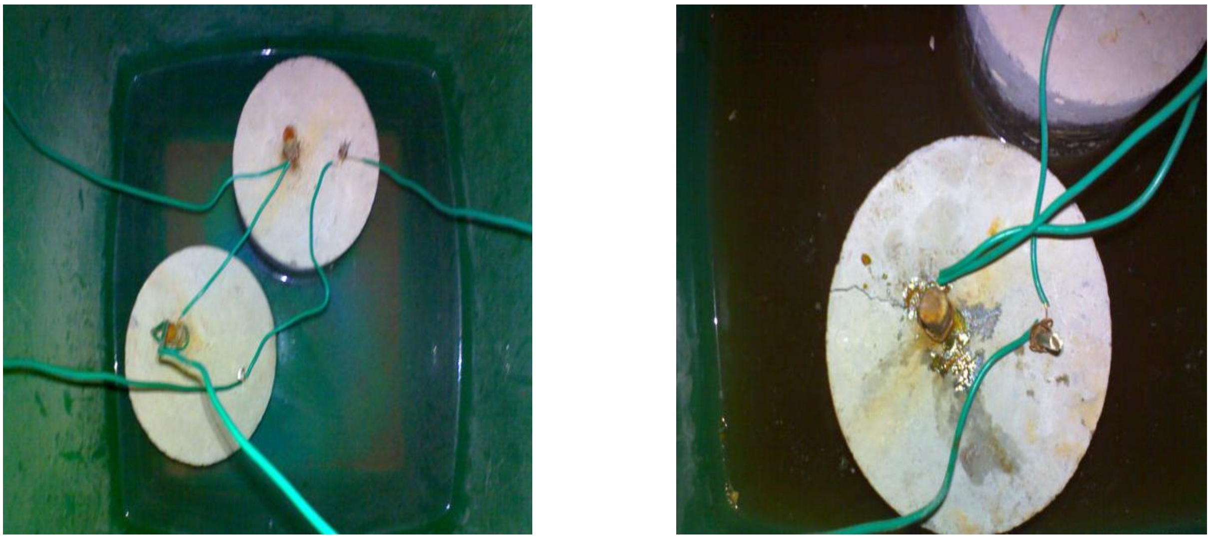

a) No initiation of corrosion till 105 hrs

b) Initial signs of corrosion

Fig. 7.9 Corrosion Effects on Plain Concrete Cylinders

Corrosion reaction has not started in plain concrete specimen till 105 hours is presented in Fig. 7.9 (a). Initial signs of corrosion in cylindrical specimens have been given in Fig. 7.9 (b). Small crack had appeared on the surface only. Color had not changed.

4. Result Comparison

- Time duration for first cracks to be visible

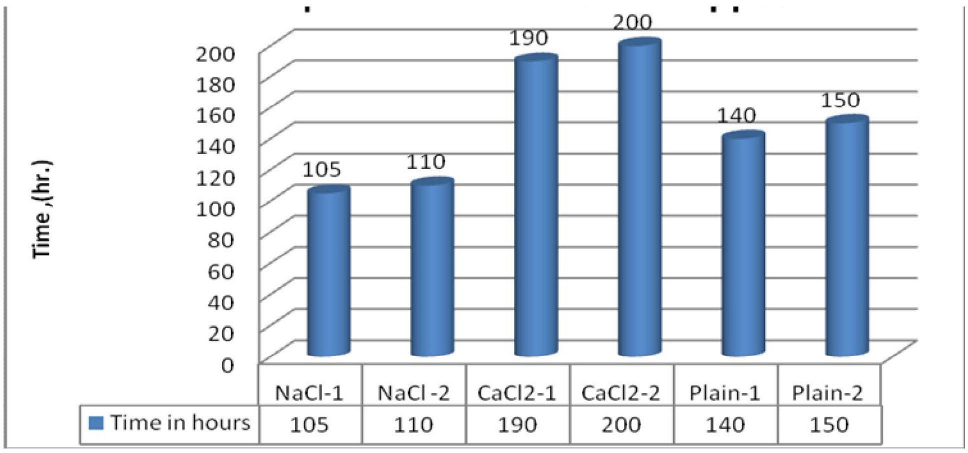

Fig. 7.10 Time required for first cracks to be visible

Comparison of time taken by different concrete specimens to exhibit effects of corrosion has been presented in Fig. 7.10. It has been observed that concrete exposed to NaCl corrodes at a faster rate compared to exposure to other environmental conditions. Specimens with $CaCl_2$ addition has proved to be slowest to react and show effects of corrosion. Thus, concrete exposed to lime requires repair attention after a longer time compared to concrete exposed to clorides.

- Half-cell potentiometer readings

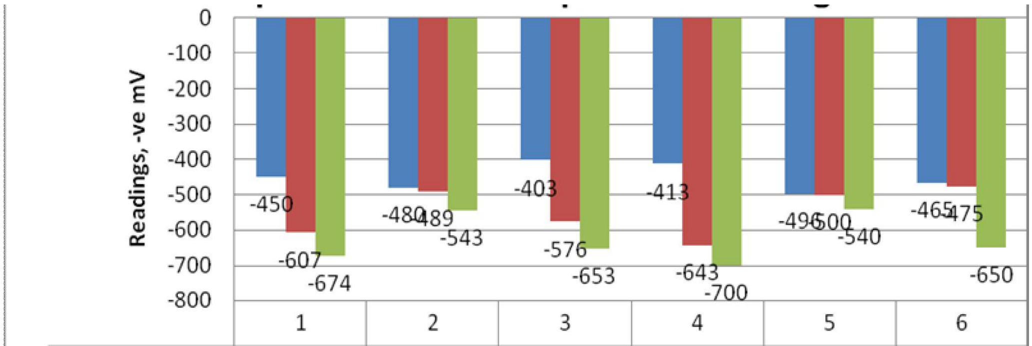

	1	2	3	4	5	6
INITIAL	-450	-480	-403	-413	-496	-465
After 105 Hours	-607	-489	-576	-643	-500	-475
After 120 Hours	-674	-543	-653	-700	-540	-650

Fig. 7.11 Half-cell potentiometer readings

It has been observed from Fig. 7.11 that concrete with NaCl is subjected to about 75% active corrosion, plain concrete shows about 40% active corrosion and concrete with $CaCl_2$ is exposed to 65% active corrosion respectively.

- Rebound Hammer readings

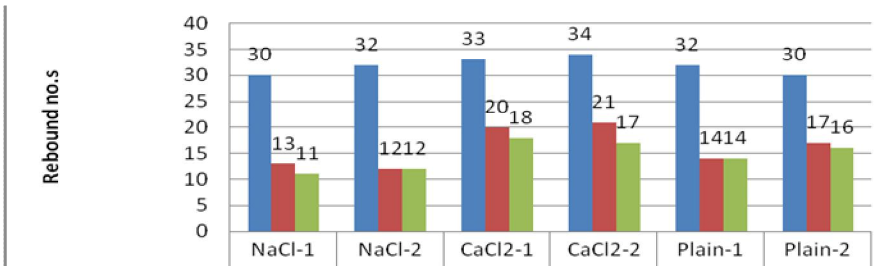

	NaCl-1	NaCl-2	CaCl2-1	CaCl2-2	Plain-1	Plain-2
Initial	30	32	33	34	32	30
After 105 hours	13	12	20	21	14	17
After 120 hours	11	12	18	17	14	16

Fig. 7.12 Comparison of Rebound Hammer Readings

Rebound hammer readings of specimens taken before 105 hrs, just after the experimental set-up before the corrosion reaction had started.

7.8 Further line of action

To get more thorough information about techniques of initiating and measurement of corrosion in concrete and repair of concrete affected due to corrosion, the experimental work described in this chapter can be further extended as discussed below.

1. Effects of addition of Sulphuric acid (H_2SO_4), Magnesium sulphate ($MgSo_4$) etc. in concrete on corrosion phenomenon can be measured.
2. Effects of addition of GGBFS, Fly ash etc. mineral admixtures in delaying corrosion of concrete can be evaluated.
3. Epoxy-Coated reinforcing steel (ECR) can be used to verify its effect and resistance against corrosion in concrete under corrosion friendly conditions.
4. Glass and Carbon Fiber reinforced composite sheets can be used to check their efficacy in resistance to corrosion in concrete.
5. Corrosion investigation performed on cylinders can be extended to concrete beam, slab and column to have more thorough knowledge about entire mechanism.
6. An attempt can be made to study performance of anodic inhibitors like sodium nitrate and zinc oxide; cathodic inhibitors like mono ethanol amine, di-ethanol amine and tri ethanol amine and mixed inhibitors in controlling rebar corrosion.
7. Concrete specimens in addition to submergence in plain water and chemicals can also be exposed to sustained loading to facilitate introduction of more cracks.
8. Instrument for measuring crack width and other non destructive testing equipment can further be used.
9. Concrete of other grades in addition to M20 can also be cast to judge effect of corrosion mechanism on stronger concrete.

Efficient, dedicated and effortful extension of work reported in this chapter is certainly anticipated to bring out meaningful results to serve humankind in a more fruitful manner.

8. SUMMARY AND FUTURE SCOPE OF WORK

8.1 Summary

An attempt has been made to study effect of incorporation of FRP reinforcement on behavior of reinforced concrete beams experimentally and theoretically in the present investigation. Details have been referred regarding flexure test, shear test, tension test, bond properties, fire performance for RC structural elements using FRP reinforcement from more than 25 research papers. For understanding about basic concept, properties, behavioural aspects and design methodology fore FRP rebars in more detail. These reference papers and India, American codes have been referred.

Design of RC beams with conventional HYSD reinforcement and RC beams with FRP reinforcement has been worked out using relevant codal provisions. An innovative concept of combined i.e. HYSD and FRP bars reinforcement for RC beam has been attempted in the present work. Theoretical comparison related to moment capacity and calculation of true moment capacity for RC beams with combined reinforcement using strain compatibility method has been computed. Additional plates have been fabricated to facilitate easier casting of RC beams in available setup of pre-tensioned PSC beam. Presently in laboratory casting of 12 RC beams has been conducted. Tensile test of HYSD and FRP bars has been completed.

Testing of beams has been carried out using two point load at loading frame. Here different parameter has been evaluated like failure load, deflection, strain at different position etc. Their comparison has been made in Chapter 6 from different results incorporated in Chapter 5. It seems that RC beams with GFRP reinforcement proved comparable to RC beams with conventional reinforcement. Partial replacement has been proved superior over all other series as it gives higher moment capacity. Some of the concluding remarks related to work carried out here has been as given in next head.

8.2 Concluding Remarks

Following concluding remarks have been made on basis of work carried out for major project.

- For design of RC beams with FRP reinforcement provisions of ACI 440.1R-03 has been used. For design of RC beams with HYSD reinforcement provisions IS 456:200 code has been referred.

- To evaluate moment capacity of RC beams with combined reinforcement strain compatibility method has been employed

- Minimum reinforcement concept has been employed for FRP reinforced beams for assessment of their flexural behavior.

- Tension test on 12 mm diameter HYSD bar and 9.5 mm diameter FRP bar has been conducted in laboratory for understanding their Load-strain relationship. True moment capacity of RC beam with combined reinforcement has been worked out from load-strain relationship with help of strain compatibility method.

- Tension tests excellent results for GFRP reinforcement. It has been measured tensile strength as 690.6 MPa.

- All beams have failed with higher amount failure load compared to theoretically evaluated failure load.

- RC beams with GFRP reinforcement as well as GFRP stirrups have performed better in terms of failure loads compared to other beams. RC beams with combined reinforcement have exhibited highest amount of experimental load carrying capacity.

- Shear strength of RC beam with HYSD reinforcement (RCB1, RCB2) has been observed higher compared to RC beam with GFRP reinforcement (RCB11, RCB12)

- RC beams with GFRP reinforcement have exhibited higher displacement compared to all other beam specimens.

- RC beams with GFRP reinforcement have exhibited higher strain compared to other beam specimen. In case of strain gauges attached to compression zone (strain position-4) for beams, results have been opposite than its in tension zone.

- Experimental moment capacity of RC beams with GFRP reinforcement has been lesser compared to theoretical moment capacity. Opposite behaviour has been observed for other beams in terms of moment capacity. RC beam with GFRP reinforcement have show lowest experimental moment capacity due to their lesser failure load.

- Majority of beams have exhibited flexure cracks in the beginning. The beams have been failed ultimately in shear and sudden failure is visible. HYSD-MS (RCB1, RCB2) beams have been failed in flexure. RC beams reinforced with GFRP bars and mild steel stirrups complete rupture of GFRP rebars have been observed.

- For RC beams with GFRP reinforcement (RCB5, RCB6 RCB11, RCB12) larger portion of concrete cover has collapsed in tension zone. This suggests poor bond strength between concrete and FRP reinforcement.

- GFRP stirrups performed well compared to mild-steel stirrups in terms of different parameters like failure load, deflection, moment capacity etc. However, these stirrups have failed at ultimate loads for RC beams.

8.3 Recommendation for Future work

Experimental work

- To Study mechanical properties of different types of FRP reinforcements.

- Study presented here can be repeated by making use of CFRP or AFRP reinforcements.

- To study enhancement in performance of prestressed concrete beams using FRP tendons.

- To evaluate effects of high temperature and fire on performance of RC/PSC beams using FRP reinforcement/tendons

- To Study bond properties between concrete and FRP reinforcement by incorporating different cementitious materials and fibers like polypropylene fibers, steel fibers etc.
- Experimental work to be conducted on other structural elements like slab, columns, beam-column junction etc.
- Use of surface mounted reinforcements for strengthening of column, beam, beam-column joint of concrete and on masonry to be studied.
- Durability of FRP reinforced beams can be evaluated and comparison is to be made with conventional reinforcement.
- Effect of freeze-thaw cycles, heating cooling cycles, wetting drying cycles, sustained load on flexural behaviour of FRP reinforced concrete beams is to be studied.

Analytical work

- Analytical study can be made using FEM modeling by incorporating non-linearity and adopting compatible material properties for RC/PSC beams.
- Analytical evaluation of bond properties of FRP reinforced beams is to be made
- Analytical study on stress-strain diagram of FRP confined concrete with different loading rate to be conducted.
- Analytical evaluation of FRP strengthening work by preparing FE model of RC structural elements.
- FEM modeling of any existing RC structure to be prepared using FRP reinforcement.
- Micro-structural analysis of FRP reinforced concrete elements is to be studied.

REFERENCES

1. Alsayed (1998), "Flexural Behaviour of Concrete Beams Reinforced with GFRP Bars", Elsevier, Cement and Concrete Composites, vol. 20, pp. 1-11
2. Sarazin and Newhook (2002), "Examination of Minimum Flexural Reinforcement for GFRP Reinforced Concrete Beams", 4th Structural Specialty Conference, Canadian Society for Civil Engineering.
3. Stratford and Burgoyne (2003), "Shear Analysis of Concrete with Brittle Reinforcement" Journal of Composites for Construction, vol. 7, no. 4, pp. 323- 330
4. Matta et al. (2007), "Size effect on shear strength of concrete beams reinforced with FRP bars", Proc. 6th Int. Conf. on Fracture Mechanics *of Concrete and Concrete Structures (FraMCoS-6)*, Catania, Italy
5. El sayed et al. (2007), "Shear strength of concrete beams reinforced with FRP bars: Design method", FRPRCS-7, SP 230-54, pp. 955-974
6. Gravina and Smith (2008), "Flexural behaviour of indeterminate concrete beams reinforced with FRP bars", Elsevier, Engineering Structures, vol. 30, pp. 2370–2380
7. Bank Lawrence (2006), "Composites for construction: Structural design with FRP materials", John Willey and Sons Inc.
8. Gangarao et al. (2007), "Reinforced concrete design with FRP composites", Taylor and Francis group, CRC Press.
9. Krishnaraju (1981), "Prestressed Concrete", Tata McGraw-Hill.
10. Shah and Karve (2005), "Illustrated Design of Reinforced Concrete Buildings", Structures publication.
11. Pecce et al. (2000), "Experimental Response and Code Models of GFRP RC Beams in Bending", Composites for Construction, vol. 4, no. 4, pp. 180-190
12. Grace et al. (1998) "Behaviour and Ductility of simple and continuous FRP reinforced beams", Composites for Construction, vol. 2, no. 4, pp. 186-194

13. Abdalla (2002), “Evaluation of deflection in concrete members reinforced with fiber reinforced polymer (FRP) bars”, Elsevier, Composite Structures, vol. 56, pp. 63–71

14. Toutanji and Youg (2003), “Deflection and crack-width prediction of concrete beams reinforced with glass FRP rods”, Elsevier, Construction and Building Materials, vol. 17, pp. 69-74

15. Sunna et al. (2004), “Deflection of FRP Reinforced concrete beams”, Building Research center, Royal Scientific Society, Jordan

16. Kocaoz et al. (2005), “Tensile characterization glass FRP bars”, Composites, part-B, vol. 36, pp.127-134.

17. Castro et al. (1998), “Tensile and Non-Destructive testing of FRP bars”, Composite construction, vol. 2, no.1, pp. 17-27.

18. Katz et al. (1999), “Effect of high temperature on bond strength of FRP rebars”, Journal of Composite construction, vol. 3, no.2, pp. 73-81.

19. Nadjai et al. (2005), “Fire Performance of Concrete beams reinforced with FRP bars”, Proceedings of International Symposium on bond behaviour of FRP in structures, pp. 401-410.

20. Galati et al. (2006), “Thermal effects on bond between FRP bars and concrete”, Composites, Part A, vol. 37, pp. 1223-1230.

21. Won et al. (2008), “Effect of fibers on bond between FRP reinforcing bars and high strength concrete”, Composites, Part B, vol. 39, pp. 745-755.

22. Tighiouart et al. (1998), “Investigation of bond in concrete member with Fiber Reinforced Polymer (FRP) bars”, Construction and Building Materials, vol. 12, pp. 453-462

23. ACI 440.1R (2003), “Guide for Design and Construction of Concrete reinforced with FRP bars”, ACI Committee 440

24. IS 456:2000, “Plain and Reinforced Cement Concrete” Bureau of Indian Standards, New Delhi

25. Broomfield J. (1997), “Corrosion of steel in Concrete: Understanding, Investigation and Repair”, E and SPON press

26. Bentur et al. (1996), “Steel Corrosion in Concrete”, CRC press .

27. Maaddawy(2006), “Effect of FRP wraps on Corrosion Activity and Concrete Cracking in Chloride-Contaminated Concrete Cylinders”, Journal of composite for construction, vol. 10, No.2, pp-139-147

28. Maaddawy(2003), “Effectiveness of impressed current technique to simulate corrosion of steel reinforcement in concrete”, Journal of Materials in Civil Engineering, vol. 15, N0.1, pp-41-47

29. Austin et al. (2004), “Electrochemical Behaviour of steel-reinforced concrete during accelerated concrete testing”, Houston, vol. 60, Issue:2, pg. 203-213

30. Pruckner and Gjorv (2004), “Effect of CaCL2 and NaCl additions on concrete corrosivity”, Elsevier, Cement and Concrete Research, 34, pp. 1209-1217

31. Andrade and Alonso (1996), “Corrosion rate monitoring in laboratory and on site”, Construction and Building Materials, vol. 10, No. 5, pp 315-318.

32. Veerachai leelarleikeit (2003), “BEM Analysis on Half-cell potential measurement for corrosion estimation”, NDT-CE (international symposium).

33. ACI 222, “Corrosion of metals in concrete”, report from ACI committee 222

34. ASTM C 876 (1991), “Standard Test Method for Half-cell Potentials of Reinforcing Steel in Concrete”, ASTM International

APPENDIX A

LIST OF USEFUL WEBSITES

- www.dextraindia.com
- www.firep.com
- www.fiberglassrebar.com
- www.asce.org
- www.scincedirect.com
- www.corrosionvector.com
- www.concretecorrosion.net
- www.pdfsearchengine.com
- www.google.com/scholar

APPENDIX B

LIST OF PAPERS TO BE COMMUNICATED

1. Barot Urvesh N. and Dave Urmil V., "Flexural behaviour of Reinforced Concrete beams using GFRP reinforcement", APFIS 2009, *Asia Pacific conference on FRP in structures*, 9-11December, seoul, Korea

2. Barot Urvesh N. and Dave Urmil V., "Shear behaviour of Reinforced Concrete beams using GFRP stirrups", *5th International conference on FRP composites in civil engineering*, CICE-2010, 27-29 September 2010, Beijing, China.

3. Barot Urvesh N. and Dave Urmil V., "Performance of Reinforced Concrete beams with partial replacement of conventional reinforcement with GFRP rebars", *NU Journal of Engineering*, Nirma University, Ahmedabad.

4. Barot Urvesh N. and Dave Urmil V., "Flexural and Shear behaviour of Reinforced Concrete beams using GFRP reinforcement", *Journal of Engineering structures.*

5. Barot Urvesh N. and Dave Urmil V., "Initiation of corrosion in concrete cylinders using accelerated technique", *NUCONE 2009, National Trends in current Technology*, Nirma University, Ahmedabad, Gujarat, 25-27 November, 2009.